



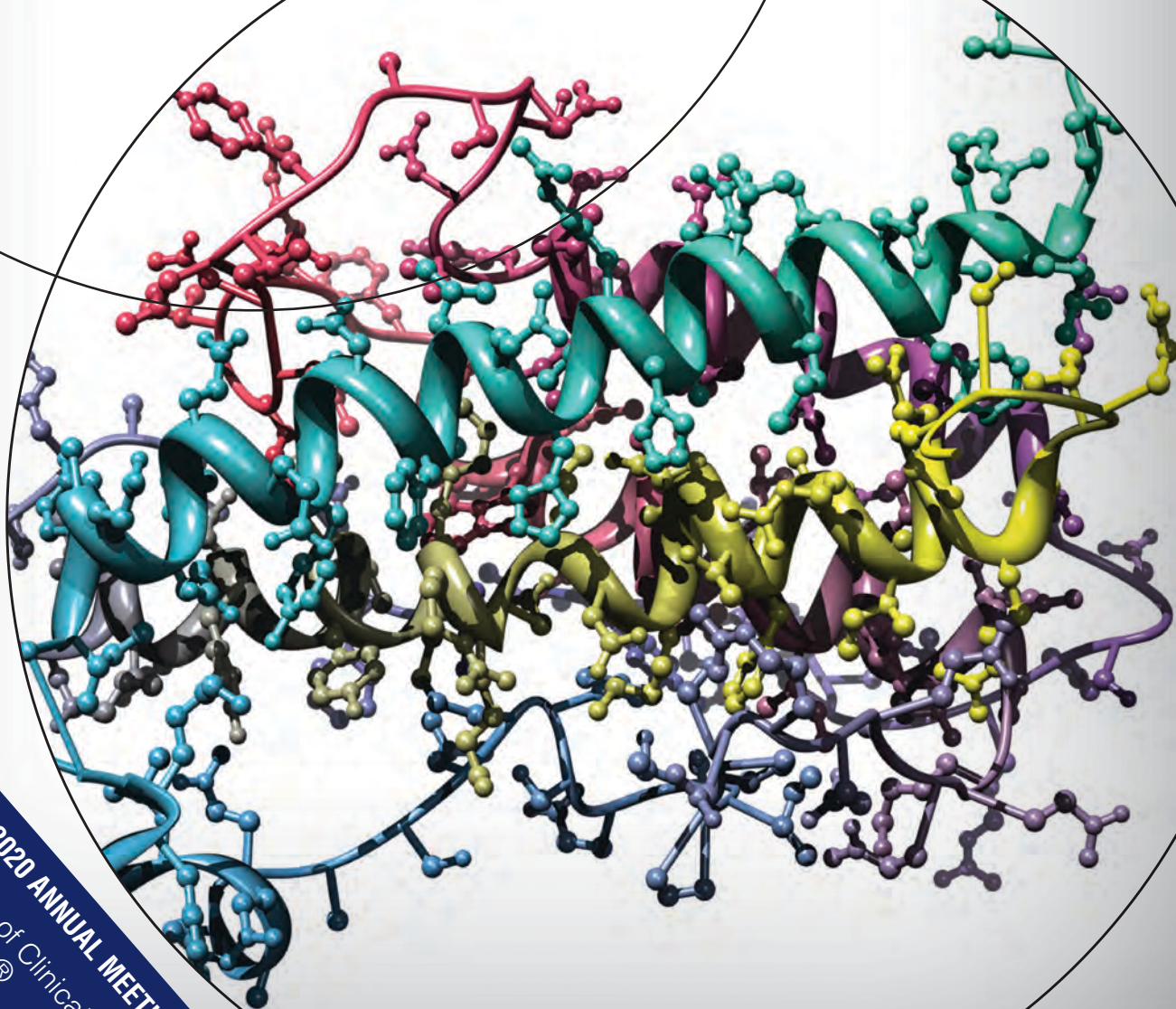
ACCP

AMERICAN COLLEGE OF CLINICAL PHARMACOLOGY  
Advancing Clinical Care through Pharmacology®

Volume 9 Number S2 September 2020

# CLINICAL PHARMACOLOGY IN DRUG DEVELOPMENT

Official Publication of the American  
College of Clinical Pharmacology®



**ABSTRACTS OF THE 2020 ANNUAL MEETING**  
American College of Clinical  
Pharmacology®  
September 21–23, 2020  
Virtual

# Clinical Pharmacology in Drug Development

Official Publication of the American College  
of Clinical Pharmacology®

---

**Abstracts: 2020 Annual Meeting  
American College of Clinical Pharmacology®  
September 21–23, 2020  
Virtual**

---

Published by:

**WILEY**

On behalf of:

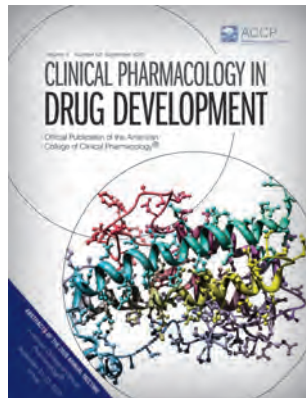


**ACCP**

AMERICAN COLLEGE OF CLINICAL PHARMACOLOGY®

*Advancing Clinical Care through Pharmacology®*

American College of Clinical Pharmacology®





## Abstracts

Clinical Pharmacology  
 in Drug Development  
 9(52) 1–75  
 © 2020, The American College of Clinical  
 Pharmacology  
 DOI: 10.1002/cpdd.858

# ACCP Abstract Booklet

## Adverse Drug Effects

Poster Number: 001

### An Evaluation of Gastrointestinal Adverse Events in Patients Receiving Tenofovir Alafenamide vs Tenofovir Disoproxil Fumarate

M. Bertoni<sup>1</sup>, B. Kennard<sup>1</sup>, D. Murrell<sup>1</sup>, D. Cluck<sup>1</sup>, J. Moorman<sup>1</sup>, K. Wang<sup>2</sup>, M. Duffourc<sup>1</sup>, S. Harirforoosh<sup>1</sup>

<sup>1</sup>East Tennessee State Univ, Johnson City, TN, USA;

<sup>2</sup>West Virginia Univ, Morgantown, WV, USA

**Statement of Purpose, Innovation or Hypothesis:** Tenofovir alafenamide (TAF) and tenofovir disoproxil fumarate (TDF) are two nucleoside reverse transcriptase inhibitors (NRTIs) formulated with emtricitabine as part of the backbone of antiretroviral regimens. Tenofovir disoproxil fumarate, when used as pre-exposure prophylaxis, has been associated with a gastrointestinal (GI) “start-up syndrome”. This study sought to determine if an association exists between respective drugs, TAF and TDF, pertaining to specific GI adverse events (AEs).

**Description of Methods and Materials:** This substudy included fifty-four subjects, which were part of a larger IRB-approved study at East Tennessee State University. Nearly 83.3%, or 45 subjects, were male with a median age of 53 yrs (IQR, 46.0–59.0 yrs). Individuals received care from the East Tennessee State University Center of Excellence (COE) for HIV/AIDS Care. Subjects received either TAF (n=25) or TDF (n=29) antiretroviral therapy. A Fisher’s exact test was used to determine associations between TDF and TAF and GI side effects. Significance ascertainment was set at  $p < 0.05$ .

**Data and Results:** An overall diarrhea occurrence was found in 31.5% of subjects; TAF 44% and TDF 20.7%. A Fisher’s exact test showed no association between the GI AE (diarrhea) and the respective NRTI ( $p=0.084$ ). An overall nausea occurrence was reported in 16.7% of subjects. 20% and 13.80% of subjects reported a nausea occurrence in TAF and TDF treatment groups, respectively. A Fisher’s exact test showed no association between the GI AE (nausea) and regimen ( $p=0.718$ ). Lastly, an overall vomiting occurrence was found in 3.7% of subjects. While 8% of TAF subjects reported a vomiting occurrence, no occurrences were found among the individual TDF regimen. A Fisher’s exact test showed no association between the GI AE (vomiting) and regimen ( $p=0.210$ ).

By contrast, there were no significant associations in a GI AE between TAF and TDF.

**Interpretation, Conclusion or Significance:** Although patients receiving TAF or TDF experienced GI adverse events, there was no statistical significance to report nonrandom associations. Additional real-world data should be obtained to determine if an association exists.

Poster Number: 002

### An Analysis of CD4 Lymphocyte Levels in HIV-infected Patients Treated With Dolutegravir, Elvitegravir or Raltegravir

B. Kennard<sup>1</sup>, M. Bertoni<sup>1</sup>, D. Murrell<sup>1</sup>, D. Cluck<sup>1</sup>, J. Moorman<sup>1</sup>, K. Wang<sup>2</sup>, M. Duffourc<sup>1</sup>, S. Harirforoosh<sup>1</sup>

<sup>1</sup>East Tennessee State Univ, Johnson City, TN, USA;

<sup>2</sup>West Virginia Univ, Morgantown, WV, USA

**Statement of Purpose, Innovation or Hypothesis:** Integrase strand transfer inhibitors (INSTIs) dolutegravir (DTG), elvitegravir (EVG) and raltegravir (RAL) are commonly used in the treatment of HIV. They are preferred agents due to an improved tolerability and efficacy profile. However, the use of INSTIs is associated with several adverse events. The purpose of this study was to compare the levels of CD4 T cells in patients grouped by respective INSTI to determine if CD4 recovery differed by INSTI-based regimen.

**Description of Methods and Materials:** This is a substudy of a larger IRB-approved study conducted from 2015–2017 at East Tennessee State University. A total of eighty-six patients (median age 52.5 yrs; interquartile range, 45.7–57.2) were divided based on receiving DTG (n=41, 88.1 % male), EVG (n=23, 87.0% male) or RAL (n=22, 86.4 %, male). Each group underwent measurement of absolute CD4 lymphocyte (ACD4) count and percentage of CD4 lymphocytes (CD4POS). The means of the three were compared by a one-way ANOVA with significance determination being set at  $p < 0.05$ . All data below is reported as mean  $\pm$  SD. It is worth noting that most patients were virologically suppressed ( $< 20$  copies/mL).

**Data and Results:** The ACD4 mean for the comprehensive group was  $748.24 \pm 387.21$  cells/mm<sup>3</sup>; while the DTG, EVG and RAL patient groups presented with means of  $699.39 \pm 349.82$  cells/mm<sup>3</sup>,  $781.65 \pm 403.88$  cells/mm<sup>3</sup> and  $804.36 \pm 440.13$  cells/mm<sup>3</sup>, respectively. After analysis with a one-way ANOVA, there was no

statistical significance ( $p=0.531$ ) in ACD4 among the three groups. In addition, the comprehensive mean value for CD4POS was  $33.90 \pm 10.63\%$ . For DTG, EVG and RAL, respective results were  $32.82 \pm 10.59\%$ ,  $35.14 \pm 10.60\%$  and  $34.62 \pm 11.01\%$ . There was no statistical significance ( $p=0.663$ ) revealed among the groups for CD4POS mean.

**Interpretation, Conclusion or Significance:** Patients receiving RAL demonstrated the highest CD4 lymphocyte levels; however, the difference did not attain statistical significance among the groups. This might be due to a longer duration of treatment with RAL compared to other INSTIs. Further studies with larger sample sizes need to be conducted to determine if a true difference exists.

## Applications of Modeling & Simulation

### Poster Number: 004

#### Comparison of Simulated Drug Concentrations With *In-vivo* Data Obtained from HIV Patients Receiving Dolutegravir-based Therapy

Z. Liu<sup>1</sup>, D. Murrell<sup>1</sup>, S. Harirforoosh<sup>1</sup>

<sup>1</sup>East Tennessee State Univ, Johnson City, TN, USA

**Statement of Purpose, Innovation or Hypothesis:** GastroPlus<sup>®</sup> is a software program that simulates a wide range of biopharmaceutics and pharmacokinetics parameters including plasma concentration of a compound based on physiochemical characteristics and some preliminary data. Concerning the prediction of pharmacokinetic (PK) factors in humans, the program will create a model and perform simulations which consider patient characteristics such as age, body mass index, gender and level of kidney function. Dolutegravir (DTG) is an integrase strand transfer inhibitor utilized in the antiretroviral therapy of HIV. The goal of this study was to evaluate the potential relationship between data generated by the simulation software program and observed plasma concentrations of DTG in HIV-infected patients.

**Description of Methods and Materials:** DTG trough concentrations collected in a previous study conducted from 2015–2017 were compared to the results obtained from GastroPlus. In that study, patients were on a dose of 50 mg DTG orally once daily, along with other HIV medicines. Utilizing patient-specific characteristics (age, body mass index, gender and level of kidney function) obtained from the previous study and DTG PK data provided by GastroPlus v9.7, simulations were performed. The model was instructed to determine DTG concentrations following 30 days of 50 mg once-a-day dosing with DTG. This would return values equivalent to steady-state trough concentrations. Observed DTG concentrations were then compared to

predicted values and evaluated through linear regression. Data are presented as mean  $\pm$  standard deviation. Statistical significance was dependent on the discovery of a  $p$ -value of less than 0.05.

**Data and Results:** The available samples ( $n=22$ ) had median age of 51.5 yrs with interquartile range of 42.0–57.0 yrs, male predominance (86.36%), mean BMI of 25.3 and mean GFR at the end of treatment 62.68 mL/min. The mean simulation concentration was  $785.8 \pm 68.9 \mu\text{g/L}$  and the original sample concentration yielded  $758.0 \pm 410.0 \mu\text{g/L}$ . Trough concentrations produced by GastroPlus were not correlated with those obtained from previous study ( $R^2=0.030$ ,  $p>0.44419$ ).

**Interpretation, Conclusion or Significance:** GastroPlus yields steady-state concentrations under perfect circumstances and without other possible influencing variables. The comparison of simulations with previous *in-vivo* study indicates that there might be other variables that influence DTG concentrations in human body. Further studies on those variables are suggested.

### Poster Number: 005

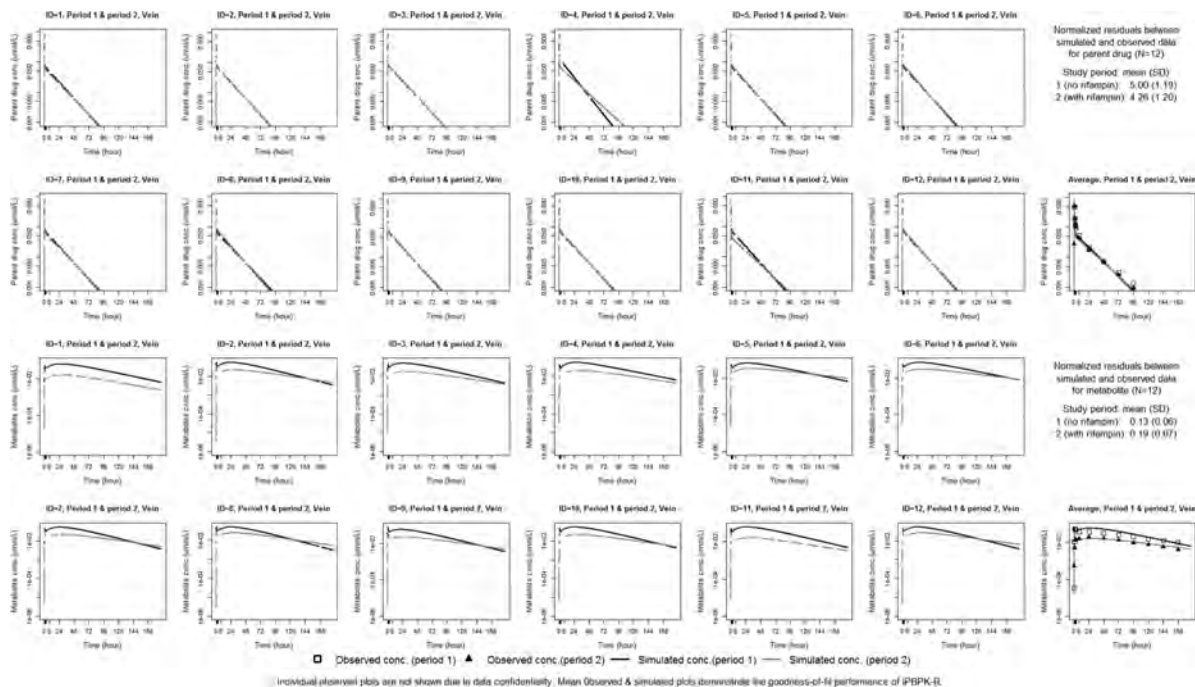
#### Use of Individualized, Physiologically-based Pharmacokinetic Modeling Using Rate Data (iPBPK-R) to Estimate the Activity of Nonrenal Elimination Pathways of Temozolomide and Its Metabolite Methylolomide

Y. Franchetti<sup>1</sup>, T. D. Nolin<sup>1</sup>

<sup>1</sup>Univ of Pittsburgh School of Pharmacy, Pittsburgh, PA, USA

**Statement of Purpose, Innovation or Hypothesis:** Temozolomide, used to treat renal cell carcinoma, is a nonrenally cleared drug with overlapping substrate specificity for multiple enzymes and transporters. It is intravenously administered and has a long half-life. Our objective is to evaluate the ability of our individualized, physiologically-based pharmacokinetic (PBPK) modeling approach using rate data (iPBPK-R) to distinguish and simultaneously estimate the contributions of nonrenal elimination pathways mediated by cytochrome P450 3A4 (CYP3A4) and P-glycoprotein (P-gp) to the disposition of temozolomide and its metabolite methylolomide within healthy individuals. In addition, we simultaneously investigate the effect of coadministered rifampin, a strong CYP3A4 inducer and P-gp modulator, on the disposition of temozolomide.

**Description of Methods and Materials:** The study included two dosing periods; temozolomide alone (period 1), followed by temozolomide with concomitant rifampin. Temozolomide 25mg was administered as a single 30-min intravenous (IV) infusion in both periods. A PBPK model comprised of seven organ compartments was built with parameters for temozolomide and methylolomide. The liver compartment included



**Poster Number: 005** **Figure 1.** Simulated Drug Concentration - Time Curves of Temsirolimus and Its Metabolite Sirolimus in the Study Period 1 and Period 2 in 12 Healthy Individuals

extracellular space and hepatocyte subcompartments. Linear CYP3A4 clearance and nonlinear P-gp clearance with a Michaelis-Menten term were included in the ordinary differential equations (ODE) related to the hepatocyte compartment. Thirteen PBPK parameters were selected based on sensitivity analysis and estimated via optimization using whole blood concentrations of temsirolimus and sirolimus, which were serially measured at 13 timepoints over seven days in period 1 and repeated in period 2. Fifteen subjects received daily oral doses (2 x 300 mg capsules) of rifampin from Days 15 to 27. Period 2 began on Day 21 with repeat dosing of temsirolimus 25 mg IV. Induction/inhibition coefficient parameters for CYP3A4 and P-gp activity were included in ODEs and independently estimated between the two periods with and without rifampin. The thirteen PBPK parameters, including velocity of efflux transport, metabolic clearance and volume of hepatocyte, were individually co-optimized across the two periods. Individual model fits were evaluated using residuals between predicted and observed drug concentrations. Simulations were performed using R v3.4.4 on the Bridges supercomputer.

**Data and Results:** The seven-compartmental iPBPK-R model simultaneously captured the time-dependent behavior of concentrations of both temsirolimus and sirolimus in 12 healthy subjects. Due to the data confidentiality, we present concentration-time plots where we applied iPBPK-R to a virtual subject with data being the sample average (Figure 1). The interim re-

sults with the 12 subjects indicated that rifampin increased CYP3A4-mediated metabolism of sirolimus by a median of 50.3%. P-gp transport of temsirolimus and sirolimus was not altered by rifampin. Simulations for the remaining three subjects will be implemented once the supercomputer becomes available (temporarily inaccessible due to the COVID-19 pandemic).

**Interpretation, Conclusion or Significance:** Our iPBPK-R modeling indicated that its application to the four sets of drug concentration data (i.e., parent and metabolite in two periods per individual) enables us to differentially quantify the changes of transporter versus enzyme-mediated elimination pathways in healthy subjects. Upon further improvement of the computation speed and accuracy of the nested co-optimization, iPBPK-R is anticipated to provide good utility for evaluating induction and inhibition effects and alterations of drug disposition caused by a concomitant drug or disease state.

**Poster Number: 006**

**Prediction of Food Effect of Paliperidone Invega® Using Physiologically-based Absorption Modeling**

S. Subhani<sup>1</sup>, C. Kim<sup>1</sup>, P. Muniz<sup>2</sup>, M. Rodriguez<sup>2</sup>, R. Cristofolletti<sup>1</sup>, S. van Os<sup>3</sup>, S. Schmidt<sup>1</sup>, V. Vozmediano<sup>1</sup>

<sup>1</sup>Univ of Florida Coll of Pharmacy, Gainesville, FL, USA; <sup>2</sup>Dynakin S.L. Derio, Biscay, Spain; <sup>3</sup>Synthon BV, Nijmegen, The Netherlands

**Statement of Purpose, Innovation or Hypothesis:**

An atypical antipsychotic drug, paliperidone, was approved by the US Food & Drug Administration in 2006 as an extended-release (ER) tablet (Invega<sup>®</sup>), for a once-daily treatment regimen in schizophrenia. Osmotic-controlled release oral delivery system (OROS) of paliperidone (PAL) offers advantages, such as prevention of fluctuation of plasma concentration and reduced dosing frequency. It is known that the administration of Invega after a high-fat or high-calorie meal increases the maximum plasma concentrations ( $C_{max}$ ) and area under the curve (AUC) values by 60% and 54%, respectively. However, food has various effects on the gastrointestinal (GI) physiology, such as changed transit times, changed volumes, pH in different gastrointestinal compartments, secretion of bile salts and increased hepatic blood flow. Consequently, this may affect the drug solubility, dissolution rate, absorption and pharmacokinetics (PK). To investigate the effect of food on Invega we have developed and qualified a physiologically-based absorption model (PBAM) as a tool to identify the most sensitive factors affecting the food effect (FE) by integrating the complex biological process with *in-vitro* dissolution data.

**Description of Methods and Materials:** The model was developed in GastroPlus<sup>™</sup> v9.7 in a step-wise manner: 1) development of a compartmental PK model to describe the disposition of PAL using data from the IR formulation; 2) link of the compartmental model to an advanced compartmental absorption and transit (ACAT) model and 3) update of the model for the OROS formulation in fasting and fed physiology to predict the food effect for the OROS formulation. The model was developed and qualified using both data from the literature as well as proprietary data provided by Synthon BV (*in vitro* dissolution data and clinical data). Clinical studies used in the present research were approved by the corresponding Institutional Review Board (IRB) and conducted in accordance with the principles of the Declaration of Helsinki.

**Data and Results:** The developed ER model for OROS formulation could successfully predict decreased absorption in the upper GI tract compared to the immediate release (IR) formulation. The developed ER model adequately predicts the GI absorption of the OROS formulation, as well as the positive FE. Under fasting conditions, absorption primarily occurs in the colon and increased through the jejunum, ileum and colon in fed conditions. Moreover, the fraction absorbed in fed condition increases due to an increased solubilization of PAL in the presence of food. The population simulations are able to not only predict the mean behavior but also to account for the variability observed in the PK of the OROS formulation in both fasted and fed states in a pilot study.

**Interpretation, Conclusion or Significance:** To our knowledge, this is the first attempt to model the food effect observed clinically for the OROS ER tablet of PAL and depicts the gastrointestinal regional absorption of the formulation. The developed and calibrated model was used to evaluate the effect of different GI parameters on the food effect and can be further applied in guiding the development and selection of generic drug products of Invega through the simulation of virtual bioequivalence trials.

**Poster Number: 007****Modeling Lamotrigine Clearance Changes During Pregnancy and Postpartum: Preliminary Results from the MONEAD Study**

A. Karanam<sup>1</sup>, P. B. Pennell<sup>2</sup>, K. J. Meador<sup>3</sup>, A. K. Birnbaum<sup>1</sup>

<sup>1</sup>Univ of Minnesota, Minneapolis, MN, USA;

<sup>2</sup>Brigham & Women's Hosp, Harvard Medical School, Boston, MA, USA; <sup>3</sup>Stanford Univ, Stanford, CA, USA

**Statement of Purpose, Innovation or Hypothesis:**

Lamotrigine (LTG) is one of the most prescribed antiepileptic drugs (AEDs) in pregnant women with epilepsy (PWWE). Management of women with epilepsy in pregnancy is complicated due to increasing LTG clearance. Moreover, approximately 25% of PWWE experience small or minimal changes in LTG clearance during pregnancy, whereas the remaining 75% experience on average ~200% linear increase in clearance (Polepally et al. 2014). Additionally, no studies directly compare LTG pharmacokinetics in PWWE and non-pregnant women with epilepsy (NPWWE). Further characterization of changes in LTG pharmacokinetics and factors that affect drug disposition during pregnancy and postpartum are needed to optimize therapy for both mother and fetus.

**Description of Methods and Materials:** MONEAD is a 20-site, prospective, observational, parallel-cohort study recruiting both PWWE and NPWWE taking AEDs. This analysis focused on women taking LTG alone or with a nonpharmacokinetic-interacting AED. For NPWWE, seven plasma samples were collected per individual, one at each of seven visits over a span of two years. In PWWE, four plasma samples were collected during pregnancy (three during pregnancy and one on the day of delivery) and three samples collected over 11 mos postpartum. A steady-state infusion model in NONMEM<sup>®</sup> with first-order conditional estimation was used to describe LTG clearance where clearance is approximated as daily dose rate/observed concentrations. In addition, the effect of gestational age, body size, race, ethnicity, smoking, alcohol use and use of hormonal medication on clearance was tested.

**Data and Results:** Analysis included 162 PWWE and 50 NPWWE. Baseline clearance ( $CL_{BL}$ ) (clearance when not pregnant for PWWE and NPWWE) was estimated to be 2.9 L/hr with 35% between-subject variability (BSV). Clearance change during pregnancy was best described by an  $E_{max}$  model as a function of gestational age. Two subpopulations were identified in PWWE using a mixture model: with approximately 92% of the PWWE having a maximum induction of 2.13-fold (39.2% BSV) over  $CL_{BL}$  with 50% of the maximum clearance being reached at 28.8 wks gestational age and the remaining 8.13% of PWWE having no statistically-significant change in clearance during gestation. Following delivery, a first-order mono-exponential decline ( $1.27 \text{ hr}^{-1}$ ) in clearance as a function of postpartum week described the return of clearance to baseline in the postpartum period. Use of estrogen-based contraceptives was the only covariate found to significantly affect  $CL_{BL}$  (increased by 31.4%). Model residual error was 29.8%.

**Interpretation, Conclusion or Significance:** We characterized the changes in LTG clearance during pregnancy and after delivery using a model-based approach in the largest known pharmacokinetic study of PWWE taking LTG. Baseline LTG clearance was similar for both PWWE and NPWWE. An  $E_{max}$  model best described the clearance increase during pregnancy, making it more physiologically relevant than the linear increase described earlier. Our analysis also confirms reported existence of two subpopulations (Polepally et al. 2014) within PWWE and the clinically significant effect of oral contraceptives on baseline LTG clearance. These findings are of clinical importance as they indicate a subpopulation without the need for dose changes in pregnancy.

*Submitted on behalf of the MONEAD Group. This work was supported by NIH NINDS, NICHD grants #U01-NS038455, 2U01-NS038455 and U01-NS050659.*

**Poster Number: 008**

**Population Pharmacokinetic/Pharmacodynamic Modeling of a Novel TAFIa Inhibitor DS-1040 in Healthy Subjects and Patients**

L. Ma<sup>1</sup>, D. Kang<sup>1</sup>, I. Patel<sup>1</sup>, M. Grosso<sup>1</sup>, O. Yin<sup>1</sup>

<sup>1</sup>Daiichi Sankyo, Basking Ridge, NJ, USA

**Statement of Purpose, Innovation or Hypothesis:** DS-1040 is an inhibitor of the activated form of thrombin-activatable fibrinolysis inhibitor (TAFIa) enzyme, currently in clinical development for the treatment of thrombotic diseases including venous thromboembolism (VTE) and acute ischemic stroke (AIS). DS-1040 inhibits enzymatic activity of TAFIa and enhances thrombolytic activity triggered by endogenously

or exogenously administered plasminogen activator (t-PA). Therefore, DS-1040 is expected to enhance the effect of endogenous t-PA, or reduce the required amount of or even eliminate the need for exogenous t-PA, without compromising the thrombolytic activity or increasing bleeding risks, suggesting that it may provide a safer therapeutic option for the treatment of AIS and VTE. Population pharmacokinetics (PopPK) and pharmacodynamics (PD) modeling for TAFIa were conducted previously in healthy subjects. The main objective of this analysis is to update the PopPK of DS-1040 and characterize the relationships between DS-1040 plasma concentrations and TAFIa activity in patients with AIS or VTE.

**Description of Methods and Materials:** Analyses were performed based on pooled data from five Phase 1 studies in healthy subjects (single oral dose from 50–400 mg or intravenous infusion from 0.1–20 mg), and two Phase 1b studies in patients (intravenous infusion from 0.6–80 mg). A total of 4,227 plasma samples and 2,868 TAFIa measurements from 361 subjects were included. Log-transformed plasma concentrations of DS-1040 following intravenous and oral administration were analyzed simultaneously. Stepwise forward addition and backwards elimination were used for covariate model building. The TAFIa activity was analyzed sequentially, using final PopPK model predicted plasma concentrations and sigmoid  $I_{max}$  model.

**Data and Results:** The DS-1040 PopPK model was best described by a three-compartment model with sequential zero- and first-order absorption and linear elimination following intravenous and oral administration. Among the significant covariate identified, renal clearance was proportional to creatinine clearance (CrCL); however, the CrCL effect on DS-1040 exposure for subjects with CrCL >70 ml/min is modest (<30%) based on simulation using 5- and 95-percentile values (71.0–193 ml/min). Peripheral volume of distribution (V3) and rate constant (Q3) for Asian was ~15% and 14% lower than Caucasian. Non-renal clearance and V3 for oral formulation were estimated to be 43% lower and 136% higher than that for intravenous (IV) formulation. Pharmacokinetic (PK)-TAFIa relationship was described by direct sigmoid  $I_{max}$  model. A rapid and strong inhibition in TAFIa activity was observed with mean (%RSE) of  $I_{max}$  and IC50 of 90.8% (1) and 2.29 (2) ng/mL. The PK parameter estimates are similar to that observed in healthy subjects with  $I_{max}$  and IC50 of 91.6% (2) and 2.16 (2) ng/mL.

**Interpretation, Conclusion or Significance:** The analyses provided an adequate description of the observed data. Overall, PopPK and PK/PD model (TAFIa) suggest that after IV administration of DS-1040, the exposure-biomarker (TAFIa activity) relationship in patients with AIS and VTE are comparable with those observed in healthy subjects. Statistically-significant

covariates did not result in clinically-meaningful impact on DS-1040 exposure for subjects with mild renal impairment or normal renal function and therefore no dose adjustment criteria have been identified at this time for subjects with CrCL >60 ml/min.

**Poster Number: 009**

**Improved Safety of Opioid Analgesic Oliceridine Compared to Morphine Assessed by Utility Function Analysis**

A. Dahan<sup>1</sup>, M. Niesters<sup>1</sup>, M. J. Fossler, Jr.<sup>2</sup>, M. A. Demitrack<sup>2</sup>, E. Olofsen<sup>1</sup>

<sup>1</sup>Leiden Univ, Leiden, The Netherlands; <sup>2</sup>Trevena Inc, Chesterbrook, PA, USA

**Statement of Purpose, Innovation or Hypothesis:**

Opioids produce potent pain relief and therefore remain the cornerstone of treatment of moderate to severe pain. Among the many opioid side effects, respiratory depression is potentially life-threatening. Given the “opioid crisis”, there is the ongoing search for potent (opioid) analgesics with less or no adverse effects. Opioids produce respiratory depression *via* activation of  $\mu$ -opioid receptors expressed on pontine respiratory neurons. Full  $\mu$ -receptors agonists produce analgesia, by activation of the G-coupled signaling pathway, and dose-dependent respiratory depression (with apnea at high doses) by activation of the  $\beta$ -arrestin pathway. Recent focus has been on the development of biased ligands, which are  $\mu$ -receptors agonists that selectively engage the G-coupled signaling pathway while avoiding the  $\beta$ -arrestin pathway.

**Description of Methods and Materials:** In the current study, we compared the respiratory and analgesic effects of three intravenous doses of the biased ligand Oliceridine (1.5, 3 and 4.5 mg) and one morphine dose (10 mg) in 30 healthy male volunteers. The descriptive analysis of this study has been published before. Here, we performed a population pharmacokinetic-pharmacodynamic analysis in NONMEM<sup>®</sup> and constructed utility functions. Utility functions are objective and precise assessments of the probability of analgesia relative to the probability of respiratory depression.

**Data and Results:** The morphine steady-state plasma concentration causing 25% ventilatory depression was  $11 \pm 2$  ng/mL (median  $\pm$  SE) and for concentration causing a doubling of the pain tolerance  $34 \pm 10$  ng/mL; the equivalent values for Oliceridine were  $27 \pm 4$  ng/mL (ventilation) and  $28 \pm 5$  ng/mL. The values are indicative for a 2.5-fold greater morphine respiratory potency compared to Oliceridine, while equipotency was observed for the analgesia efficacy of the two opioids. Additionally, Oliceridine equilibrates more rapidly than morphine with its effects compartment. The two utility curves that were constructed, i.e. the probability of analgesia minus the probability of respiratory depres-

sion and the probability of analgesia without respiratory depression, were all in favor of Oliceridine compared to morphine, indicative that following treatment with Oliceridine the probability of analgesia exceeds that of respiratory depression, over the dose range studied, in contrast to morphine, where the probability of respiratory depression exceeded that of analgesia.

**Interpretation, Conclusion or Significance:** We conclude that Oliceridine has a favorable safety profile when considering both analgesia and respiratory depression.

**Encore:** Presented at the Annual Meeting of the American Society of Anesthesiologists, October 2019.

**Clinical Pharmacokinetics (ADME)**

**Poster Number: 010**

**S-warfarin Concentrations to Estimate Exposure and Cytochrome P450 (CYP) 2C9 Activity Using Limited Sampling Strategy With a Population Pharmacokinetic Approach**

L. Tran<sup>1</sup>, M. Nikanjam<sup>2</sup>, E. V. Capparelli<sup>2</sup>, J. S. Bertino, Jr.<sup>3</sup>, A. Nafziger<sup>3</sup>, A. D. Kashuba<sup>4</sup>, S. Turpault<sup>5</sup>, J. D. Ma<sup>6</sup>

<sup>1</sup>Univ of North Carolina Eshelman School of Pharmacy, Blue Bell, PA, USA; <sup>2</sup>Univ of California San Diego, San Diego, CA, USA; <sup>3</sup>Bertino Consulting, Schenectady, NY, USA; <sup>4</sup>Univ of North Carolina at Chapel Hill, Chapel Hill, NC, USA; <sup>5</sup>Sanofi, Malvern, PA, USA; <sup>6</sup>Univ of California San Diego, La Jolla, CA, USA

**Statement of Purpose, Innovation or Hypothesis:** S-warfarin is a probe drug to phenotype cytochrome P450 (CYP) 2C9 activity. S-warfarin limited sampling models (LSMs) were evaluated using a population pharmacokinetic (PopPK) approach.

**Description of Methods and Materials:** A single oral dose of warfarin 10 mg was administered with and without potential CYP2C9 inducers to 100 healthy volunteer adults (65 M, 35 F) who were genotyped for CYP2C9 via PCR. Intensive pharmacokinetic (PK) sampling was obtained ( $\geq 8$  plasma concentrations over 72 hrs). A PopPK model was developed using nonlinear mixed-effects modeling (NONMEM<sup>®</sup> v7.3). LSMs using single- or two-time point concentrations were compared with full PK profiles using empiric Bayesian post hoc estimations of S-warfarin AUC derived from the PopPK model. Preset criterion, precision and bias estimates were determined.

**Data and Results:** S-warfarin concentrations (n=2,508) were well described with a two-compartment model. Mean clearance was 0.56 L/hr and volume of distribution was 35.5 L. Clearance decreased by 33% with the CYP2C9 \*3 allele and increased by 42% with

**Poster Number: 010 Table 1. Assessment of S-warfarin limited sampling models in healthy adults (n=100)**

Sampling Times (hr)	R <sup>2</sup> (≥0.90)	%MPE (-5% to 5%)	%MAE (≤10%)	%RMSE (≤15%)
24	0.83	4.64%	16.23%	16.23%
48	0.89	-2.18%	7.66%	11.23%
72	0.93	-5.56%	7.12%	9.91%
24 and 48	0.89	-0.71%	7.77%	11.48%
<b>24 and 72</b>	<b>0.94</b>	<b>-2.86%</b>	<b>5.85%</b>	<b>8.97%</b>
<b>48 and 72</b>	<b>0.94</b>	<b>-4.76%</b>	<b>6.80%</b>	<b>9.67%</b>

\*Bolded values denote LSMs that were within acceptable limits for correlation, bias, and/or precision.

R<sup>2</sup>: Coefficient of determination.

%MPE: Relative percent mean prediction error.

%MAE: Relative percent mean absolute error.

%RMSE: Relative percent root mean squared prediction error.

lopinavir coadministration in the final PopPK model. LSMs of bias and precision are summarized in the table.

**Interpretation, Conclusion or Significance:** 24 and 72 hrs LSM and 48 and 72 hrs LSM accurately estimate S-warfarin AUC and thus CYP2C9 activity in healthy adults even in the setting of coadministration of a CYP2C9 inducer or the CYP2C9 \*3 allele.

#### Poster Number: 011

##### Mass Balance Studies of [<sup>14</sup>C]-Labeled Poziotinib

J. J. Deppas<sup>1</sup>, D. Greene<sup>2</sup>, B. M. Miller<sup>3</sup>, H. Vu<sup>2</sup>, D. Davar<sup>4</sup>, T. F. Burns<sup>4</sup>, B. T. McLaughlin<sup>4</sup>, S. Chawla<sup>2</sup>, E. Chu<sup>4</sup>, J. H. Beumer<sup>1</sup>

<sup>1</sup>Univ of Pittsburgh School of Pharmacy, Pittsburgh, PA, USA; <sup>2</sup>Spectrum Pharmaceuticals, Irvine, CA, USA; <sup>3</sup>UPMC Hillman Cancer Ctr, Pittsburgh, PA, USA; <sup>4</sup>Univ of Pittsburgh School of Medicine, Pittsburgh, PA, USA

##### Statement of Purpose, Innovation or Hypothesis:

**Background:** Poziotinib is an investigational, irreversible pan-HER tyrosine kinase inhibitor. Unlike currently approved tyrosine kinase inhibitors, poziotinib is a potent inhibitor of cancer cells with EGFR or HER2 exon 20 insertion mutations. To characterize the

metabolic fate and excretion pathways of poziotinib, [<sup>14</sup>C]-poziotinib mass balance studies were conducted.

##### Description of Methods and Materials: Methods:

**Rats:** Male Sprague-Dawley rats were administered an intravenous (IV) bolus or an oral (PO) dose of 3 mg/kg [<sup>14</sup>C]-poziotinib (~80 μCi/animal). Urine and feces were collected through 120 hrs. Additional animals were bile-duct cannulated and dosed PO. **Humans:** Two patients with advanced non-small cell lung cancer (NSCLC) (1 M/1 F; average age 62.5 yrs) were enrolled. Both patients were administered a capsule with ~12 mg [<sup>14</sup>C]-poziotinib (~100 μCi). Blood, urine and feces were collected through 168 hrs and analyzed for radioactivity by liquid scintillation counting. LC-MS/MS analyses of poziotinib and metabolic profiling are ongoing.

**Data and Results: Results:** Rats: After an IV or PO dose, peak radioactivity in plasma was observed at 5 mins and 1 h postdose, respectively, with half-lives of 73 hrs and 49 hrs, respectively. By 24 hrs post treatment, ~5% and ~66% was excreted in urine and feces, respectively after PO or IV dosing. By 120 hrs, greater than 80% was excreted into feces, with ~5% in urine resulting in a total recovery of more than 90% after IV or PO dosing. Carcass retained 2–4% of the administered radioactive dose after IV or PO dosing. In the bile-duct cannulated group, 61% was excreted in bile. **Humans:** Peak radioactivity in plasma was observed at 6–12 hrs

**Poster Number: 011 Table 1. Mean excretion recoveries of radioactivity following [<sup>14</sup>C]-poziotinib administration**

Species	Design			Mean (SD) recovery			
	Route	Dose	Collection Interval	Feces	Urine	Carcass	Total
(n)		(mg/kg)	(h)	(%dose)	(%dose)	(%dose)	(%dose)
Rat (4)	IV	3	0–120	80.9 (4.8)	5.2 (0.8)	4.1 (0.5)	90.5* (4.0)
Rat (4)	PO	3.1	0–120	82.1 (3.0)	5.1 (0.9)	2.8 (0.6)	90.5* (2.3)
Rat (4)	PO	3.2	0–120		Bile: 61.4 (3.1)		
Human (2)	PO	12	0–168	83.3	1.3	NA	84.6

after dosing, with an elimination half-life of radioactivity in plasma >140 hrs. By 24 hrs post treatment, ~1% and ~50% was excreted in urine and feces, respectively. More than 82% of radioactive dose after PO dosing was excreted into feces, with ~1.3% in urine and a total recovery of almost 85%. The majority of excretion occurred within 96 hrs postdose (~97% of ultimate excretion).

**Interpretation, Conclusion or Significance: Conclusion:** Results of both rat and human studies demonstrate that poziotinib is primarily excreted in the feces with urinary excretion playing a negligible role. Thus, dose adjustment of poziotinib will likely not be indicated in patients with renal impairment.

**Poster Number: 012**

**Pharmacokinetics and QT/QTc Interval Prolongation With Concentration-QT Analysis of Trastuzumab Deruxtecan in Patients With HER2-Expressing Metastatic and/or Unresectable Breast Cancer**

E. Kamiyama<sup>1</sup>, T. Garimella<sup>2</sup>, T. Yamashita<sup>3</sup>, A. Shimomura<sup>4</sup>, F. LaCreta<sup>2</sup>, H. Ishizuka<sup>1</sup>, M. Abutarif<sup>2</sup>

<sup>1</sup>Daiichi Sankyo Co Ltd, Shinagawa-ku, Tokyo, Japan;

<sup>2</sup>Daiichi Sankyo Inc, Basking Ridge, NJ, USA;

<sup>3</sup>Kanagawa Cancer Ctr, Yokohama, Kanagawa, Japan;

<sup>4</sup>National Ctr for Global Health & Medicine, Shinjuku-ku, Tokyo, Japan

**Statement of Purpose, Innovation or Hypothesis:** Trastuzumab deruxtecan (T-DXd; DS-8201) is a novel antibody-drug conjugate composed of a humanized anti-HER2 antibody, peptide-based cleavable linker and topoisomerase I inhibitor payload (DXd). T-DXd has a drug-to-antibody ratio of  $\approx 8$ . T-DXd was recently approved for the treatment of unresectable or metastatic HER2-positive breast cancer (BC) and its pharmacokinetics (PK) were well characterized. In this study, the T-DXd/DXd concentration-QT/QTc relationship was evaluated after multiple dosing.

**Description of Methods and Materials:** This is a multicenter, open-label, nonrandomized Phase 1 study in patients with HER2-expressing metastatic BC dosed with T-DXd at 6.4 mg/kg Q3W (NCT03366428). Pharmacokinetic parameters of T-DXd, total anti-HER2 antibody and DXd were determined using noncompartmental analysis. Twelve-lead ECGs were performed in triplicate at specific time points before and after dosing of T-DXd, and PK samples were collected at the same time points as the ECGs. The concentration-QT relationship using the baseline-adjusted QTcF was quantified using linear mixed effects modeling.

**Data and Results:** Fifty-one patients enrolled and received T-DXd; all were assessed for PK and two were excluded for C-QT analysis due to concomitant use of QTc prolonging drugs. The AUC for T-DXd increased

**Poster Number: 012 Table 1. Relationship between Concentration of T-DXd and DXd and QTcF Interval**

QTcF Interval	T-DXd (N=49)
<b>T-DXd</b>	
At mean $C_{max}$ on Cycle 1	
$\Delta$ QTcF interval	1.3
90%CI	-1.2, 3.8
At mean $C_{max}$ on Cycle 3	
$\Delta$ QTcF interval	1.4
90%CI	-1.1, 3.9
<b>DXd</b>	
At mean $C_{max}$ on Cycle 1	
$\Delta$ QTcF interval	2.7
90%CI	0.1, 5.3
At mean $C_{max}$ on Cycle 3	
$\Delta$ QTcF interval	0.7
90%CI	-1.4, 2.7

in Cycle 3 compared to Cycle 1 by approximately 36%, but not  $C_{max}$ . The  $V_{ss}$  of T-DXd was 60.9 mL/kg at Cycle 1, which was similar to serum volume. DXd exposure was much lower than that of T-DXd, indicating good stability of the T-DXd molecule in systemic circulation. There was little or no accumulation observed for DXd. The concentration-time profile of the total anti-HER2 antibody was similar to that of T-DXd. Three (6.1%) patients had a QTcF increase >30 ms during the study; none had QTcF increases >60 ms. The maximum QTcF value remained below 480 ms. The upper bound of the 90% CI for the observed mean  $\Delta$ QTcF was below 10 ms at all assessed time points, which was the primary endpoint. A trend towards an increase in change in QTcF with increase in concentrations of T-DXd and DXd was observed. However, the relationship between change in QTcF and concentrations of T-DXd was much shallower than that observed for the relationship between change in QTcF and concentrations of DXd. The upper bound of the 90% CI for the relationship between concentrations of DXd and  $\Delta$ QTcF was slightly over 10 ms at the highest concentration of DXd, but not at the point estimate. Estimation of the mean change in QTcF at the mean observed  $C_{max}$  values for both T-DXd and DXd using the linear model equation indicated that the value was less than 10 ms.

**Interpretation, Conclusion or Significance:** Pharmacokinetic parameters after a single dose of T-DXd were consistent with previous studies and moderate accumulation of T-DXd was observed. The upper bound of the 90%CI for  $\Delta$ QTcF at the observed mean  $C_{max}$  for each analyte (T-DXd and DXd) in the linear model of concentration versus  $\Delta$ QTcF for Cycles 1 and 3 was under 10 ms. In conclusion, T-DXd dosed at 6.4 mg/kg Q3W was not associated with clinically relevant QTcF prolongation.

**Poster Number: 013****Pharmacokinetic Profile of Asenapine Transdermal System HP-3070 Secuado®: The First Antipsychotic Patch in the US**

M. Castelli<sup>1</sup>, K. Suzuki<sup>1</sup>, M. Komaroff<sup>1</sup>, C. Zeni<sup>1</sup>, L. Citrome<sup>2</sup>

<sup>1</sup>Noven Pharmaceuticals Inc, Jersey City, NJ, USA;

<sup>2</sup>New York Medical Coll, Valhalla, NY, USA

**Statement of Purpose, Innovation or Hypothesis:** Asenapine transdermal system (HP-3070) was developed to effectively deliver asenapine. HP-3070 is the first antipsychotic patch approved and available in the US for the treatment of adults with schizophrenia. The purpose of this study was to characterize the pharmacokinetic (PK) profile of HP-3070.

**Description of Methods and Materials:** HP-3070 was assessed in three open-label, randomized, Phase 1 studies: a multiple ascending-dose study; a single-center, single-dose, three-way crossover study and a single-center, single-dose, five-period crossover study. These three studies were designed to assess the single-/multiple-dose PK and dose proportionality of HP-3070; the effect of external heat on HP-3070 bioavailability (BA) and the relative BA of HP-3070 versus sublingual asenapine (SLA, Saphris®); and the effects of application sites and race on HP-3070 BA. Studies were conducted in healthy subjects, with the exception of the multiple ascending-dose study that was performed in adults with schizophrenia.

**Data and Results:** After HP-3070 administration, asenapine concentrations increased gradually over time. Asenapine total daily exposure (AUC) for HP-3070 was well within the range of that for SLA, whereas peak exposure ( $C_{max}$ ) for HP-3070 was significantly lower. AUC values of the HP-3070 3.8 mg/24h and 7.6 mg/24h doses corresponded to those of SLA 5 mg and 10 mg BID, respectively. The PK profile for HP-3070 reached steady state in approximately 72 hrs and exhibited low peak-to-trough fluctuations with a  $C_{max}/C_{min}$  ratio of 1.5. The PK of HP-3070 was dose-proportional, was not affected by site of administration and was similar across the ethnic groups studied. The application of external heat increased both the rate and extent of absorption.

**Interpretation, Conclusion or Significance:** Overall, HP-3070 exhibited a consistent, dose-dependent PK profile that was unaffected by site of administration or race. While its AUC was similar to that of SLA, HP-3070 PK had a more predictable absorption profile and lower peak-to-trough fluctuations. Based on these preferable PK characteristics, HP-3070 could address the PK challenges observed with SLA. As the first and only transdermal antipsychotic available in the US, HP-3070 provides patients, caregivers and HCPs

with a novel once-daily treatment formulation for schizophrenia.

**Supported by:** Hisamitsu Pharmaceutical Co Inc

**Poster Number: 014****Pharmacokinetics and Exposure-Response Relationship of Teprotumumab, an Insulin-like Growth Factor-1 Receptor (IGF-1R) Blocking Antibody in Active Thyroid Eye Disease**

Y. Xin<sup>1</sup>, F. Xu<sup>2</sup>, Y. Gao<sup>2</sup>, N. Bhatt<sup>1</sup>, J. Chamberlain<sup>1</sup>, M. Kovalenko<sup>1</sup>, S. Sile<sup>1</sup>, R. Sun<sup>1</sup>, R. Holt<sup>1</sup>, S. Ramanathan<sup>1</sup>

<sup>1</sup>Horizon Therapeutics plc, Lake Forest, IL, USA;

<sup>2</sup>Shanghai Qiangshi Information Technology Co Ltd, Shanghai, China

**Statement of Purpose, Innovation or Hypothesis:** Teprotumumab treatment resulted in statistically- and clinically-meaningful improvements across multiple facets of active thyroid eye diseases (TED) and was generally well tolerated in Phase 2 and 3 trials.<sup>1,2</sup> An initial intravenous infusion of 10 mg/kg followed by 20 mg/kg every 3 wks was selected based on *in vitro* activity and clinical pharmacokinetic (PK) profile, to maintain pharmacologically active exposures and >90% saturation of IGF-1R over dosing intervals and to achieve efficacy at a well-tolerated dose for this vision-threatening disease.

**Description of Methods and Materials:** Population PK analyses were performed on data from a Phase 1 oncology study (n=60)<sup>3</sup> and Phase 2 and 3 studies in Active TED (n=83) and covariate effect on PK was assessed. Exposure-response relationship was evaluated in TED studies for key efficacy endpoints (proptosis response rate, % patients with a clinical activity score value of 0 or 1, and diplopia responder rate) and selected safety variables (hyperglycemia and muscle spasms).

**Data and Results:** Teprotumumab PK was linear in TED patients and consistent with other immunoglobulin G1 monoclonal antibodies (IgG1 mAbs), with low systemic clearance (0.334 L/day), low volume of distribution (3.9 L for central compartment and 4.2 L for peripheral compartment) and long elimination half-life (19.9 days)<sup>4,5</sup>. Model-predicted mean ( $\pm$  standard deviation) steady-state area under the concentration curve ( $AUC_{ss}$ ), peak ( $C_{max,ss}$ ) and trough ( $C_{min,ss}$ ) concentrations in TED patients were 131 ( $\pm$  30.9) mg•hr/mL, 643 ( $\pm$  130)  $\mu$ g/mL and 157 ( $\pm$  50.6)  $\mu$ g/mL, respectively, suggesting low intersubject variability. Population PK analysis indicated no significant impact of baseline age, gender, race, weight, smoking status, renal impairment (mild/moderate) and hepatic function (total bilirubin, aspartate and alanine aminotransferases) on teprotumumab PK. Female patients had 15% higher

$C_{\max,ss}$  but similar AUC compared to male patients, which is not considered clinically relevant. Exposure-response analysis from the TED dose regimen indicated no meaningful correlations between exposures ( $AUC_{ss}$ ,  $C_{\max,ss}$  and  $C_{\min,ss}$ ) and key efficacy endpoints or selected safety variables, supporting the demonstrated, favorable benefit-risk profile of the TED dose regimen.<sup>2</sup>

**Interpretation, Conclusion or Significance:** Teprotumumab PK was characterized in TED patients by long elimination half-life, low systemic clearance and low volume of distribution, consistent with other IgG1 mAbs. There was no meaningful exposure-response relationship at the selected TED dose regimen for both efficacy and safety endpoints, supporting the teprotumumab dose regimen used in TED patients.

#### References

1. Smith TJ, et al. *N Engl J Med* 2017;376:1748-1761.
2. Douglas RS, et al. AACE 2019 late-breaking abstract.
3. ClinicalTrials.gov: NCT00400361.
4. Dirks NL et al. *Clin Pharmacokinet.* 2010;49(10):633-59.
5. Ryman JT et al. *CPT Pharmacometrics Syst Pharmacol.* 2017;6(9):576-88.

**Encore:** Presented at the Endocrine Society Meeting, March, 2020; Published in the *Journal of the Endocrine Society*, Vol. 4, Issue Supplement\_1, April-May 2020.

#### Poster Number: 015

##### Effects of Different Meal Types on Pexidartinib Pharmacokinetics in Healthy Subjects

H. Zahir<sup>1</sup>, W. Tap<sup>2</sup>, H. Gelderblom<sup>3</sup>, S. Stacchiotti<sup>4</sup>, A. J. Wagner<sup>5</sup>, C. Hsu<sup>6</sup>, F. LaCreta<sup>1</sup>, T. Kakkar<sup>1</sup>

<sup>1</sup>Daiichi Sankyo Inc, Basking Ridge, NJ, USA; <sup>2</sup>Memorial Sloan Kettering Cancer Ctr, New York, NY, USA; <sup>3</sup>Leiden Univ Medical Ctr, Leiden, The Netherlands; <sup>4</sup>Fondazione IRCCS Istituto Nazionale dei Tumori, Milan, Italy; <sup>5</sup>Dana-Farber Cancer Inst, Boston, MA, USA; <sup>6</sup>Daiichi Sankyo Inc, Basking Ridge, NJ, USA

**Statement of Purpose, Innovation or Hypothesis:** Pexidartinib, a novel, orally-administered, small molecule kinase inhibitor with selective activity against colony-stimulating factor-1 receptor, is approved in the United States for treatment of adult patients with symptomatic tenosynovial giant cell tumor (TGCT) that is associated with severe morbidity or functional limitations and is not amenable to improvement with surgery. Pexidartinib has a Risk Evaluation and Mitigation Strategy (REMS) program to mitigate the risk of serious and potentially fatal hepatotoxicity. Here we present results from four separate studies conducted to evaluate the effect of food (i.e., high- or low-fat meal) on pexidar-

tinib pharmacokinetics (PK) in healthy subjects; these results provide the basis for the currently approved labeling that pexidartinib be taken on an empty stomach.

**Description of Methods and Materials:** Healthy subjects received single doses of pexidartinib in three open-label, randomized, crossover studies at doses ranging from 200–600 mg. In an additional study, healthy subjects received high doses of pexidartinib (1200 mg and 1800 mg) in a single sequence in fasted and fed conditions. The objective of each study was to determine the effect of food on pexidartinib PK. Subjects received single doses of pexidartinib under fasting conditions (10 hrs overnight fast) or within 30 mins after a high-calorie (800–1000 Kcal), high-fat (~50% of calories from fat) meal or a low-calorie (400–500 Kcal), low-fat meal (~25% of calories from fat). Plasma samples were assayed using a validated liquid chromatography/mass spectrometry/mass spectrometry method. Pharmacokinetic parameters were calculated with actual dosing and sampling time points using a noncompartmental approach in WinNonlin<sup>®</sup>.

**Data and Results:** Overall, 121 subjects received pexidartinib across the four studies and were included in the analysis (Table 1). Pexidartinib peak (maximum plasma concentration [ $C_{\max}$ ]) and total (area under the plasma concentration time curve [AUC]) increased from 400 mg to 1800 mg. When pexidartinib was administered after a high-fat meal, there was an approximate doubling of  $C_{\max}$  and AUC compared with the fasted state for doses ranging from 400 mg to 1800 mg. When pexidartinib was administered (200 mg and 400 mg) with a low-fat meal, exposure increased by approximately 60% (Table 1). When administered with food (irrespective of meal type), median time to maximum plasma drug concentration ( $T_{\max}$ ) was delayed by approximately 2.5 hrs (from 2.5 hrs to 5.0 hrs). Pexidartinib was generally well tolerated in healthy subjects and the safety profile was consistent across studies.

**Interpretation, Conclusion or Significance:** Administering pexidartinib after a high-fat meal resulted in an approximate doubling (i.e., 100% increase) of pexidartinib exposure when compared to administering pexidartinib in a fasted state, while a low-fat meal increased pexidartinib exposure by approximately 60%. The presence of food increases pexidartinib exposure and may increase the risk of hepatotoxicity; therefore, pexidartinib should be taken on an empty stomach, at least 1 hr before or 2 hrs after a meal or snack. These dosing instructions support a positive benefit/risk profile for TGCT patients defined in the indication section of the labeling. Patients must follow labeling recommendations and only take pexidartinib on an empty stomach, as outlined in the product label.

**Encore:** Presented at the Annual Meeting of the American Society for Clinical Pharmacology and Therapeutics, March 2018.

**Poster Number: 015 Table 1. Effects of a High-fat and Low-fat Meal on Pexidartinib Pharmacokinetics**

Pexidartinib Dose	Geometric LSMean <sup>a</sup>		Ratio of Geometric Mean [Fed/fasted], %(90% CI for Ratio)
	Fasted	Fed	
<b>High-fat Meal</b>			
400 mg (n = 29)			
C <sub>max</sub> , ng/mL	3,150	6,235	197.9 (176.6, 221.8)
AUC <sub>last</sub> , ng•h/mL	50,262	106,085	211.1 (191.9, 232.2)
AUC <sub>inf</sub> , ng•h/mL	51,070	107,304	210.1 (191.0, 231.1)
600 mg (n = 27)			
C <sub>max</sub> , ng/mL	3,025	4,631	153.1 (114.5, 204.7)
AUC <sub>last</sub> , ng•h/mL	55,675	106,360	191.0 (145.5, 250.8)
AUC <sub>inf</sub> , ng•h/mL	57,733	108,822	188.5 (144.0, 246.7)
1200 mg (n = 8)			
C <sub>max</sub> , ng/mL	7,746	14,688	189.6 (142.2, 252.8)
AUC <sub>last</sub> , ng•h/mL	135,517	292,997	216.2 (169.0, 276.7)
AUC <sub>inf</sub> , ng•h/mL	137,696	296,422	215.3 (168.1, 275.7)
1800 mg (n = 9)			
C <sub>max</sub> , ng/mL	10,947	20,576	188.0 (159.6, 221.4)
AUC <sub>last</sub> , ng•h/mL	207,293	465,658	224.6 (200.8, 251.4)
AUC <sub>inf</sub> , ng•h/mL	211,071	471,459	223.4 (199.8, 249.7)
<b>Low-fat Meal</b>			
200 mg <sup>b</sup> (n = 24)			
C <sub>max</sub> , ng/mL/mg	2,219	3,799	171.2 (160.3, 182.7)
AUC <sub>last</sub> , ng•h/mL/mg	31,017	51,710	166.7 (153.9, 180.6)
AUC <sub>inf</sub> , ng•h/mL/mg	31,620	52,584	166.3 (153.6, 180.1)
400 mg (n = 24)			
C <sub>max</sub> , ng/mL	4,438	6,904	155.6 (146.2, 165.5)
AUC <sub>last</sub> , ng•h/mL	62,035	98,905	159.4 (146.8, 173.2)
AUC <sub>inf</sub> , ng•h/mL	63,240	100,374	158.7 (146.2, 172.3)

AUC<sub>last</sub>, area under the plasma concentration time curve from time 0 to the last quantifiable dose; AUC<sub>inf</sub>, area under the plasma concentration time curve from time 0 extrapolated from the last time to infinity; CI, confidence interval; C<sub>max</sub>, maximum plasma concentration; LSMean, least squares mean.

<sup>a</sup> Geometric least squares mean from ANOVA, calculated by transforming the natural log means back to the linear scale (i.e., geometric least squares mean).

<sup>b</sup> Individual exposure parameters for the fasted state were derived by dose-normalizing the exposure parameters of 400 mg pexidartinib in the fasted state to 200 mg.

### Poster Number: 016

#### Influence of Rheumatoid Factor and Anti-citrullinated Protein Antibodies on the Pharmacokinetics of IgG-based Therapeutic Proteins

Y. Xu<sup>1</sup>, Y. Chen<sup>1</sup>, J. Leu<sup>1</sup>, Y. Zhuang<sup>1</sup>, S. Sheng<sup>1</sup>, Y. Liu<sup>1</sup>, P. Agarwal<sup>1</sup>, H. Zhou<sup>1</sup>, Z. Xu<sup>1</sup>

<sup>1</sup>Janssen Research & Development LLC, Spring House, PA, USA

#### Statement of Purpose, Innovation or Hypothesis:

Rheumatoid factor (RF) and anti-citrullinated protein antibodies (ACPA) are autoantibodies that are directed against the Fc portion of the immunoglobulin G (IgG) and the peptides and proteins that are citrullinated, respectively. High levels of RF and ACPA in the blood are often associated with autoimmune diseases, such as rheumatoid arthritis (RA). Rheumatoid factor (RF) and ACPA may have an impact on the pharmacokinetics (PK) of IgG-based therapeutic proteins

since they may form a complex with the therapeutic proteins leading to an accelerated clearance. However, this hypothesis has not been investigated or reported in the literature. To understand the effect of RF and ACPA on the PK of therapeutic monoclonal antibodies (mAbs), we have conducted a retrospective analysis using sirukumab and golimumab (human IgG monoclonal antibodies [mAbs] targeting interleukin-6 [IL-6] and tumor necrosis factor [TNF], respectively) as case examples.

**Description of Methods and Materials:** Correlation analyses were conducted to explore the relationships between baseline serum RF or ACPA levels and the serum drug concentrations of sirukumab and golimumab using data from four Phase 3 trials in patients with active RA, i.e., pooled data from studies (SIRROUND-D and SIRROUND-T) with sirukumab, and from studies (GO-BEFORE and GO-FORWARD) with golimumab, respectively. Distribution of the steady-state serum drug concentrations versus the baseline RF

and ACPA status were explored and summarized for each drug.

**Data and Results:** Based on the distribution plots and the descriptive analyses of the pooled data, weak correlations were observed between serum drug concentration and the serum RF and ACPA levels, where patients with higher RF or ACPA levels tended to have lower median drug exposures. The median serum sirukumab trough concentrations at steady state were approximately 20–22% lower in subjects who were positive for RF (i.e., RF  $\geq$  15 IU/mL) compared to subjects with negative RF, and approximately 12–20% lower in subjects who were positive for ACPA (i.e., ACPA  $\geq$  20 IU/ml) versus subjects with negative ACPA levels. Similar trends were also observed between serum golimumab trough concentrations at steady state and the baseline RF or ACPA levels. Rheumatoid arthritis patients with higher ACPA tended to have higher RF levels. For both sirukumab and golimumab trials, lower median drug exposures were observed for patients who were higher in both RF and ACPA levels compared to the single positive condition, though these results were limited by the small sample size of RF and ACPA double negative or single negative populations.

**Interpretation, Conclusion or Significance:** Our analyses indicate that RF and ACPA may affect the PK of IgG mAbs, where patients with higher RF and/or ACPA levels tend to have lower drug exposure. In addition, there is a potential of a combined RF and ACPA effect on the PK of mAbs, though data may be limited by the small sample size. Further work is needed to understand the effect of RA or ACPA on the PK of other IgG-based biologics and whether the resultant decreased drug exposure may subsequently influence drug efficacy.

**Poster Number: 018**

**Olorinab (APD371), a Highly-selective and Peripherally-acting Full Agonist of the Cannabinoid Receptor 2 (CB2), Pharmacokinetics and Safety in Healthy Adults**

K. Stauber<sup>1</sup>, D. Oh<sup>1</sup>, B. Lindstrom<sup>1</sup>, B. A. English<sup>1</sup>, C. H. Cabell<sup>1</sup>, J. Ruckle<sup>2</sup>, S. Searle<sup>3</sup>, J. Kam<sup>4</sup>, R. W. Jones<sup>5</sup>, J. S. Grundy<sup>1</sup>

<sup>1</sup>Arena Pharmaceuticals Inc, San Diego, CA, USA;

<sup>2</sup>Pacific Pharma Group LLC, Tacoma, WA, USA;

<sup>3</sup>PRA Health Sciences, Salt Lake City, UT, USA;

<sup>4</sup>Covance, Dallas, TX, USA; <sup>5</sup>Colorado Clinic, Aurora, CO, USA

**Statement of Purpose, Innovation or Hypothesis:** Olorinab is currently under investigation for the treatment of abdominal pain associated with irritable bowel syndrome and inflammatory bowel disease. The purpose of this study was to evaluate the safety and phar-

macokinetics (PK) of single and multiple doses of olorinab in healthy adults.

**Description of Methods and Materials:** Healthy adult subjects (18–45 yrs of age) were randomly assigned to receive orally-administered olorinab either one time (10, 20, 30, 60, 120, 250 or 400 mg) in a single ascending-dose (SAD) study (6:2 active: placebo at each dose) or three times daily (TID) for ten days and once on day 11 (50, 100 or 200 mg) in a multiple ascending-dose (MAD) study (9:3 active: placebo at each dose). Pharmacokinetic analyses of olorinab and its metabolites (M1–M5 in SAD and M1, M2 and M4 in MAD) were performed on plasma and urine samples using validated liquid chromatography-mass spectrometry methods. The safety of olorinab was assessed based on adverse events (AEs), clinical laboratory tests, vital signs, physical examinations, 12-lead safety electrocardiograms (ECGs) and continuous telemetry (5-lead ECG).

**Data and Results:** The systemic exposure of olorinab increased with increasing doses, but less than dose proportionally in both studies (per maximum plasma concentration and area under the curve). Furthermore, there was no accumulation of olorinab following repeated dosing in the MAD study. Across both studies, the median time to maximum concentration of olorinab ranged from 1 to 4 hrs after administration, whereas the mean half-life ranged from 3 to 5 hrs. Urinary excretion of olorinab was low. Metabolites M1, M2 and M4 were the predominant circulating metabolites, with systemic exposures increasing with the dose of olorinab. Both studies support the tolerability of olorinab in healthy adults, with AEs occurring in  $\leq$ 45% of subjects administered any dose of olorinab and  $\leq$ 33% of subjects receiving placebo in either study; AEs were mild in 91% and 100% of cases in the SAD and MAD studies, respectively, and none were serious.

**Interpretation, Conclusion or Significance:** Olorinab had a favorable safety and PK profile in healthy adult subjects and may represent a novel treatment option for abdominal pain management without use-limiting psychoactive effects.

**Additional Author:** Yong Q. Tang (affiliation: Arena Pharmaceuticals Inc, San Diego, CA, USA)

**Encore:** Published in *Clinical Pharmacology & Therapeutics*, Vol 107, March 2020.

**Poster Number: 019**

**Effect of Mild and Moderate Hepatic Impairment (defined by Child Pugh [CP] Classification) on Pexidartinib Pharmacokinetics**

H. Zahir<sup>1</sup>, J. Greenberg<sup>1</sup>, T. Marbury<sup>2</sup>, K. Lasseter<sup>3</sup>, L. Xu<sup>1</sup>, F. LaCreta<sup>1</sup>, T. Kakkar<sup>1</sup>

<sup>1</sup>Daichi Sankyo Inc, Basking Ridge, NJ, USA;

<sup>2</sup>Orlando Clinical Research Ctr, Orlando, FL, USA;

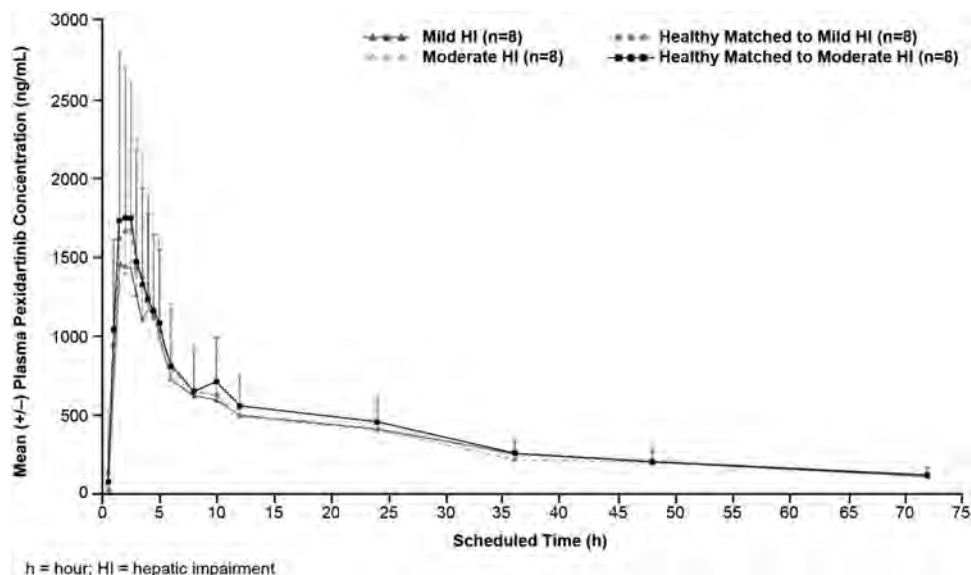
<sup>3</sup>Clinical Pharmacology of Miami, Miami, FL, USA

**Statement of Purpose, Innovation or Hypothesis:** Pexidartinib is a novel, oral, small-molecule tyrosine kinase inhibitor targeting the colony stimulating factor 1 receptor. Pexidartinib undergoes extensive hepatic metabolism via multiple cytochrome P450 and uridine 5'-diphospho-glucuronosyl transferase (UGT) enzymes. ZAAD-1006a, an N-glucuronide, is the only major metabolite in human plasma. As pexidartinib is extensively metabolized, there is potential that hepatic impairment (HI) may lead to increased exposure of pexidartinib in HI. The objective was to determine the pharmacokinetics (PK) of pexidartinib after a single 200 mg dose in subjects with mild and moderate HI compared to healthy subjects.

**Description of Methods and Materials:** This was a Phase 1, open-label, single-dose PK study conducted in subjects with mild (CP A classification, n=8) and moderate (CP B classification, n=8) HI and matched controls (healthy subjects with normal hepatic function, n=16) according to sex, age ( $\pm 10$  yrs) and body mass index ( $\text{kg}/\text{m}^2 \pm 15\%$ ). A single 200 mg dose of pexidartinib was administered following an overnight fast of  $\geq 10$  hrs. Subjects continued to fast for four hrs after dosing. Blood samples were collected for PK analysis of pexidartinib and ZAAD-1006a at predose through 168 hrs postdose. Samples were analyzed by a validated LC-MS/MS method for pexidartinib and by a qualified LC-MS/MS method for ZAAD-1006a. Primary endpoints included maximum observed concentration ( $C_{\text{max}}$ ), area under the plasma concentration-time curve (AUC) extrapolated to infinity ( $\text{AUC}_{\text{inf}}$ ) and AUC up to the last measurable concentration ( $\text{AUC}_{\text{last}}$ ). Pharmacokinetic parameters were compared using ANOVA analysis.

**Data and Results:** Following oral administration, maximum concentration of pexidartinib generally appeared at 2.5 hrs post dose (Figure 1). Exposure to pexidartinib ( $C_{\text{max}}$ ,  $\text{AUC}_{\text{last}}$  and  $\text{AUC}_{\text{inf}}$ ) was similar in subjects with mild and moderate HI and respective matched controls (Table 1). The percentage ratios of the geometric least square (LS) mean  $\text{AUC}_{\text{inf}}$  values were 109% (90% CI: 73.8%, 160%) and 99.6% (90% CI: 74.0%, 134%) in subjects with mild and moderate HI, respectively. Mean  $C_{\text{max}}$  of ZAAD-1006a was similar for subjects with mild HI and normal hepatic function, but was higher for subjects with moderate hepatic impairment than for matched controls.  $\text{AUC}_{\text{inf}}$  of ZAAD-1006a was higher for subjects with mild HI (28% higher) and moderate HI (49% higher) compared to control groups, as was the metabolite-to-parent (M/P) molar ratio of area under the concentration-time curve (AUC) (up to 42% higher). This may be due to increased UGT activity in the viable part of the liver or upregulation of the extrahepatic UGTs. Plasma protein binding of pexidartinib was similar (mean protein binding  $>99.96\%$ ) in subjects with normal hepatic function and subjects with mild to moderate HI. Pexidartinib was well tolerated and demonstrated a safety profile consistent with previous findings. This study had only two moderate HI subjects according to the National Cancer Institute (NCI) Organ Dysfunction Working Group (ODWG) criteria. The sponsor is conducting an additional study in subjects with moderate HI as defined by NCI criteria.

**Interpretation, Conclusion or Significance:** This study demonstrated that mild to moderate HI (defined by CP classification) does not affect the PK of pexidartinib. No pexidartinib dose adjustment is recommended for



**Poster Number: 019** Figure 1. Mean Plasma Pexidartinib Concentrations in Subjects With Mild and Moderate Hepatic Impairment and Normal Hepatic Function

**Poster Number: 019 Table 1. Statistical Comparison (using ANOVA) of Exposure Parameters of Pexidartinib and ZAAD-1006a (Subjects With Mild Hepatic Impairment versus Matching Controls and Subjects With Moderate Hepatic Impairment and Matching Controls)**

PK Parameter (unit)	Geometric LS Means		Ratio of Geometric LS Means (%) <sup>a</sup>	90% CI for Ratio (%)	Geometric LS Means		Ratio of Geometric LS Means (%)	90% CI for Ratio (%)
	Mild HI n = 8	Normal = 8			Moderate HI = 8	Normal n = 8		
<b>Pexidartinib</b>								
C <sub>max</sub> (ng/mL)	1449	1655	87.6	51.7, 148	1566	1722	91.0	51.3, 161
AUC <sub>last</sub> (ng·h/mL)	29,010	26,810	108	73.6, 159	29,778	30,534	97.5	73.7, 129
AUC <sub>inf</sub> (ng·h/mL)	29,989	27,641	109	73.8, 160	31,212	31,341	99.6	74.0, 134
<b>ZAAD-1006a</b>								
C <sub>max</sub> (ng/mL)	1650	1780	92.7		1960	1690	116	
AUC <sub>last</sub> (ng·h/mL)	61,500	48,400	127		67,400	47,700	141	
AUC <sub>inf</sub> (ng·h/mL)	63,500	49,800	128		72,300	48,700	149	

AUC<sub>inf</sub> = area under the plasma concentration-time curve from time of dosing extrapolated to infinity; AUC<sub>last</sub> = area under the plasma concentration-time curve from time 0 to the time of the last quantifiable measurement; CI = confidence interval; C<sub>max</sub> = maximum observed plasma concentration; h = hour; LS = least squares; n = number of subjects.

Notes: The model was performed on logarithm-transformed PK parameters including study group as a factor. The geometric LS means presented are LS means from the model with back transformation to the original scale.

<sup>a</sup>Ratio = geometric LS mean (mild/moderate)/geometric LS mean (normal).

<sup>b</sup>The 90% CIs are presented after back transformation to the original scale.

subjects with mild to moderate HI on the basis of PK alone.

#### Poster Number: 020

##### Pharmacokinetic Study of Colchicine in Oral Solution (0.6 mg) and Exposure Comparison With Probenecid/Colchicine Tablets USP Under Fasted and Fed Condition in Healthy Adult Subjects

J. Yin<sup>1</sup>, N. Vishnupad<sup>2</sup>, M. Willett<sup>1</sup>, J. Lederman<sup>1</sup>, D. Fan<sup>3</sup>, P. Guo<sup>3</sup>, J. Lin<sup>3</sup>, L. Diamond<sup>1</sup>, I. Muni<sup>2</sup>

<sup>1</sup>Frontage Clinical Svcs Inc, Secaucus, NJ, USA;

<sup>2</sup>Romeg Therapeutics LLC, Woburn, MA, USA;

<sup>3</sup>Frontage Laboratories Inc, Exton, PA, USA

##### Statement of Purpose, Innovation or Hypothesis:

Colchicine was used for treatment of familial Mediterranean fever and acute flares of gout approved by the US Food & Drug Administration (FDA) in 2009. Colchicine oral solution was developed with dosage form flexibility and for patients with difficulty of swallowing colchicine oral tablets and approved by the FDA in 2019. The objective of the study was to evaluate the pharmacokinetics of colchicine oral solution, determine the relative bioavailability of colchicine oral solution, 0.6 mg and Probenecid and Colchicine Tablets USP, 500 mg/0.5 mg under fasted conditions and to assess the effect of food on the absorption of colchicine oral solution under fed versus fasted conditions.

**Description of Methods and Materials:** This was an open-label, single-dose, randomized, three-period, crossover design study to evaluate the relative bioavailability of a single oral dose of colchicine oral solution (0.6 mg) and a single oral dose of one Probenecid

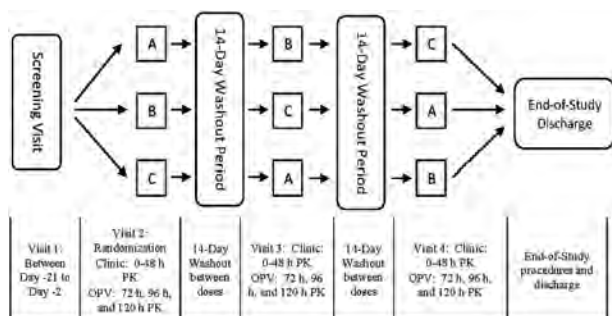
and Colchicine tablets USP, 500 mg/0.5 mg under fasted conditions in healthy subjects. Furthermore, the study evaluated the food effect of a single oral dose of colchicine oral solution, 0.6 mg under fed and fasted conditions. Pharmacokinetic (PK) parameters for colchicine including C<sub>max</sub>, T<sub>max</sub>, AUC<sub>0-t</sub>, AUC<sub>0-inf</sub>, K<sub>el</sub> and t<sub>1/2</sub> were calculated using a noncompartmental analysis method by Phoenix<sup>®</sup> WinNonlin. Log transformed PK parameters dose normalized AUC<sub>0-t</sub>, AUC<sub>0-inf</sub>, and C<sub>max</sub> were analyzed for bioavailability and food effect using an analysis of variance (ANOVA) model by SAS<sup>®</sup> v9.3.

**Data and Results:** Pharmacokinetic results of colchicine are summarized in Table 1. Similar plasma PK profiles suggest that colchicine absorption in the oral solution was similar to the probenecid and colchicine tablet formulation. Median T<sub>max</sub> for the oral solution was the same as the tablet formulation (1 hr). The apparent terminal half-life (31 hrs) of colchicine oral solution was also similar to the tablet formulation (30 hrs). Dose-normalized colchicine mean C<sub>max</sub> for colchicine oral solution (3.60 ng/mL) was similar to the dose-normalized C<sub>max</sub> for probenecid and colchicine tablet (3.66 ng/mL). Dose-normalized colchicine mean AUC<sub>0-t</sub> for colchicine oral solution (31.0 h\*ng/mL) was similar to that of probenecid and colchicine tablet (30.9 h\*ng/mL). In the fed state, median T<sub>max</sub> increased to 2 hrs compared to 1 hr in the fasted state. Mean C<sub>max</sub> was 78.0% when comparing fed state to fasted state. Mean AUC<sub>0-t</sub> was 92.5% when comparing fed state to fasted state.

**Interpretation, Conclusion or Significance:** In healthy adults, colchicine in oral solution reached a mean C<sub>max</sub> of 2.16 ± 0.87 ng/mL in 1 hr (range 0.5 to 2 hrs)

**Poster Number: 020 Table 1. Mean Pharmacokinetic Parameters of Colchicine in Healthy Adults**

Parameter	Statistic	Colchicine Oral Solution, 0.6 mg Fasted (N=34)	Colchicine Oral Solution, 0.6 mg Fed (N=34)	Probenecid and Colchicine Tablets USP, Fasted (N=34)
AUC <sub>0-t</sub> (h*ng/mL)	Mean (SD)	18.59 (4.635)	17.20 (4.231)	15.54 (5.021)
AUC <sub>0-inf</sub> (h*ng/mL)	Mean (SD)	19.90 (4.736)	18.47 (4.290)	16.70 (4.988)
C <sub>max</sub> (ng/mL)	Mean (SD)	2.161 (0.8741)	1.685 (0.3945)	1.828 (0.7096)
T <sub>max</sub> (h)	Median (Min-Max)	1.000 (0.5: 2)	2.000 (1: 4)	1.000 (0.5: 1.8)
T <sub>1/2</sub> (h)	Mean (SD)	31.00 (6.090)	30.56 (5.218)	31.18 (6.789)
Kel (1/h)	Mean (SD)	0.0232 (0.0049)	0.0233 (0.0036)	0.0231 (0.0046)

**Poster Number: 020 Figure 1. Study Design Scheme**

after a single dose administered under fasting conditions. The comparisons of colchicine exposure (dose normalized C<sub>max</sub>, AUC<sub>0-t</sub> and AUC<sub>0-inf</sub>) between the oral solution and the tablet satisfied the bioequivalence criteria as C<sub>max</sub>, AUC<sub>0-t</sub> and AUC<sub>0-inf</sub> GMRs were fully contained within the 80 to 125% boundaries. The study showed that a minimum food effect was observed when colchicine oral solution was administered following a high fat high calorie meal.

**Poster Number: 021****Clinical Pharmacokinetics and Response Assessments of the Novel Anti-EGFRvIII BiTE<sup>®</sup> (Bispecific T-Cell Engager) AMG 596 In Patients With Glioblastoma**

J. Kast<sup>1</sup>, M. Bose<sup>1</sup>, K. Mehta<sup>1</sup>, S. Stienen<sup>2</sup>, S. Dutta<sup>3</sup>, V. Upreti<sup>1</sup>

<sup>1</sup>Amgen Inc, South San Francisco, CA, USA; <sup>2</sup>Amgen Inc, Munich, Germany; <sup>3</sup>Amgen Inc, Thousand Oaks, CA, USA

**Statement of Purpose, Innovation or Hypothesis:** Glioblastoma (GBM) is an aggressive brain tumor with extremely poor prognosis. Median overall survival is 9 mos for patients with recurrent glioblastoma and there is an unmet need for new treatment options. The investigational drug AMG 596 is a novel BiTE<sup>®</sup> (Bispecific T cell Engager) immune therapy that engages patients own T cells to kill EGFRvIII-expressing GBM cells. We report preliminary clinical pharmacokinetic (PK) and

response data of continuously infused AMG 596 in patients with EGFRvIII-positive GBM from the dose escalation phase of the trial.

**Description of Methods and Materials:** In this ongoing Phase 1 open-label, sequential dose-escalation/expansion study, patients received AMG 596 as continuous infusion at constant flow rate for seven-day on/seven-day off cycles or for 28-day on/14-day off cycles, until confirmed disease progression per modified Response Assessment in Neuro-Oncology Criteria (RANO) criteria or treatment discontinuation due to adverse events. Serum PK results are reported for dose cohorts between 4.5 and 1000 µg/day. Mean steady-state serum concentrations (C<sub>ss</sub>) for the 1<sup>st</sup> cycle were calculated by averaging the exposures from 24 hrs until the end of infusion duration. Population PK were described using nonlinear mixed effects modeling.

**Data and Results:** Preliminary PK data are presented for 18 patients (56% male, median age 55 [44–69] yrs) with recurrent GBM that were enrolled in the dose escalation phase. The AMG 596 PK was best described by a one-compartment linear PK model. Mean C<sub>ss</sub> values for the seven-day infusion group were 0.95 and 1.1 ng/mL at doses of 4.5 and 15 µg/day. Mean C<sub>ss</sub> values for the 28-day infusion group were 2.0, 3.7, 9.5, 26 and 53 ng/mL at doses of 15, 45, 150, 500 and 1,000 µg/day, respectively. As of September 16, 2019, no grade ≥4 treatment-emergent adverse events were reported. One patient exhibited a sustained confirmed partial response (PR) after five treatment cycles with a mean C<sub>ss</sub> of 2.3 ng/mL in cycle 1 after receiving 15 µg/day. One patient received an initial dose of 1,500 µg/day (mean C<sub>ss</sub>: 52 ng/mL) and received a 15 µg/day dose in the remaining cycle 1 (mean C<sub>ss</sub>: 0.72 ng/mL) and cycle 2. This patient exhibited an initial 54.6% tumor shrinkage qualifying for PR after cycle 1, which was ultimately unconfirmed as subsequent scans showed stable disease followed by progressive disease. Four additional patients who achieved C<sub>ss</sub> levels of 3.3, 3.5, 22 and 60 ng/mL had stable disease, eleven patients had progressive disease at varying C<sub>ss</sub> and for one patient response assessment was not available at time of analysis.

**Interpretation, Conclusion or Significance:** Glioblastoma patients treated with AMG 596 by continuous intravenous infusion achieved steady-state exposures rapidly (within 1 to 2 days of the start of treatment), consistent with its relatively short terminal elimination half-life. The AMG 596 steady-state serum exposures in patients with GBM increased approximately dose-proportionally across all cohorts in a predictable manner and were well described by a one-compartment population PK model. Preliminary evidence for AMG 596 antitumor activity was observed at dose levels evaluated. Intersubject differences in blood-brain barrier penetration of AMG 596 potentially contribute to observed response variability at evaluated dose cohorts.

**Poster Number: 022**

**A Phase 1 Healthy Volunteer Study of the Safety, Tolerability and Pharmacokinetics of TRV250, A G Protein-selective Delta Receptor Agonist**

M. A. Demitrack<sup>1</sup>, M. S. Kramer<sup>1</sup>, K. Arscott<sup>1</sup>, I. A. James<sup>2</sup>, M. J. Fossler, Jr.<sup>1</sup>

<sup>1</sup>Trevena Inc, Chesterbrook, PA, USA; <sup>2</sup>Consultant, Chesterbrook, PA, USA

**Statement of Purpose, Innovation or Hypothesis:** The delta opioid receptor (DOR) has been implicated in an array of neuronal processes of relevance to major central nervous system disorders. For example, DOR agonists have demonstrated activity in nonclinical models of migraine, nociceptive, inflammatory and neuropathic pain, depression and anxiety. Studies in rats and monkeys evaluating abuse potential for DOR ligands suggest that these agonists may not demonstrate high abuse liability. Functional activity at the DOR has been linked to the calcitonin gene related peptide (CGRP), which is thought to play a role in migraine. Diffuse dural innervation peptidergic CGRP-expressing C fibers co-express the DOR, suggesting that DOR agonists could exert antimigraine effects by inhibition of CGRP release, providing a novel therapy for the treatment of migraine. Attempts at development of a DOR agonist has been hampered by on-target convulsant effects. Data suggest that  $\beta$ -arrestin2 recruitment plays a critical role in DOR-mediated convulsions. Hence, a potent DOR agonist with reduced  $\beta$ -arrestin2 recruitment could offer an improved therapeutic index over previous candidates in this class TRV250 is a novel small molecule agonist of the DOR that acts in a manner preferentially selective for G-protein signaling, with relatively little activation of the  $\beta$ -arrestin2 post-receptor signaling pathway. TRV250 significantly reduces nitroglycerin-evoked hyperalgesia in rodents, a model of acute migraine and is being developed for the acute treatment of migraine in humans.

Nonclinical studies indicate that TRV250 shows a substantial reduction in pro-convulsant activity compared to other, non-G protein-selective DOR agonists.

**Description of Methods and Materials:** This was a two-part, single ascending-dose study. Part A included four cohorts of healthy adults (n=38). Each cohort was dosed on three occasions (placebo and two different dose levels of TRV250, allocated in randomized order and administered by subcutaneous route). In part B, a single cohort (n=9) of subjects received an oral dose administration of either TRV250 or placebo in a fed or fasted state. Serial blood samples were obtained for pharmacokinetic determination across a 24-hrs post-dose period. Safety assessments included clinical laboratory measures, vital signs, 12-lead ECGs and electroencephalograms pre- and postdosing.

**Data and Results:** TRV250 was well tolerated in both study parts. There were no serious adverse events, and all treatment-related adverse events were mild in severity. There were no clinically-significant changes in any safety parameters. Specifically, no subject experienced abnormalities in EEGs, and no subject experienced a change from baseline in rate-corrected QT interval (QTcF) greater than 60 msec, or an absolute QTcF interval greater than 480 msec at any postdosing observation. Peak and total plasma exposure to TRV250 increased in a dose-proportional manner following 0.1 to 30 mg subcutaneous (SC) doses, with the mean half-life ranging from 2.39 to 3.76 hrs. Oral bioavailability of TRV250 ranged from 14% (fasting) to 20% (fed) relative to SC dosing, while administration with food reduced the rate of absorption as reflected by a modest delay in median  $T_{max}$  and a slight reduction in  $C_{max}$ .

**Interpretation, Conclusion or Significance:** In this First-in-Human study, TRV250, a G protein-selective DOR agonist, showed safety, tolerability and a pharmacokinetic profile supporting its potential use in the treatment of acute migraine.

**Encore:** Presented at the Annual Meeting of the American College of Neuropsychopharmacology, December, 2019.

**Poster Number: 023**

**Relative Bioavailability, Food Effect and Intra-subject Variability of Cenobamate, a Newly-approved Antiepileptic Drug for the Treatment of Focal (Partial-onset) Seizures**

S. A. Greene<sup>1</sup>, L. Orlinski<sup>1</sup>, K. Glenn<sup>1</sup>, L. Vernillet<sup>1</sup>

<sup>1</sup>SK Life Science Inc, Paramus, NJ, USA

**Statement of Purpose, Innovation or Hypothesis:** A clinical study was conducted in healthy subjects using three cohorts to assess the intra-subject variability (ISV), food effect (FE) and relative bioavailability (BA) of a single oral dose of cenobamate.

**Description of Methods and Materials:** Pharmacokinetic (PK) parameters (AUC and  $C_{max}$ ) of cenobamate were estimated for all cohorts using Phoenix<sup>®</sup> WinNonlin (v7.0). Geometric mean ratios (GMRs) and 90% confidence intervals (CIs) were calculated for each cohort to assess the difference between formulations or fed status. Treatment was considered bioequivalent if 90% CIs were within the 0.80 to 1.25 reference range. Cohort 1 (18 subjects) and Cohort 3 (24 subjects) were enrolled to assess the relative BA of 200 mg (Cohort 1) or 100 mg (Cohort 3) of cenobamate as a 2x100 mg or 1x200 mg (Cohort 1) and 2x50 mg or 1x100 mg (Cohort 3), respectively (two-way crossover in fasting condition). Cohort 2 included FE and ISV assessments with a 200 mg cenobamate tablet. Eighteen subjects were randomized to one of six sequences (three-way crossover), including one cenobamate administration in fasting condition on two occasions (ISV) or one cenobamate administration in fed condition.

**Data and Results:** For Cohort 1,  $C_{max}$  and AUC GMRs (90% CI) were 1.0101 (0.95925–1.0636) and 0.98197 (0.94016–1.0256) for the comparison between 1x200 mg and 2x100 mg. For Cohort 2,  $C_{max}$  and AUC GMRs (90% CI) were 0.90220 (0.85305–0.95419) and 0.98250 (0.95225–1.0137) for the comparison between 200 mg dose under fed versus fasted conditions. For Cohort 3,  $C_{max}$  and AUC GMRs (90% CI) were 0.99617 (0.92912–1.0681) and 0.97987 (0.95110–1.0172) for the comparison between 1x100 mg to 2x50 mg. The ISV of 200-mg cenobamate tablet (Cohort 2) was 13.7% for  $C_{max}$  and 4.61% for AUC. Cenobamate administration was safe and well tolerated across all cohorts.

**Interpretation, Conclusion or Significance:** From this study, the disposition of cenobamate was not significantly affected by food or the different oral tablet strengths tested (50, 100 or 200 mg). Intra-subject variability after a single oral tablet of 200 mg cenobamate was low.

Supported by: SK Life Science Inc

#### Poster Number: 024

#### Meta-analysis of Dose Escalations for Monoclonal Antibodies in First-in-Human Trials

J. Shao<sup>1</sup>, B. Hartingsveldt<sup>1</sup>, H. Zhou<sup>1</sup>, Z. Xu<sup>1</sup>, Y. Xu<sup>1</sup>

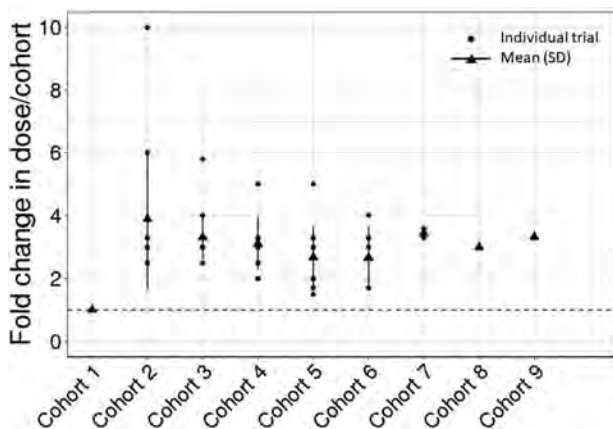
<sup>1</sup>Janssen Research & Development LLC, Spring House, PA, USA

**Statement of Purpose, Innovation or Hypothesis:** First-in-Human (FIH) studies represent a milestone in the drug development of therapeutic monoclonal antibodies (mAbs). Single ascending dose (SAD) is the first step to characterize safety, tolerability,

pharmacokinetics (PK), immunogenicity and possibly target engagement or early pharmacodynamic read outs. Due to continued development of new biologics, examination on the study designs for these studies evolved over the last two decades may provide informative understanding for early clinical development of mAbs. We hereby described a meta-analysis summarizing the study designs and practices commonly used in conducting mAb's FIH studies at Janssen R&D, with the focus being on SAD dose-escalation approaches.

**Description of Methods and Materials:** Eighteen (n=18) mAbs from the Janssen pipeline that have undergone FIH studies since the year of 2000 were included in the analysis. These mAbs were developed for immune-mediated inflammatory diseases (n=15), infectious diseases (n=2) and neurological disease (n=1). Monoclonal antibodies developed for the indications in oncology are excluded from this analysis since its early development strategy is very different. To summarize the parameters of interest, descriptive statistics were conducted.

**Data and Results:** Most of the studies were conducted as double-blinded and placebo-controlled, with a 5:2, 6:2 or 3:1 active/placebo randomization scheme. The majority of the trials were conducted in healthy subjects (15/18, 83%) and a few (3/18) in patients (with inflammatory diseases). Almost all trials started with intravenous administration in SAD (17/18, 94%) regardless of the intended therapeutic route of administration (intravenous or subcutaneous). Several different approaches were used in the starting dose selection and multiple approaches were often used together for a given mAb. No-observed-adverse-effect-level (NOAEL)-based approach was the most frequently used (15/18, 83%), followed by pharmacologically-active-dose (PAD) approach (9/18, 50%) and minimal-anticipated-biological-effect-level (MABEL) approach (7/18, 39%). Other approaches, including comparison to biologics with similar mechanisms of action and PK/target engagement modeling, were also applied. First-in-Human SAD typically consisted of five dose cohorts (range three to nine) with a median dose range of 100-fold (range 10 to 37,500-fold) and a median dose escalation of 3-fold between two adjacent cohorts (Figure 1). Larger dose escalations tended to occur between earlier cohorts. And the maximum escalation between two adjacent cohorts was ten-fold. The minimum escalation, which was about 1.5- to 1.7-fold of the previous dose, often occurred at the highest dose cohorts. For most studies, actual dose escalations were adaptive in nature and generally determined by emerging safety and PK data from the proceeding cohorts. Approximately 90% of the studies reached the planned highest dose.



**Poster Number: 024** **Figure 1.** Dose Escalation Between Adjacent Cohorts in FIH Trials Single Ascending Dose Part

**Interpretation, Conclusion or Significance:** Our analysis suggests that an approximately three-fold escalation of dose is the most commonly used escalation approach in FIH SAD studies of mAbs, with larger escalations (up to ten-fold) at earlier cohorts and smaller increments (1.5-fold to 1.7-fold) at later higher dose cohorts. These results may help inform the SAD design of future FIH studies for mAbs, when there are pharmacologically-relevant animal studies showing no irreversible toxicities, and safety margins for planned FIH doses are sufficiently large.

## Clinical Trials

### Poster Number: 026

#### The Effect of Modafinil on the Safety and Pharmacokinetics of Lorlatinib: A Phase 1 Study in Healthy Participants

J. Li<sup>1</sup>, J. Gong<sup>2</sup>, K. Lee<sup>3</sup>, Y. Pithavala<sup>4</sup>, J. Chen<sup>4</sup>

<sup>1</sup>Pharmacometrics, Pfizer Inc, La Jolla, CA, USA;

<sup>2</sup>Clinical Development & Operations, Pfizer Inc, New York, NY, USA; <sup>3</sup>Clinical Pharmacology, Pfizer Inc, Groton, CT, USA; <sup>4</sup>Clinical Pharmacology, Pfizer Inc, La Jolla, CA, USA

**Statement of Purpose, Innovation or Hypothesis:** Lorlatinib is a third-generation tyrosine kinase inhibitor approved for treatment of anaplastic lymphoma kinase (ALK)-positive metastatic non-small cell lung cancer. A previous clinical drug-drug interaction study of lorlatinib and rifampin, a strong CYP3A inducer, revealed that, in addition to reducing lorlatinib plasma exposure, coadministration with rifampin was associated with grade 2-4 elevations in aspartate aminotransferase (AST) and alanine aminotransferase (ALT). Hence, lorlatinib is contraindicated with strong CYP3A inducers. The current study evaluates the

impact of a moderate CYP3A inducer, modafinil, on lorlatinib safety and pharmacokinetics.

**Description of Methods and Materials:** This Phase 1, open-label, fixed sequence, two-period study enrolled healthy participants who each were to receive two single doses of lorlatinib, one alone followed by five days of washout (Period 1) and one coadministered with modafinil 400 mg preceded and followed by 14 days of lead-in and four days of follow-on, respectively, daily modafinil 400 mg doses (Period 2). For safety precautions, this study employed a sentinel dosing design with lorlatinib administered in escalating dosing cohorts of 50 (n=2), 75 (n=2), or 100 mg (n=2) prior to the expanded 100 mg cohort (n=10). Blood samples for safety, including liver function tests (LFTs), and pharmacokinetic measurements were collected for 120 hrs following each lorlatinib dose. A mixed effect model estimated the adjusted geometric mean ratios and 90% confidence intervals (CI) for  $AUC_{inf}$  and  $C_{max}$ . Since modafinil lead-in doses were administered outpatient, samples for 6 $\beta$ -hydroxycortisol/cortisol (urine) and 4 $\beta$ -hydroxycholesterol/cholesterol (blood) were collected to confirm adequate CYP3A induction.

**Data and Results:** Sixteen participants received at least one dose of lorlatinib. Ten participants completed the study, including four participants in the 50 mg and 75 mg cohorts and six participants in the 100 mg cohorts; six participants, all in the expanded 100 mg cohort, discontinued due to adverse events (AEs) during the modafinil lead-in doses. The following results are from the six completers in the 100 mg cohorts. Four participants experienced treatment-emergent AEs following coadministration of lorlatinib and modafinil, most of which were single incidences of central nervous system or gastrointestinal AEs, and all of which were mild and resolved within three days. While small increases from baseline of AST and ALT median values were observed, all individual values remained below the upper limit of normal. The adjusted geometric mean ratios [90% CI] of lorlatinib  $AUC_{inf}$  and  $C_{max}$  were 76.60% [66.30, 88.49] and 77.84% [67.52, 89.74], respectively, when lorlatinib 100 mg coadministered with modafinil was compared to lorlatinib administered alone. While the 6 $\beta$ -hydroxycortisol/cortisol ratio was variable, the 4 $\beta$ -hydroxycholesterol/cholesterol confirmed adequate CYP3A induction in those participants.

**Interpretation, Conclusion or Significance:** A lorlatinib 100 mg single dose coadministered with modafinil, a moderate CYP3A inducer, was well tolerated without clinically significant elevations in LFTs, indicating that lorlatinib 100 mg may be administered with moderate CYP3A inducers without serious hepatotoxicity. The presence of moderate CYP3A induction resulted in 23% and 22% lower lorlatinib  $AUC_{inf}$  and  $C_{max}$ , respectively.

**Poster Number: 027****Pharmacokinetics and Pharmacodynamics of JNJ-64232025 in Healthy Participants from a Phase 1 First-in-Human Single Ascending-Dose Study**

J. Leu<sup>1</sup>, J. Lee<sup>1</sup>, N. Sabins<sup>1</sup>, A. Piantone<sup>1</sup>, Q. Wang<sup>1</sup>, Z. Xu<sup>1</sup>

<sup>1</sup>Janssen Research & Development LLC, Spring House, PA, USA

**Statement of Purpose, Innovation or Hypothesis:** JNJ-64232025 is a monoclonal antibody targeting CD154 (also known as CD40 ligand), which is being developed for T cell-mediated autoimmune disorders. A Phase 1, First-in-Human, randomized, double-blind, placebo-controlled, single ascending-dose (SAD) study was conducted. The objective of this study was to assess the safety and tolerability of JNJ-64232025 following single ascending intravenous (IV) administrations and a single subcutaneous (SC) administration in healthy participants. The secondary objectives included 1) the assessment of the pharmacokinetics (PK) and immunogenicity of JNJ-64232025 following single IV or SC administration in healthy participants and 2) the estimation of the relative bioavailability of a single SC administration of JNJ-64232025 and 3) the evaluation of the effects of JNJ-64232025 on primary and recall immune challenges.

**Description of Methods and Materials:** Participants in this study were randomly assigned to an IV cohort (0.3, 1, 3, 10 and 30 mg/kg) or SC cohort (3 mg/kg) in a total of 48 subjects. Keyhole limpet hemocyanin (KLH) and tetanus toxoid (TT) were injected intramuscularly (in separate locations) approximately three days after administration of study intervention for evaluation of primary response (anti-KLH antibodies) and recall response (anti-TT antibodies), respectively. Subject safety was evaluated throughout the duration of the study. JNJ-64232025 concentrations and anti-drug antibodies (ADA) were evaluated via validated assays in plasma due to high levels of target interference expected in serum. Free and total soluble CD154 levels were evaluated in platelet poor plasma samples. A population pharmacokinetic/pharmacodynamic model was developed to characterize the relationship of the PK and anti-KLH IgG/anti-TT IgG.

**Data and Results:** There were no clinically-significant changes for coagulation, serum chemistry, hematology, urinalysis, vital signs, physical examination or ECG. There were no infusion reactions, injection site reactions or allergic reactions related to JNJ-64232025 reported. In the dose range of 0.3 mg/kg to 30 mg/kg, after single IV infusion of JNJ-64232025, there was an approximately dose-proportional increase in maximum observed serum concentration. For the area under the concentration-time curve (AUC) an approximately

dose-proportional increase was observed in the dose range of 0.3 mg/kg to 10 mg/kg, while the AUC increased more than dose proportionally following the dose increase from 10 mg/kg to 30 mg/kg. Mean  $T_{1/2}$  after a single IV infusion ranged from 3.9 to 14.7 days, and mean  $T_{1/2}$  after a SC injection of 3.0 mg/kg was 10.3 days. The mean absolute bioavailability of JNJ-64232025 was 70.8%. Four of 36 subjects receiving active treatment were positive for anti-JNJ-64232025 antibodies. None of the positive ADA samples were associated with an apparent effect on the PK exposure of JNJ-64232025. The effects of JNJ-64232025 on KLH and TT challenges support the hypothesis that blocking CD154 lowers humoral responses to antigen and that a recall response may require a higher dose of JNJ-64232025 than what is needed to blunt a primary response. A two-compartmental model with first-order elimination and a modified indirect response model appropriately described the PK/PD of JNJ-64232025.

**Interpretation, Conclusion or Significance:** Overall, single IV and SC doses of JNJ-64232025 or placebo were well tolerated without apparent safety concerns in healthy participants and warrants further development for autoimmune diseases.

**Poster Number: 028****Effectiveness of Flakozid Against Recurrent Genital Herpes Simplex Infections: Result of Clinical Trial**

V. V. Bortnikova<sup>1</sup>, L. V. Krepkova<sup>1</sup>, V. V. Karabaeva<sup>1</sup>, P. G. Mizina<sup>1</sup>, G. F. Sidel'nikova<sup>1</sup>, K. M. Job<sup>2</sup>, C. MT Sherwin<sup>3</sup>, E. Y. Enioutina<sup>2</sup>

<sup>1</sup>All-Russian Scientific Research Inst of Medicinal & Aromatic Plants, Moscow, Russia; <sup>2</sup>Univ of Utah School of Medicine, Salt Lake City, UT, USA; <sup>3</sup>Wright State Univ Boonshoft School of Medicine, Dayton, OH, USA

**Statement of Purpose, Innovation or Hypothesis:** We have recently reported that Flakozid, a natural flavonoid glycoside, demonstrated effectiveness in treating HepA or HepB infections. Our *in vitro* studies showed that Flakozid exhibits anti-herpes simplex and herpes zoster virus activities. The purpose of the current study was to evaluate the efficacy and safety of Flakozid in patients with recurrent genital herpes simplex (rGHS) infection.

**Description of Methods and Materials:** Open-label clinical studies were carried out in one hospital (Moscow, Russia) to determine the efficacy and safety of Flakozid in patients (age 19–80 yrs old; 35 men and 30 women) with rGHS (n=65). The duration of the disease ranged from 1.5–15 yrs. Participants were prescribed 0.2 g Flakozid taken three times/day for 7–10 days (rGHS). Flakozid 0.1g/day for seven days was recommended to all participants during relapses.

**Poster Number: 028 Table 1. Comparison of Therapeutic Effectiveness of Flakozid and Alpizarin in Patients With Recurrent Genital Herpes Simplex**

Drug	Total Number of Patients	Results of Treatment					
		Significant Improvement		Improvement		No Effect	
		N Patients	%	N Patients	%	N Patients	%
Flakozid	65	25	38.4	28	53.2	12	18.4
Alpizarin	15	0	0	6	40	9	60

A control group of participants (n=15) with rGHS received orally alpizarin, a botanical drug approved for rGHS treatment, 0.1g three times/day for 7–10 days. Participants were followed for 10–11 mos. The effectiveness of antiviral therapy during relapse was analyzed based on 1) duration of inflammation and edema, 2) days to lesion re-epithelization and 3) reduction of herpes relapse duration (>2.5 times – significant improvement; at least 2 times – improvement).

**Data and Results:** The rGHS lesions presented as grouped vesicles, erosions and crusts on inflamed edematous tissue in a genital area and skin of the buttocks. Patients complained of itching, burning and soreness in the area of the lesions. Flakozid treatment in patients with rGHS led to a reduction of inflammation and edema on day 2–3 after treatment initiation, a decrease in pain and neuralgia and accelerated lesion epithelization on day 3–6 after treatment initiation. Full resolution of herpetic rashes was observed in patients within 8–15 days. Flakozid treatment in patients with rGHS resulted in improvement in 91.6% of cases and exceeded the effects of Alpizarin (Table 1). Remission periods increased 1.5–2 times in 15% and >2 times in 9.2% patients using Flakozid in 4–5 consecutive relapses. Both Flakozid and Alpizarin were well tolerated; no adverse effects were noted.

**Interpretation, Conclusion or Significance:** Previously, Flakozid was demonstrated to be effective against HepA and HepB (DNA viruses). Now, Flakozid shows superior effectiveness in the treatment of rGHS, caused by an RNA virus. These observations suggest that Flakozid may be used as a complementary medicine to treat a variety of viral infections. Clinical pharmacologists need to be aware that some antimicrobial drugs of natural origin may possess a broad spectrum of antimicrobial activity (viruses, bacteria, and fungi). These drugs can be used as complementary treatments of difficult to treat and mixed infections.

#### Poster Number: 029

#### Effect of the Glucosylceramide Synthase Inhibitor Lucerastat on Cardiac Repolarization: Results from a Thorough QT Study in Healthy Subjects

M. S. Mueller<sup>1</sup>, P. N. Sidharta<sup>1</sup>, C. Voors-Pette<sup>2</sup>, J. Dingemans<sup>1</sup>

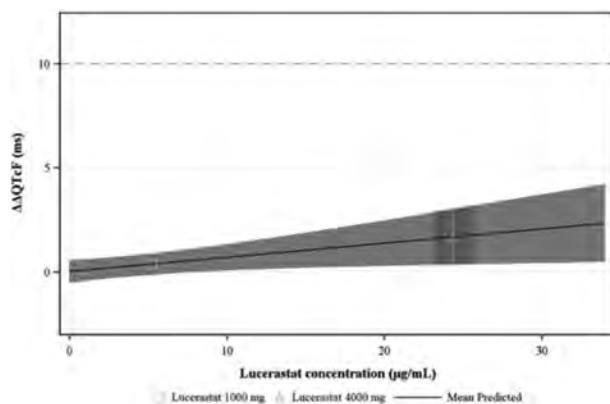
<sup>1</sup>Idorsia Pharmaceuticals Ltd, Allschwil, Switzerland;

<sup>2</sup>QPS Netherlands BV, Groningen, The Netherlands

#### Statement of Purpose, Innovation or Hypothesis:

Lucerastat is an orally available iminosugar molecule with potential to provide substrate reduction therapy in the treatment of Fabry disease, regardless of the patient's underlying gene mutation. A thorough QT (TQT) study was conducted to investigate its effect on cardiac repolarization.

**Description of Methods and Materials:** A single-center, randomized, double-blind, placebo- and open-label moxifloxacin-controlled, two-part Phase 1 study (NCT03832452) was conducted in healthy subjects (age: 18–54 yrs). Part A was a pilot study to determine the suprathreshold dose for Part B. In Part A, six healthy male subjects received 2,000 and 4,000 mg lucerastat on Day 1 and 3, respectively, and two received placebo on both days. Part B was a four-period crossover study in 36 healthy male and female subjects who received in a random sequence a single oral dose of: 1,000 mg lucerastat (proposed therapeutic dose, currently investigated in a Phase 3 study in Fabry patients [NCT03425539]), 4,000 mg lucerastat (suprathreshold dose), placebo and 400 mg moxifloxacin. ECG variables were extracted in replicates at predefined time points from continuous 12-lead Holter ECG recordings over 36 hrs. Pharmacokinetic (PK)



**Poster Number: 029 Figure 1.** Predicted  $\Delta\Delta\text{QTcF}$  at lucerastat geometric mean  $C_{\text{max}}$

plasma samples were obtained at corresponding time points. Data was analyzed using concentration-QTc modeling with the objective to demonstrate that lucerastat at therapeutic and supratherapeutic doses does not exhibit an effect on the QT interval corrected with Fridericia's formula (QTcF) exceeding 10 ms. Safety and tolerability were evaluated based on adverse event (AE), vital signs, 12-lead ECG, clinical laboratory and physical examination data.

**Data and Results:** Across all doses, lucerastat was rapidly absorbed with maximum plasma concentrations ( $C_{max}$ ) occurring between 0.5 and 4.0 hrs post-dose; geometric mean  $t_{1/2}$  ranged from 8.0 to 10.0 hrs. The PK of lucerastat appeared dose proportional and PK characteristics of moxifloxacin were in line with published data. Based on concentration-QTc analysis, the lower bound of the 90% confidence interval (CI) of baseline- ( $\Delta$ ) and placebo- ( $\Delta\Delta$ ) corrected QTcF was  $>5$  ms at moxifloxacin  $C_{max}$ , demonstrating assay sensitivity. The effect of lucerastat on  $\Delta\Delta$ QTcF was predicted as 0.39 ms (90% CI: -0.13, 0.90) and 1.69 ms (90% CI: 0.33, 3.05) at the observed lucerastat geometric mean  $C_{max}$  after dosing with 1,000 mg (5.2  $\mu\text{g/mL}$ ) and 4,000 mg (24.3  $\mu\text{g/mL}$ ), respectively (Figure 1). A QTcF effect exceeding 10 ms could be excluded within the observed range of lucerastat plasma concentrations up to approximately 34.0  $\mu\text{g/mL}$ . There were no subjects with QTcF  $>480$  ms and no subjects with  $\Delta$ QTcF  $>30$  ms. Lucerastat was safe and well tolerated across all doses. AEs were all mild in intensity and the most frequently reported AE was headache. There was no clear difference in the incidence of treatment-emergent AEs across doses of lucerastat or as compared to placebo.

No clinically relevant effects on other safety parameters were observed.

**Interpretation, Conclusion or Significance:** These results constitute a negative TQT study, demonstrating that lucerastat up to a dose of 4,000 mg does not have any clinically relevant liability to prolong the QT interval.

The solid black line with gray shaded area denotes the predicted mean (90% CI)  $\Delta\Delta$ QTcF. The darker shaded areas denote the predicted mean (90% CI)  $\Delta\Delta$ QTcF with a square and a triangle at the geometric mean (90% CI)  $C_{max}$  of lucerastat 1,000 mg and lucerastat 4,000 mg, respectively. CI = confidence interval;  $C_{max}$  = maximum plasma concentration;  $\Delta\Delta$  = baseline- and placebo-corrected; QTcF = QT interval corrected with Fridericia's formula.

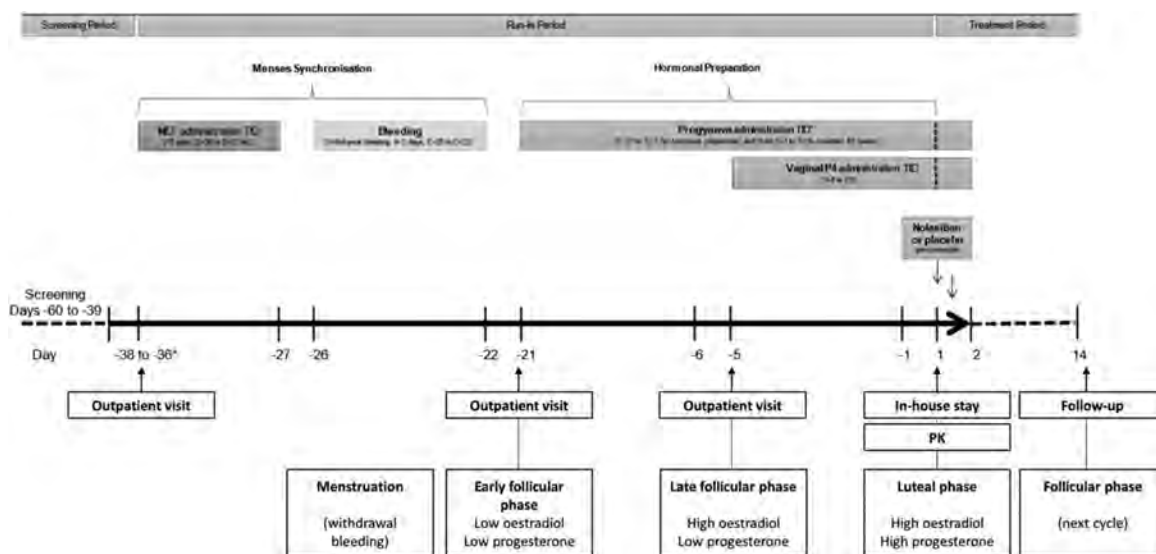
**Poster Number: 030**

**Effects of Progesterone and Estradiol on Subintervals Over the Course of a Menstrual Cycle**

J. Taubel<sup>1</sup>, U. Lorch<sup>1</sup>, C. Spencer<sup>2</sup>, A. Freier<sup>3</sup>, D. Djumanov<sup>4</sup>, G. Ferber<sup>5</sup>, J. Gotteland<sup>6</sup>, O. Pohl<sup>6</sup>

<sup>1</sup>Richmond Pharmacology Ltd, London, United Kingdom; <sup>2</sup>Richmond Pharmacology Ltd, Cranmer Terrace, United Kingdom; <sup>3</sup>Richmond Research Inst, London, England, United Kingdom; <sup>4</sup>Richmond Pharmacology Ltd, London, United Kingdom; <sup>5</sup>Statistik Georg Ferber GmbH, Riehen, Switzerland; <sup>6</sup>ObsEva, Geneva, Switzerland

**Statement of Purpose, Innovation or Hypothesis:** Observed sex differences in the QT interval have led to the



**Poster Number: 030** **Figure 1.** Diagram of synchronized run-in period. Each study day except for Day 1 includes an outpatient visit where a meal was served prior to ECG screening. NET - norethisterone, PK - pharmacokinetics, TID - three times a day. \* Outpatient visit was carried out from Day -38 to Day -36, NET self-administration began on Day -36 for all volunteers

**Poster Number: 030 Table 1. Significant Estimates of Fixed Effects of Sex Hormones on Cardiac Parameters**

Parameter	Model	AIC	Effect	Effect estimate	SE	d.f.	T value	90% CI	
Heart rate	Progesterone, without baseline	1,065.8	Progesterone [ms per nmol/L]	-0.158	0.0218	Inf	-7.23	-0.194	-0.122
			Intercept [ms]	0.5	0.82	Inf	0.59	-0.9	1.8
QTcF	Oestradiol without baseline	1,225.5	Oestradiol [ms per ng/L]	0.013	0.008	Inf	1.58	-0.001	0.026
			Intercept [ms]	1.3	0.91	Inf	1.41	-0.2	2.8
QRS	None	726.5	Intercept [ms]	0.5	0.21	Inf	2.28	0.1	0.8
JTpc	Oestradiol without baseline	1,144.8	Oestradiol [ms per ng/L]	0.02	0.006	Inf	3.41	0.011	0.03
			Intercept [ms]	0.7	0.85	Inf	0.81	-0.7	2.1
TpTe	Baseline only	940.5	Baseline [ms per ms]	-0.16	0.056	Inf	-3.19	-0.27	0.09
			Intercept [ms]	-0.1	0.39	Inf	-0.25	-0.7	0.5

postulation of hormonal influences on cardiac repolarization. Women have longer QTc intervals than men, with onset at puberty, and changes in the duration of QTc across the menstrual cycle and during pregnancy have been observed.

**Description of Methods and Materials:** This Phase 1, double-blinded, single-center, randomized, placebo-controlled study in 45 healthy women of child-bearing age examined the effects of the sex hormones estradiol and progesterone on the QT interval (Figure 1). Changes in ECG variables (heart rate, QTcF, QRS, JTcJ, Tpeak-Tend) were compared with changes in plasma hormone levels using concentration-effect modeling over the course of a full, standardized menstrual cycle. Women were treated with an identical hormonal preparation as that used for women undergoing frozen-thawed embryo transfer.

**Data and Results:** A clear variation in ECG parameters and hormone levels occurred over the menstrual cycle. Modeling indicated a highly-significant relationship between progesterone level and heart rate, whereby heart rate increased as progesterone levels decreased. The estimated effect size was -0.158 bpm per nmol/L progesterone. Concentration-effect modeling also indicated a positive relationship between estradiol levels and the duration of the JTcJ subinterval, with an estimated effect size of 0.02 ms per ng/L estradiol (Table 1).

**Interpretation, Conclusion or Significance:** It has been observed that women of child-bearing potential have a longer QTc interval. Our findings highlight that this is due to prolongation of the JTcJ subinterval. Estrogens are suspected to cause QT-prolongation by downregulation of cardiac ion channels including potassium channel I<sub>ks</sub>. This is consistent with our findings. Further, our data confirmed a previously proposed correlation between progesterone levels and changes in heart rate. Future research is needed to

examine the causal relationship between sex hormones and cardiac repolarization.

#### Poster Number: 031

#### Identifying Appropriate Outcome Measures and Methodology to Evaluate the Abuse, Misuse, Dependence and Impairing Effects of CNS-active Drugs in Healthy Volunteer and Patient Trials

B. Setnik<sup>1/2</sup>

<sup>1</sup>Altasciences Clinical Research, Laval, QC, Canada;

<sup>2</sup>Univ of Toronto, Toronto, ON, Canada

**Statement of Purpose, Innovation or Hypothesis:** Characterizing the pharmacological profile of a CNS-active drug, including abuse/dependence potential and impairing effects, is an important component of establishing the safety and risk profile. Such an evaluation is based on a composite of various data including *in vitro*, preclinical, clinical and any available post-marketing data.

**Description of Methods and Materials:** A review of regulatory guidances, literature and unpublished data were reviewed to provide examples of strategies for evaluating CNS drug risk evaluation.

**Data and Results:** Studies such as human abuse potential and driving simulation studies are often required to provide surrogate data to identify risks. However, all preclinical and clinical data is reviewed for risks. Several strategies to obtain data related to aberrant drug behaviors (i.e. abuse, misuse and/or diversion) can be considered. This includes monitoring key adverse events (AEs), urine drug testing, risk assessment questionnaires, drug accountability and noncompliance, amongst other measures. Cognitive impairment may also be assessed throughout a clinical program. In addition, new tools are emerging to specifically probe on such events in the patient population

particularly because most events related to abuse, misuse, diversion, overdose, dependence and addiction will likely require further evaluation and interpretation. Examination of aberrant behaviors would benefit from a structured method to collect information that may aid in understanding whether a specific behavior or adverse event is related to abuse or misuse.

**Interpretation, Conclusion or Significance:** Specific AEs and questionnaires may be utilized to evaluate drug withdrawal and dependence and contribute to the abuse potential evaluation of a drug's safety profile. The available methods and limitations will be reviewed.

## Decision Making in Research & Development

Poster Number: 032

### Development of an Innovative First-in-Human Intelligent Visualization Tool to Drive Enhanced Decision-making and Promote Patient Safety

R. Sonty<sup>1</sup>, S. Jadidi<sup>2</sup>, D. Kim<sup>2</sup>, V. Tran<sup>1</sup>, S. Ramakrishnan<sup>3</sup>, S. Rani<sup>3</sup>, M. Kelley<sup>4</sup>, R. Goldsmith<sup>4</sup>, V. Sinha<sup>2</sup>

<sup>1</sup>Johnson & Johnson, Horsham, PA, USA; <sup>2</sup>Johnson & Johnson, Titusville, NJ, USA; <sup>3</sup>Johnson & Johnson, Raritan, NJ, USA; <sup>4</sup>Johnson & Johnson, Spring House, PA, USA

**Statement of Purpose, Innovation or Hypothesis:** Ensuring study participant safety in First-in-Human (FIH) trials is an imperative. Safe dose selection is based on a review of diverse nonclinical safety data and predicted clinical data drawn from myriad systems. Appropriately compiling these data is a major challenge for teams. Given a lack of off-the-shelf systems, the work is manual, burdensome and time consuming.

**Description of Methods and Materials:** To address this gap, Janssen leadership assembled a cross-functional analytics team to develop a FIH intelligent automation platform for synthesis and visualization of the varied nonclinical safety and predicted clinical data for enhancing decision making at the FIH stage.

**Data and Results:** The team collaborated with their JRD, data science and design partners in developing a FIHEDC Intelligent Automation tool that can create comprehensive, dynamic and intuitive visualizations of diverse nonclinical and predicted clinical data. A successful pilot of the tool was conducted in Dec 2018. The benefits were obvious: rapid and enhanced decision making, reduced burden for teams and safeguarding of participants enrolled in FIH studies. The team is exploring the usefulness of the tool beyond the FIH stage and across all of development.

**Interpretation, Conclusion or Significance:** The path forward for the tool is exciting as AI (Artificial Intelligence) extensions are added. As system performance improves there will be a transition to fully automated data extraction from reference documents using Natural Language Processing leveraging models such as Graph IE model which effectively captures information in the local, non-local and non-sequential contexts. Moving forward, the FIH tool will have access to voluminous and rapidly growing nonclinical, clinical and translational data sourced from an R&D data lake. Potential future applications of the tool in collaboration with relevant functions include predicting safety issues with the analogues of the compound of interest, leveraging the molecular structure from the data lake or the mechanisms of action from the data lake or of the compound and/or the class of compounds. Publicly available tissue-based expression profiles could be leveraged

## AViiD: A Novel FIH Visualization Platform For Enhanced FIH Decision-making

Non-clinical and projected clinical safety data distributed across documents (e.g. IB), manually tabulated and graphed for FIHEDC review

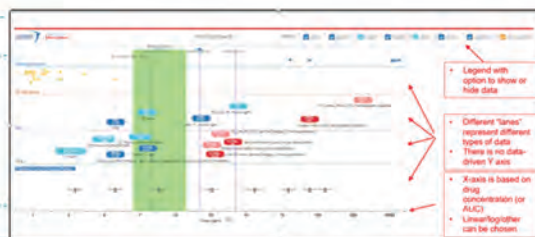


Dynamic, interactive, visual display of FIH data with key parameters identified and linked to source data



### HIGHLIGHTS

- Integrated and interactive views of non-clinical and projected clinical data based on drug concentration facilitate safety insights
- Easy link to source document (e.g. IB)
- Significant opportunity to extend use beyond FIH stage
- Prospect of connecting to numerous and varied sources through data lake
- In 2020, AI/Machine learning extensions will be added to automate data extraction and import



Poster Number: 032 Figure 1. Introduction to the AViiD platform

through Neural Network based Knowledge Graphs to identify and predict toxicities of the compound of interest, as well as its analogues.

We have developed an innovative, industry-leading, intelligent visualization platform that helps drive decision-making at the FIH stage and thus enhances trial participant, patient and consumer safety.

**Encore:** Presented at the Annual Meeting of the Drug Information Association, June 2020.

## Drug Development

### Poster Number: 033

#### Non-invasive Thermo-responsive Formulation for Peripheral Nerve Injury

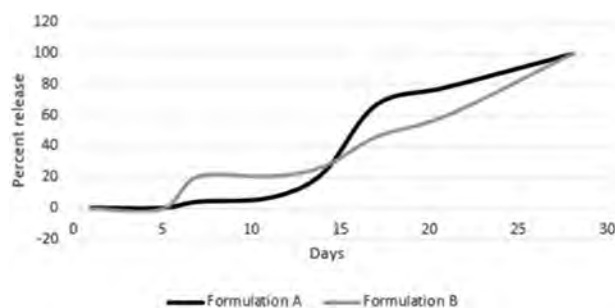
A. J. Sperry<sup>1</sup>, J. Yan<sup>1</sup>, A. Chayhan<sup>1</sup>

<sup>1</sup>Medical Coll of Wisconsin, Greenfield, WI, USA

**Statement of Purpose, Innovation or Hypothesis:** Severe peripheral nerve injury is very common in US military personnel during war. Immediately after primary nerve injury, an accompanying overwhelming calcium influx occurs at the site of injury. Excessive accumulation of calcium results in activation of various intracellular cascades resulting in secondary and more severe damage. Our group has reported a strong correlation between the degree of injury and the accumulated amount of calcium and electrophysiological recovery. It was shown that even a small increase in calcium negatively affects Schwann cell survival in nerve cell culture without calcitonin. However, with calcitonin, Schwann cells survive normally and grow. Calcium channel blockers were also tested for their ability to block calcium influx and they demonstrated the same protective effect as calcitonin. We have used osmotic pumps to deliver calcitonin into the rat model post nerve injury and it showed that the slow release of calcitonin helps in nerve regeneration. But this approach needs multiple surgical interventions. Hence, we are proposing a thermogel based biodegradable polymeric formulation, which provides sustained delivery of calcitonin and calcium channel blockers at the site of nerve injury for nerve regeneration.

**Description of Methods and Materials:** Poly(lactic-co-glycolic) acid (PLGA)- based copolymers were used to prepare various calcitonin formulations. Different copolymers were explored at various ratios and concentrations. These polymer-drug formulations were evaluated for gelling time, stability, drug entrapment and drug release.

**Data and Results:** This formulation remains as a liquid at cold temperature and forms gel at the body temperature. The polymer-drug formulations showed sustained drug release for four weeks intended for noninvasive thermo-responsive application. The tested



**Poster Number: 033** Figure 1. Calcitonin Drug Release from PLGA-Copolymers

formulations degraded during the study period and hence are biodegradable. Moreover, these polymers were stable for six months during refrigeration.

**Interpretation, Conclusion or Significance:** This data indicates that these polymer formulations have potential to treat patients with peripheral nerve injury while avoiding costly and time taking surgery. Moreover, this formulation can then reduce the number of surgeries needing to be performed due to its biodegradability.

### Poster Number: 034

#### Interspecies Comparison and Irradiation Effect on Pharmacokinetics of BIO 300, A Nanosuspension of Genistein, Following Different Routes of Administration in C57BL/6J Mice and Non-human Primates

A. M. Salem<sup>1</sup>, I. L. Jackson<sup>2</sup>, M. D. Kaytor<sup>3</sup>, A. A. Serebrenik<sup>3</sup>, Z. Vujaskovic<sup>2</sup>, J. Gobburu<sup>1</sup>, M. Gopalakrishnan<sup>1</sup>

<sup>1</sup> Univ of Maryland Baltimore, Pharmacy Practice & Science, Baltimore, MD, USA; <sup>2</sup> Univ of Maryland Baltimore, Radiation Oncology, Baltimore, MD, USA; <sup>3</sup>Humanetics Corp, Edina, MN, USA

**Statement of Purpose, Innovation or Hypothesis:** BIO 300 is being developed as a medical countermeasure for the prevention and treatment of the delayed effects of acute radiation exposure. BIO 300 is a nanosuspension of synthetic unconjugated genistein, which enhances the bioavailability and aqueous solubility of the poorly soluble compound. This study aimed to characterize and compare the pharmacokinetics (PK) of BIO 300 following administration via different routes in mice and non-human primates (NHPs) upon total body irradiation (TBI) with bone marrow (BM) sparing or no irradiation. The analysis objectives were to: (i) assess the effect of radiation on BIO 300 PK, (ii) inform the optimal route of administration to be used in future studies and (iii) explore interspecies differences in BIO 300 PK.

**Description of Methods and Materials:** The PK study included the following sex-matched treatment groups: TBI/BM2.5 and non-irradiated C57BL/6J mice

(n=60) receiving 400 mg/kg BIO 300 through oral gavage (OG), TBI/BM2.5 C57BL/6J mice (n=54) receiving 200 mg/kg BIO 300 subcutaneously (SC), non-irradiated C57BL/6J mice (n=108) receiving 100 mg/kg or 200 mg/kg BIO 300 SC, non-irradiated C57BL/6J mice (n=48) receiving 200 mg/kg BIO 300 intramuscularly (IM) and TBI/BM5 Rhesus Macaque NHPs (n=7) receiving 100 mg/kg BIO 300 OG. Unconjugated (aglycone) genistein serum concentrations were measured in all groups for 72 hrs postdose. The composite group mean PK metrics were obtained using standard noncompartmental analysis (NCA) engine of Pumas v0.10.0.

**Data and Results:** For the 400 mg/kg OG group, the TBI/BM2.5 mice showed 11% and 19% reduction in  $C_{max}$  and  $AUC_{0-inf}$ , respectively compared to the nonirradiated group. In contrast, in the 200 mg/kg SC group, the TBI/BM2.5 mice showed a 53% increase in  $AUC_{0-inf}$  but a 28% reduction in  $C_{max}$  compared to the nonirradiated group. The relative bioavailability of OG route to SC and IM routes in mice were 9% and 7%, respectively. The mean terminal elimination rate constant for OG was  $0.23 \text{ hr}^{-1}$  compared to  $0.02 \text{ hr}^{-1}$  and  $0.03 \text{ hr}^{-1}$  for IM and SC, respectively. The difference could possibly be due to the slow absorption of a fraction of the administered IM and SC dose, resulting in a flip-flop phenomenon. The dose-normalized  $AUC_{0-inf}$  was  $1,337 \text{ ng}\cdot\text{hr}/\text{mL}$  in TBI/BM2.5 mice compared to  $695 \text{ ng}\cdot\text{hr}/\text{mL}$  in TBI/BM5 NHPs. The linear regression analysis of log-transformed apparent clearances and log-transformed weights of mice and NHPs yielded an interspecies scaling coefficient of 1.06 (95% CI: 0.98-1.16), indicating a perfect linear relationship between the apparent clearance and body weight.

**Interpretation, Conclusion or Significance:** The effect of radiation on BIO 300 PK led to slightly lower  $C_{max}$  in mice (consistent between OG and SC routes) and slightly higher  $AUC_{0-inf}$  in the SC group. Despite this inconsistency, overall, the radiation effect is considered minimal. Compared to OG route, SC and IM routes seemed to be superior options for achieving satisfactory exposures of BIO 300 for future studies. The estimated interspecies scaling coefficient confirmed the body weight related changes in clearance and would be useful in estimating the BIO 300 doses in species having body weights between mice and NHPs. To project human equivalent BIO 300 dose, standard allometric principles will be used.

#### Poster Number: 035

#### Assessment on the Formulation Similarity of Approved Generic Drug Products and Their Respective Reference Products Which are Considered as Potential BCS Class 3 Drugs

T. Chan<sup>1</sup>, P. Ren<sup>1</sup>, W. Yang<sup>1</sup>, Y. Wang<sup>1</sup>, M. Luke<sup>1</sup>, M. Kim<sup>1</sup>, Y. Zhang<sup>1</sup>

<sup>1</sup>US Food & Drug Administration, Silver Spring, MD, USA

**Statement of Purpose, Innovation or Hypothesis:** A biowaiver of *in vivo* bioequivalence (BE) studies for Biopharmaceutics Classification System (BCS) Class 3 drugs may be considered provided that formulations are qualitatively (Q1) the same and quantitatively (Q2) very similar to the reference drug product as per the US Food & Drug Administration (FDA) BCS guidance. However, formulation development remains a major challenge for generic drug applicants when pursuing this approach due to the challenges meeting the stringent Q1/Q2 and dissolution criteria in FDA's guidance. The stringent criteria for biowaiver for BCS Class 3 drugs are mainly due to concerns on the potential effects of excipients on drug absorption. The purposes of the study were to investigate the impact of formulation similarity on the drug absorption through assessing BE study results of the approved generic (test, T) products that are potential BCS Class 3 drugs and to explore the possible level of formulation similarity for BCS Class 3 drugs that may not impact BE.

**Description of Methods and Materials:** A total of 110 approved abbreviated new drug applications (ANDAs) were examined for 11 potential BCS Class 3 drugs formulated as immediate-release solid dosage forms (tablets and capsules). For each ANDA, the formulation compositions from both T and reference drug products (reference, R) were compared and categorized based on Q1 and Q2. The excipients used in these formulations were analyzed based upon the function and percent of total weight (%w/w). In addition, the pharmacokinetic (PK) parameters ( $AUC_{0-t}$ ,  $AUC_{0-i}$  and  $C_{max}$ ), T/R ratios of these PK parameters and 90% confidence intervals (CIs) of these T/R geometric mean ratios were collected from a total of 204 BE studies (115 fasting and 95 fed BE studies).

**Data and Results:** Of the 110 ANDAs, 5.5% of T formulations surveyed were Q1/Q2 same, 22.7% Q1 same/Q2 very similar, 18.2% Q1 same/Q2 different and 53.6% Q1/Q2 different compared to their corresponding R formulations. In these formulations, a total of 30 excipients of various amounts were used, none of which were novel or in atypically large amounts. The top five common excipients were magnesium stearate, microcrystalline cellulose, povidone, starch and colloidal silicon dioxide. The excipients identified in Q2 different formulations were mostly glidant, disintegrant, diluent and binder. The T/R ratios and respective 90% CIs for all PK parameters met the BE criteria under fasting and fed conditions in all 204 BE studies from these 110 approved ANDAs.

**Interpretation, Conclusion or Significance:** Although the majority of formulations (~72%) in our study may not be eligible for BCS Class 3 biowaiver as per the

FDA BCS Guidance, the *in vivo* BE study results suggested that the observed Q1/Q2 differences may not impact *in vivo* BE. In addition, the excipients (30 in total assessed in the study) do not seem to affect the absorption of these potential BCS Class 3 drugs. Because there is a potential bias of our dataset that we only included formulations that passed BE, future studies, combining data-driven and mechanistic approaches, are warranted to further investigate the data and evidence needed to support a possible biowaiver for these apparently non-Q1/Q2 BCS Class 3 drugs.

**Poster Number: 036**

**Clinical Pharmacology Considerations in Clinical Development of Testosterone Replacement Therapy Products**

M. Cho<sup>1</sup>, C. Yu<sup>2</sup>

<sup>1</sup>Univ of Illinois at Chicago, Chicago, IL, USA; <sup>2</sup>US Food & Drug Administration, Silver Spring, MD, USA

**Statement of Purpose, Innovation or Hypothesis:** Testosterone replacement therapy (TRT) has been approved in the US since the 1950s for male hypogonadism, which shows a deficiency or absence of endogenous testosterone. Depending on the route of administration, each product has a different dosage and administration instruction, often including a dose titration scheme to achieve the optimal testosterone dose for each individual. The purpose of this investigation is to survey the currently approved TRT products and summarize the various clinical pharmacology considerations that were made in the clinical development of TRT products.

**Description of Methods and Materials:** Testosterone replacement therapy products approved during the period of 1953–2019 were surveyed for the following key elements involved in clinical drug development using information available at the [Drugs@FDA.gov](mailto:Drugs@FDA.gov) website:

- Route of administration and dosage regimen
- Pharmacokinetic (PK) characteristics
- Phase 3 trial designs aspects:
  - Inclusion/exclusion criteria
  - Dose titration scheme (when applicable)
  - Treatment period
  - Normal testosterone concentration range
  - Efficacy and safety endpoints and outcomes
- Bioanalytical methods

Testosterone replacement therapy products with various administration routes such as topical, oral, buccal, nasal and intramuscular or subcutaneous injections were included in the survey. Testosterone replacement therapy products that were discontinued were also included. Information on additional types of studies con-

ducted during clinical development of TRT products depending on administration routes were also collected and summarized.

**Data and Results:** A total of 17 TRT products have been approved by the US Food & Drug Administration and seven of these products have been discontinued. Nearly two thirds of the approved TRT products (65%) are given through topical administration and additional studies were conducted to address safety concerns such as interpersonal transferability. Pharmacokinetic characteristics are different among TRT products with different routes of administration which could warrant considerations that are unique to the route of administration. Three of the five most recent TRT product approvals were for testosterone pro-drugs. In the case of a recently approved oral testosterone pro-drug product, special considerations for food effect, sample collection and handling conditions and associated bioanalytical methods had to be made. Key features of Phase 3 study designs were surveyed and summarized. In addition information on currently ongoing safety post-marketing requirement studies were collected.

**Interpretation, Conclusion or Significance:** This survey is the first comprehensive survey that summarized the clinical pharmacology considerations made in the clinical development of all approved TRT products. This survey shows that clinical pharmacology plays a very important role in the successful development of TRT products. As different administration routes result in different PK characteristics and each individual responds differently to treatment, clinical pharmacology considerations are pivotal in determining the optimal dosage and administration recommendations (including the dose titration scheme, when applicable) to ensure the safe and effective restoration of testosterone in hypogonadal men. Information obtained from this survey provides insights on clinical pharmacology considerations that may be useful for future development of TRT products.

## Drug Effectiveness

**Poster Number: 037**

**Use of Intravenous Immunoglobulins for Treatment of Pediatric Patients with Epilepsy: Is it Effective?**

A.H. Balch<sup>1</sup>, J. Wilkes<sup>2</sup>, E. Y. Enioutina<sup>1</sup>

<sup>1</sup>Univ of Utah School of Medicine, Salt Lake City, UT, USA; <sup>2</sup>Intermountain Healthcare, Salt Lake City, UT, USA

**Statement of Purpose, Innovation or Hypothesis:** Epilepsy is a chronic neurological condition characterized by episodic occurrence of seizures. Thirty-five million people suffer from epilepsy globally. Although

many patients' symptoms are well controlled by the anticonvulsant medications, 30% of patients have refractory epilepsy that is difficult to control with anticonvulsant drugs. Some healthcare providers use intravenous immunoglobulins (IVIG) for the treatment of such conditions. Anecdotally, it has been reported that the administration of IVIG led to seizure control and cognitive improvements in a 9.5 yr old boy with refractory epilepsy. The purpose of this research is to determine effectiveness of IVIG in pediatric patients with epilepsy.

**Description of Methods and Materials:** We performed a retrospective analysis of medical records of 319,517 pediatric patients with epilepsy admitted to 47 US-based hospitals during 2004–2015 period. We queried the Pediatric Health Information System<sup>®</sup> (PHIS) for all inpatients age <18 yrs discharged with pharmacy charges for IVIG and epilepsy-relevance ICD-9/10 codes. Summary statistics were calculated and a linear regression model was developed to assess equal slopes for immunoglobulin (IG)-treated and untreated patients.

**Data and Results:** We have found 1.3% of patients with epilepsy received IVIG. Cohorts were comparable by age, sex and race. Both cohorts had comparable Risk of Mortality (ROM) at admission. IVIG patients received on average 35 drugs during admission compared to no-IVIG patients receiving only nine drugs. Pharmacy charges were higher in patients receiving IVIG (\$266,354 versus \$19,920). Overall mortality in the IVIG patients was high compared to their counterparts (Odds Ratio, OR=7.21). Stratification by the ROM scores revealed that mortality of IVIG patients increases with high ROM scores (OR 7.2, CL95% 2.6;19.5). Overall, IVIG patients had higher chance to receive ECMO (0.84% versus 0.02%). We have observed a significant increase in a number of patients receiving IVIG, who were diagnosed with Grand Mal Status Epilepticus (GMSE, OR=14.86) or Non-intractable Unspecified Epilepsy (OR=11.23). About 1% of patients with GMSE received IVIG treatment during study period. The death rate was much higher in GMSE patients receiving IVIG (11.5% versus 0.9%; OR 14.9, CL95% 9.7; 22.9). Chance of GMSE IVIG patients to be admitted to the ICU was higher (87.9% versus 54.8%). About 0.5% of patients with Complex Intractable Epilepsy received IVIG treatment (CIE). Mortality rate in these patients was comparable to CIE no-IVIG patients (OR 0.99 CL95% 0.992; 0.995), while chance to be admitted to the ICU was lower. Interestingly, patients with Complex Non-Intractable Epilepsy receiving and non-receiving IVIG had a similar rate of death, but patients on IVIG were more often admitted to ICU.

**Interpretation, Conclusion or Significance:** Our data indicate IVIG prescriptions to pediatric inpatients are on the rise, specifically to GMSE patients and patient

with epilepsy of unknown etiology. IVIG patient with epilepsy are more often admitted to the ICU and have a higher chance to die. The Academy of Neurology has no specific clinical practice guideline on IVIG use in patients with epilepsy. We can conclude that there are no obvious benefits to pediatric patients with epilepsy from IVIG treatment. Further studies are needed to identify whether IVIG decreases frequencies of seizure and hospital admissions. Supported by CSL Behring.

## Drug Interactions

**Poster Number: 038**

**An R Shiny App for Calculating *In Vitro* Drug-Drug Interaction R Values Based on Equations from Regulatory Guidances (FDA, EMA and PMDA)**

Y. S. Wu<sup>1</sup>, L. Lohmer<sup>2</sup>, B. Furmanski<sup>2</sup>

<sup>1</sup>Univ of North Carolina at Chapel Hill, Durham, NC, USA; <sup>2</sup>Nuventra Pharma Sciences Inc, Durham, NC, USA

**Statement of Purpose, Innovation or Hypothesis:** Drug regulatory agencies, including the US Food & Drug Administration (FDA), European Medicines Agency (EMA) and Pharmaceuticals & Medical Devices Agency (PMDA), routinely require evaluation of the potential for a new molecular entity (NME) to cause drug-drug interactions (DDIs). Typically, DDI potential is assessed through *in vitro* metabolic enzyme and drug transport studies, the results of which are used to predict exposure ratios (R values) in the presence and absence of the perpetrator, and subsequently compared to guidance specified thresholds. If the R value is above the guidance threshold, then a sponsor may need to conduct a clinical DDI study or further analysis through modeling and simulation (e.g., physiologically-based pharmacokinetics). Early determination of R values is needed to determine appropriate exclusion criteria for protocols and to evaluate whether dedicated clinical DDI studies are warranted prior to initiating patient studies. However, describing DDI potential of an NME in terms of an R value is seldom found in First-in-Human IND submissions and/or investigators brochures and calculation of R values typically only occurs after Phase 1/2. When eventually performed, the R values are commonly calculated by entering formulas from regulatory guidances into a spreadsheet type software. However, spreadsheets are prone to errors, corruptible, lack transparency and traceability, and can ultimately lead to version control issues if the spreadsheet is not locked down properly. To address these limitations and to improve consistency, an open source R Shiny app was developed that calculates R values according to the guidances

## Drug Interaction Calculator

	CYP Enzyme	IC50	Unit	R1	R1Gut
1	1A2		uM		
2	2B6		uM		
3	2C8		uM		
4	2C9		uM		
5	2C19		uM		
6	2D6		uM		
7	3A		uM		

Poster Number: 038 Image 1. R Shiny DDI Calculator

from the various health authorities (FDA, EMA and PMDA).

**Description of Methods and Materials:** The app was developed using R v3.6.1 making use of the Shiny (v1.4.0) and rhandsontable (v0.3.7) packages. Functions were created for the various equations for R values and the appropriate functions were used for each appropriate metabolic enzyme or transporter. The app utilized CSS visuals to warn the user of invalid input (red) and mark significant R values requiring further investigation (pink). The results can be outputted in a standard report for submission to regulatory agencies. The app was checked by an independent programmer and then validated using multiple previously calculated R values data from publicly available information.

**Data and Results:** The R Shiny DDI calculator is available at: <https://nuventra.shinyapps.io/dditool/> and a screenshot of the preliminary app is included.

**Interpretation, Conclusion or Significance:** The code for this R Shiny app is publicly available, which allows for greater transparency, ease of use and greater consistency, thus addressing the current limitations of ad hoc methods for calculating R values to determine DDI risk for an NME.

Poster Number: 039

**A Three-cohort, Open-label, Two-period, Sequential Study to Assess the Effects of Strong, Moderate and Weak 3A4 Inhibitors on the Pharmacokinetics of Colchicine Oral Solution in Healthy Adult Subjects**

J. Yin<sup>1</sup>, N. Vishnupad<sup>2</sup>, M. Willett<sup>1</sup>, J. Lederman<sup>1</sup>, D. Fan<sup>3</sup>, P. Guo<sup>3</sup>, J. Lin<sup>3</sup>, L. Diamond<sup>1</sup>, I. Muni<sup>2</sup>

<sup>1</sup>Frontage Clinical Svcs Inc, Secaucus, NJ, USA;

<sup>2</sup>Romeg Therapeutics LLC, Woburn, MA, USA;

<sup>3</sup>Frontage Laboratories Inc, Exton, PA, USA

**Statement of Purpose, Innovation or Hypothesis:** Colchicine tablet product was approved by the US Food & Drug Administration (FDA) in 2009 and used for treatment of familial Mediterranean fever, acute flares of gout and for the prophylactic treatment of gout. Colchicine oral solution was developed as a new formulation and approved by FDA in 2019. Colchicine's drug-drug interaction potential, as a P-gp substrate and cytochrome P450 substrate, specifically CYP3A4, has been reported in the literature. The three medications selected in this study to evaluate for their potential to interact with colchicine are posaconazole, ciprofloxacin hydrochloride and amlodipine besylate, which are considered strong, moderate and weak CYP3A4 inhibitors, respectively. The primary objective was to compare the pharmacokinetic (PK) variables, plasma colchicine AUC<sub>0-last</sub>, AUC<sub>0-inf</sub> and C<sub>max</sub>, after a single oral 0.6 mg dose of colchicine solution administered on Day 1 and when coadministered with either a strong (posaconazole), moderate (ciprofloxacin hydrochloride) and weak (amlodipine besylate) CYP3A4 inhibitor dosed to steady state. Secondary objective was to assess the safety and tolerability of a single oral 0.6 mg dose of colchicine solution administered alone and in combination with posaconazole, ciprofloxacin hydrochloride and amlodipine besylate.

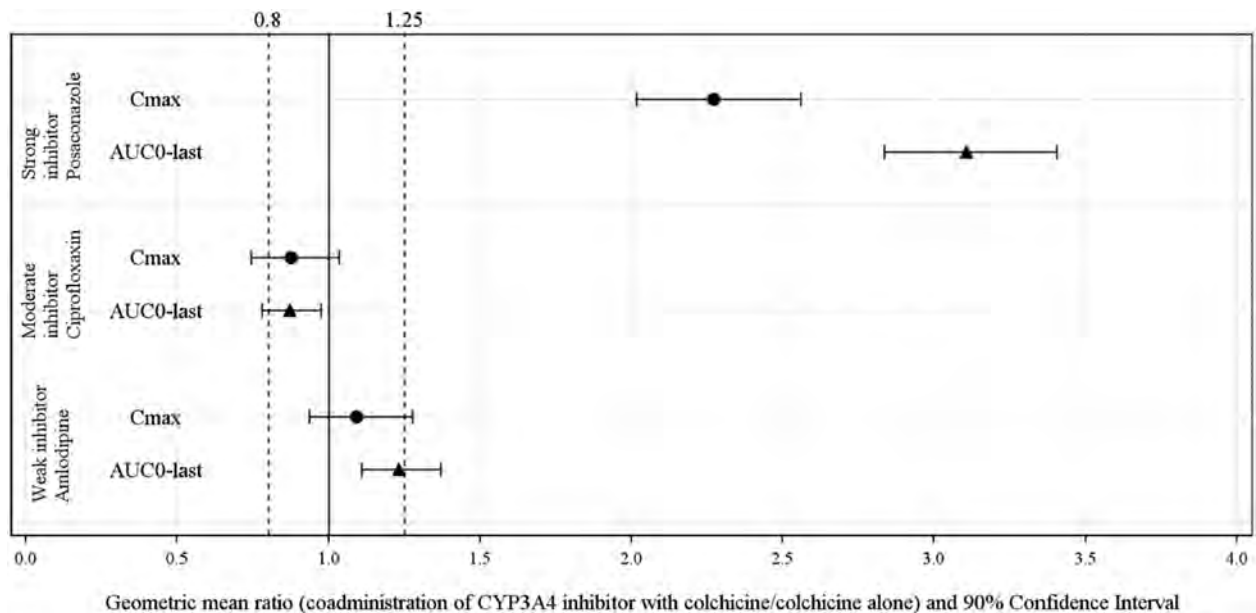
**Description of Methods and Materials:** This was a three-independent cohort, open-label, two-period

**Poster Number: 039 Table 1. Effect of Strong, Moderate and Weak CYP3A4 Inhibitors on Colchicine Pharmacokinetics**

PK Parameter	Least Squares Geometric Means				Percent GMR (%) T/R	Percent GMR 90% CI T/R	Intra-Subject CV%	
	n	T	n	R				
Strong inhibitor (Posaconazole)	$C_{max}$ (ng/mL)	22	4.498	22	1.98	227.1	(201.6–255.8)	23.26
	$AUC_{0-last}$ (h*ng/mL)	22	45.36	22	14.6	310.7	(283.7–340.4)	17.69
Moderate inhibitor (Ciprofloxacin Hydrochloride)	$AUC_{0-inf}$ (h*ng/mL)	20	49.31	20	15.98	308.7	(281.0–339.0)	17.27
	$C_{max}$ (ng/mL)	20	2.241	20	2.556	87.65	(74.25–103.5)	31.06
Weak inhibitor (Amlodipine Besylate)	$AUC_{0-last}$ (h*ng/mL)	20	18.19	20	20.87	87.16	(78.02–97.37)	20.47
	$AUC_{0-inf}$ (h*ng/mL)	19	19.94	19	22.68	87.92	(78.69–98.23)	19.9
Weak inhibitor (Amlodipine Besylate)	$C_{max}$ (ng/mL)	21	2.099	21	1.921	109.2	(93.52–127.6)	29.83
	$AUC_{0-last}$ (h*ng/mL)	21	20.29	21	16.46	123.3	(110.8–137.1)	20.26
$AUC_{0-inf}$ (h*ng/mL)	20	22.23	20	18.27	121.7	(109.1–135.7)	20.15	

R = Colchicine 0.6 mg.

T = Colchicine 0.6 mg + Posaconazole/Ciprofloxacin Hydrochloride/Amlodipine Besylate.

**Poster Number: 039 Figure 1. Forest Plot for Drug-Drug Interaction Assessment After Administration of Colchicine 0.6 mg Alone and in Combination with CYP3A4 Inhibitors**

study to assess the effects of multiple oral doses of the CYP3A4 inhibitors, posaconazole, ciprofloxacin hydrochloride and amlodipine besylate, on the PK of a single dose of colchicine oral solution 0.6 mg (0.12 mg/mL, 5 mL) in healthy male and female adults. The study was designed such that the enrollment of the three cohorts was independent of each other, in sequence. Pharmacokinetic parameters for colchicine including  $C_{max}$ ,  $T_{max}$ ,  $AUC_{0-t}$ ,  $AUC_{0-inf}$ ,  $K_{el}$  and  $t_{1/2}$  were calculated using a noncompartmental analysis method by Phoenix<sup>®</sup> WinNonlin. Log-transformed PK parameters dose normalized  $AUC_{0-t}$ ,  $AUC_{0-inf}$ , and  $C_{max}$  were analyzed for drug-drug interaction using an analysis of variance model by SAS<sup>®</sup> v9.3.

**Data and Results:** The drug-drug interaction assessment after administration of colchicine 0.6 mg alone and in combination with CYP3A4 inhibitors are summarized in Table 1. Forest plot for assessment of drug-drug interactions is displayed in Figure 1.

**Interpretation, Conclusion or Significance:** Pharmacokinetic and drug-drug interaction assessment is summarized above. Significant increases of plasma colchicine  $C_{max}$  and  $AUC_{0-last}$  were observed following the coadministration of colchicine and posaconazole (a CYP3A4 strong inhibitor) compared to colchicine alone. Strong CYP3A4 inhibitors may therefore interact with colchicine oral solution. A small decrease in  $C_{max}$  and  $AUC_{0-last}$  was observed following the

coadministration of colchicine and ciprofloxacin hydrochloride (a CYP3A4 moderate inhibitor). This effect is considered not to be clinically meaningful. Following the coadministration of colchicine and amlodipine (a CYP3A4 weak inhibitor), a modest increase of  $C_{max}$  and  $AUC_{0-last}$  was observed. This effect is also considered not to be clinically meaningful. Safety evaluation showed that colchicine oral solution was well tolerated in the study when administered orally as 0.6 mg alone and in combination with posaconazole, ciprofloxacin hydrochloride, or amlodipine besylate in healthy male and female subjects. The most common treatment-emergent adverse events were gastrointestinal disorders.

#### Poster Number: 040

#### A Phase 1, Open-label, Two-period, Sequential Study to Assess the Effects of Carvedilol Phosphate on the Pharmacokinetics of Colchicine Oral Solution in Healthy Adult Subjects

J. Yin<sup>1</sup>, N. Vishnupad<sup>2</sup>, M. Willett<sup>1</sup>, J. Lederman<sup>1</sup>, D. Fan<sup>3</sup>, P. Guo<sup>3</sup>, J. Lin<sup>3</sup>, L. Diamond<sup>1</sup>, I. Muni<sup>2</sup>

<sup>1</sup>Frontage Clinical Svcs Inc, Secaucus, NJ, USA;

<sup>2</sup>Romeg Therapeutics LLC, Woburn, MA, USA;

<sup>3</sup>Frontage Laboratories Inc, Exton, PA, USA

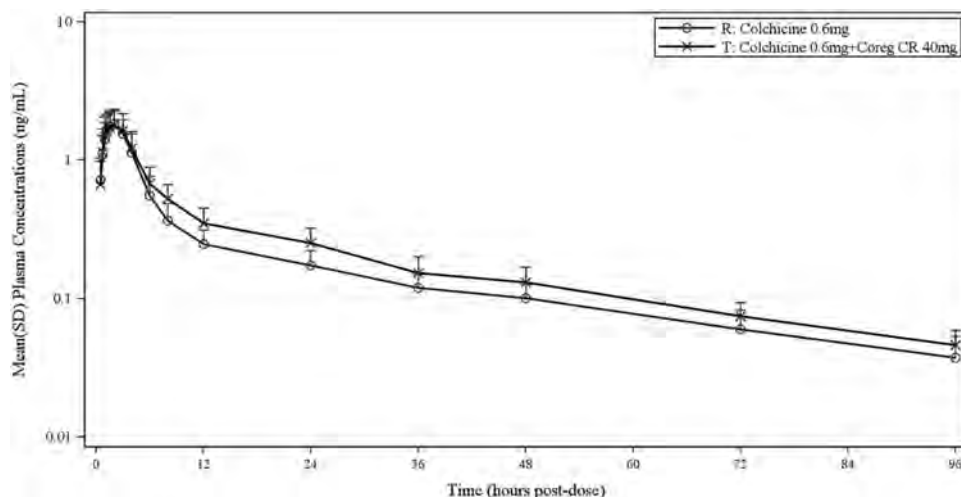
#### Statement of Purpose, Innovation or Hypothesis:

Colchicine was used for treatment of familial Mediterranean fever and acute flares of gout approved by the US Food & Drug Administration (FDA) in 2009. Colchicine oral solution was developed with dosage form flexibility and for patients with difficulty of swallowing colchicine oral tablets and approved by FDA in 2019. Colchicine is a known substrate of the P-gp transporter. Since it is likely that some patients will take colchicine and Coreg CR<sup>®</sup> concomitantly, it is clinically relevant to study the effect of carvedilol as an inhibitor of the P-gp transporter on the plasma concentrations

and pharmacokinetics of colchicine to evaluate if colchicine dosage adjustments may be warranted when the two drugs are concomitantly administered. The primary objective of the study was to compare the pharmacokinetic (PK) variables of plasma colchicine after a single oral 0.6 mg dose of colchicine solution administered on Day 1 and when coadministered with carvedilol phosphate extended-release capsules dosed for seven days to steady state. The secondary objective was to assess the safety and tolerability of a single oral 0.6 mg dose of colchicine solution administered alone and in combination with multiple doses of carvedilol phosphate extended-release capsules administered.

**Description of Methods and Materials:** This was an open-label, two-period, sequential study to assess the effects of multiple oral doses of Coreg CR<sup>®</sup> (Carvedilol Phosphate) Extended-release Capsules on the pharmacokinetics of a single oral dose of Colchicine Oral Solution 0.6 mg (0.12 mg/mL, 5 mL) in healthy male and female adults. Pharmacokinetic parameters for colchicine including  $C_{max}$ ,  $T_{max}$ ,  $AUC_{0-t}$ ,  $AUC_{0-inf}$ ,  $K_{el}$  and  $t_{1/2}$  were calculated using a noncompartmental analysis method by Phoenix<sup>®</sup> WinNonlin. Log-transformed PK parameters of  $AUC_{0-t}$ ,  $AUC_{0-inf}$ , and  $C_{max}$  were analyzed for drug-drug interactions using an analysis of variance model by SAS<sup>®</sup> v9.3.

**Data and Results:** Mean colchicine plasma concentrations versus time profiles are shown in Figure 1 on a semilogarithmic scale. A summary table of the effect of Coreg CR<sup>®</sup> (Carvedilol Phosphate) on the pharmacokinetics of colchicine is displayed in Table 1. Similar plasma PK profiles were observed for colchicine when administered alone and when coadministered with carvedilol. However, when colchicine was coadministered with carvedilol, the terminal phase profile was slightly higher than colchicine alone, but both terminal phase profiles were parallel. Mean  $C_{max}$  for colchicine alone (1.973 ng/mL) was similar to the  $C_{max}$  for



Poster Number: 040 Figure 1. Mean (SD) Colchicine Plasma Concentrations versus Time (Semilog Scale)

**Poster Number: 040 Table 1. Effect of Coreg CR<sup>®</sup> (Carvedilol Phosphate) on the Pharmacokinetics of Colchicine**

PK Parameter	Least Square Geometric Means				Ratio of Geometric Means (%) T/R	Ratio of Geometric Means 90% CI (%) T/R	Intra-subject CV%
	n	T	n	R			
C <sub>max</sub> (ng/mL)	21	1.855	21	1.94	95.59	(89.64–101.9)	12.11
AUC <sub>0-last</sub> (ng <sup>h</sup> /mL)	21	21.35	21	18.11	117.9	(112.0–124.1)	9.673
AUC <sub>0-inf</sub> (ng <sup>h</sup> /mL)	19	23.54	19	19.99	117.8	(111.8–124.0)	9.22

R = Colchicine 0.6 mg.

T = Colchicine 0.6 mg + Coreg CR<sup>®</sup> 40 mg.

co-administration with carvedilol (1.920 ng/mL). Mean AUC<sub>0-last</sub> for colchicine co-administration with carvedilol (22.06 h\*ng/mL) was 23% higher than that of colchicine alone (17.91 h\*ng/mL).

**Interpretation, Conclusion or Significance:** Drug-drug interaction assessment showed that the 90% CIs of geometric means percent ratios (coadministration with carvedilol/colchicine alone) for C<sub>max</sub>, AUC<sub>0-last</sub> and AUC<sub>0-inf</sub> were within the no-effect boundaries of 80.00 to 125.00%. A lack of an interaction of the P-gp inhibitor carvedilol on plasma colchicine exposure was observed. Colchicine oral solution was well tolerated in the study when administered as a single oral 0.6 mg dose alone and in combination with multiple doses of carvedilol phosphate extended-release capsules in adult male and female subjects. The most common treatment-emergent adverse events included nervous system disorders such as dizziness and headache.

**Poster Number: 041****The Dual Orexin Receptor Antagonist Daridorexant Does Not Affect the Pharmacokinetics of the BCRP Substrate Rosuvastatin**C. Muehlan<sup>1</sup>, I. Zenklusen<sup>1</sup>, J. Liška<sup>2</sup>, I. Ulč<sup>2</sup>, J. Dingemans<sup>1</sup><sup>1</sup>Idorsia Pharmaceuticals Ltd, Allschwil, Switzerland;<sup>2</sup>Ctr for Pharmacology & Analysis (CEPHA) s.r.o., Pilsen, Czech Republic

**Statement of Purpose, Innovation or Hypothesis:** Daridorexant is a dual orexin receptor antagonist in clinical development for the treatment of insomnia. Breast cancer resistant protein (BCRP) is an efflux pump highly expressed in the intestinal epithelium and in hepatocytes, contributing to the absorption, distribution and elimination of drugs and endogenous compounds. *In vitro*, daridorexant inhibits BCRP with an IC<sub>50</sub> of 3.0 μM. The BCRP substrate rosuvastatin is a cholesterol-lowering drug, recommended by regulatory bodies for clinical drug-drug interaction (DDI) studies. In order to exclude an inhibitory effect of daridorexant on BCRP, the primary aim of this

study was to evaluate the effect of daridorexant at steady state on the pharmacokinetics (PK) of single-dose rosuvastatin (10 mg). In addition, safety and tolerability of concomitant administration of daridorexant and rosuvastatin and the PK of daridorexant at predose (trough) were assessed.

**Description of Methods and Materials:** This was a single-center, open-label, one-sequence, two-treatment study to investigate the effect of daridorexant at steady state on the PK of rosuvastatin in 20 healthy male subjects. Each subject received a single oral dose of 10 mg rosuvastatin on Day 1 followed by 96 h observation. Thereafter, 25 mg daridorexant was administered on Day 5–8 and in combination with 10 mg rosuvastatin on Day 8. On Day 9–12, subjects received 25 mg daridorexant alone. Daridorexant was formulated as hydrochloride salt and provided in hard gelatin capsules for oral administration. Pharmacokinetic sampling for rosuvastatin alone and in combination with daridorexant was performed for 96 and 120 h following the dose on Day 1 and Day 8, respectively. Trough concentrations of daridorexant were determined on Day 5–13. Plasma concentrations of rosuvastatin and daridorexant were determined by validated LC-MS/MS methods with a lower limit of quantification of 0.04 and 0.5 ng/mL, respectively. Safety and tolerability were also assessed.

**Data and Results:** When administered concomitantly, rosuvastatin exposure showed small changes compared to rosuvastatin alone, with geometric mean ratios (90% CI) (rosuvastatin+daridorexant/rosuvastatin) of 0.93 (0.82, 1.04) and 0.93 (0.84, 1.02), for C<sub>max</sub> and AUC<sub>0-∞</sub>, respectively. The t<sub>1/2</sub> was also essentially unchanged, with a geometric mean ratio (90% CI) of 1.09 (0.92, 1.30). Daridorexant showed no apparent accumulation with steady-state conditions reached on the second day of administration. Three mild or moderate adverse events (AEs) were reported. There were no serious AEs or any relevant changes in ECG, vital signs, or laboratory data.

**Interpretation, Conclusion or Significance:** Concomitant administration of 25 mg daridorexant once daily at steady state did not affect the exposure parameters of 10 mg rosuvastatin in a relevant way for both C<sub>max</sub>

and  $AUC_{0-\infty}$ . Administration of a single dose of 10 mg rosvastatin alone or in combination with multiple doses of 25 mg daridorexant was well tolerated. In conclusion, daridorexant and BCRP substrates can be safely administered together without the need for dose adjustment.

#### Poster Number: 042

### Pharmacokinetic and Pharmacodynamic Interactions Between Daridorexant, a Dual Orexin Receptor Antagonist, and Citalopram, a Selective Serotonin Reuptake Inhibitor, in Healthy Subjects

B. Berger<sup>1</sup>, R. Kornberger<sup>2</sup>, J. Dingemans<sup>2</sup>

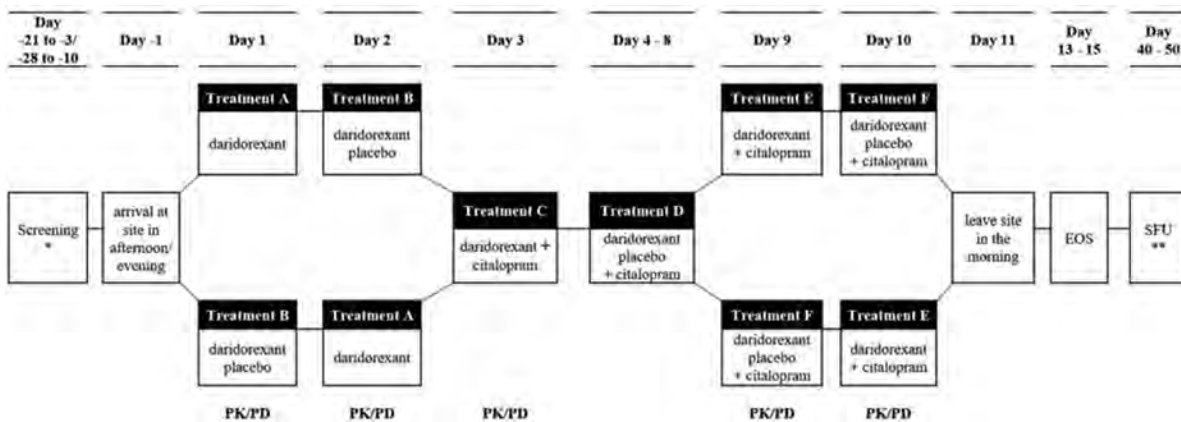
<sup>1</sup>Idorsia Pharmaceuticals Ltd, Allschwil, Basel-Landschaft, Switzerland; <sup>2</sup>Parexel Intl Corp, Berlin, Germany

**Statement of Purpose, Innovation or Hypothesis:** Daridorexant is a new potent and selective dual orexin receptor antagonist being evaluated for the treatment of insomnia. Insomnia is a common comorbidity of depression as well as anxiety and so daridorexant is likely to be administered concomitantly with agents used to treat these disorders. Citalopram, a selective serotonin reuptake inhibitor (SSRI), is one of the most widely prescribed antidepressants in many countries. The aim of this study was to investigate the pharmacokinetic (PK) and pharmacodynamic (PD) interactions between daridorexant (50 mg) and citalopram (20 mg), as well as the safety and tolerability of the coadministration.

**Description of Methods and Materials:** This was a single-center, single-blind, randomized, placebo-controlled, sequential design Phase 1 study with the inclusion of two double-blind nested crossover parts conducted in 24 healthy male and female subjects (29 – 54 yrs). Citalopram was administered together with a light breakfast while daridorexant or matching placebo was given 2 hrs later. The PK of daridorex-

ant and citalopram as well as a battery of PD tests, encompassing objective and subjective assessments on alertness, motor coordination and cognitive functions, were evaluated as shown in Figure 1. Blood sampling for PK evaluations and safety assessments (clinical laboratory, vital signs, adverse events [AEs] and ECG) were performed regularly. Pharmacokinetic parameters of daridorexant and citalopram were determined by noncompartmental analysis.

**Data and Results:** There were no relevant effects of citalopram (single dose or at steady state) on daridorexant exposure and vice versa. Pharmacodynamic variables measured after morning administration of daridorexant alone showed effects consistent with a sleep-promoting compound, including significant reduction of saccadic peak velocity, digit symbol substitution test score, visual analog scale (VAS) alertness, VAS mood and a significant increase in simple reaction time and score on the Karolinska Sleepiness Scale (KSS). Coadministration of daridorexant with a single dose of citalopram had no relevant interactions on PD parameters compared to daridorexant alone. Coadministration of daridorexant with citalopram at steady state did not lead to relevant changes in objective PD endpoints compared to daridorexant alone, apart from a decrease in unstable tracking. Relevant changes in subjective PD endpoints were only observed for VAS alertness (decrease) and the KSS score (increase) after coadministration of daridorexant with citalopram at steady state. No serious or severe AEs were reported. Overall, the most commonly reported AEs included somnolence (in 100% of subjects), headache (42%), dizziness (38%), dry mouth (29%), nausea (25%) and sleep disorder (25%). All AEs were either of mild or moderate intensity. One AE leading to study treatment discontinuation (PR prolongation) following administration of daridorexant alone resolved within 2 hrs of treatment administration. No other clinically-relevant treatment-emergent effects on ECG parameters, clinical laboratory or vital signs were observed.



Poster Number: 042 Figure 1. Study Design

**Interpretation, Conclusion or Significance:** All treatments were generally well tolerated without serious AEs. No changes in PK parameters were observed upon coadministration of daridorexant and citalopram. The effects on objective and subjective PD assessments following coadministration of daridorexant and citalopram were shown to be mainly driven by the expected CNS effects of daridorexant. Doses up to 50 mg daridorexant can be safely coadministered with citalopram.

**Poster Number: 043**

**Lack of Clinically-relevant Drug-drug Interactions for Tolvaptan at BCRP and the Oxobutyric Acid Metabolite at OATP1B1 and OAT3 Transporters in Healthy Adult Subjects**

S. E. Shoaf<sup>1</sup>, P. Bricmont<sup>1</sup>, J. Repella Gordon<sup>1</sup>

<sup>1</sup>Otsuka Pharmaceutical Development & Commercialization Inc, Rockville, MD, USA

**Statement of Purpose, Innovation or Hypothesis:** The US Food & Drug Administration (FDA) recently finalized a guidance document intended to help drug developers determine the drug-drug interaction potential of an investigational drug product. *In vitro* studies indicated that tolvaptan (TLV, IC<sub>50</sub> 8.32 μM) was a breast cancer resistance protein (BCRP) inhibitor while the oxobutyric acid metabolite of TLV (DM-4013) was an inhibitor of organic anion transport polypeptide (OATP) 1B1 (IC<sub>50</sub> 0.255 μM) and organic anion transporter (OAT) 3 (IC<sub>50</sub> 0.425 μM); the guidance indicated potential for clinical inhibition for the highest regimen of 90 + 30 mg used in autosomal dominant polycystic kidney disease (ADPKD) trials. The FDA required post-marketing clinical studies despite lack of differences in the incidence of adverse events for subjects taking TLV alone versus TLV + statins (BCRP, OATP1B1 substrates) in ADPKD trials or for subjects taking TLV + furosemide (OAT3 substrate) in congestive heart failure trials.

**Description of Methods and Materials:** Trial 1 was a four-period sequential crossover in 16 healthy adult subjects; 14 subjects completed with two subjects discontinuing in Period 1. A 5 mg dose of rosuvastatin (BCRP and OATP1B1 substrate) was administered in the fasted state in Periods 1 (Day 1), 2 (Day 3) and 4 (Day 13) with plasma PK sampling for 48 hr. A 90-mg (200 μmol) dose of tolvaptan was coadministered with rosuvastatin in Period 2. DM-4103 has a half-life around 180 hr and reaches steady state in 8 wk.<sup>1</sup> In order to rapidly achieve plasma concentrations observed following the 90 + 30 mg dose regimen of tolvaptan in ADPKD clinical trials (15.7 μM), in Period 3, 300 mg tolvaptan was given once daily for seven days (Days 5 to 11) followed by a 48-hr washout to allow time for tolvaptan to be eliminated leaving only DM-4103 in the plasma to be tested as an inhibitor of OATP1B1. Trial 2 was a three-period sequential crossover in 14 healthy adult subjects; all subjects completed. A 40-mg dose of furosemide was administered in the fasted state on Day 1 and Day 11 with plasma PK sampling for 48 hr. Tolvaptan was administered as in Trial 1 (Days 3 to 9) to produce elevated concentrations of DM-4103. Noncompartmental analysis was used to determine the three primary parameters of C<sub>max</sub>, AUC<sub>t</sub> and AUC<sub>∞</sub> for rosuvastatin and furosemide.

**Data and Results:** See Table 1. For the BCRP interaction, rosuvastatin geometric mean ratios (90% confidence intervals) for C<sub>max</sub> were 1.54 (1.26–1.88) and for AUC<sub>t</sub> were 1.69 (1.34–2.14), indicating no clinically-significant interaction at BCRP. DM-4103 produced no clinically-meaningful changes in rosuvastatin or furosemide, indicating no inhibition at OATP1B1 or OAT3.

**Interpretation, Conclusion or Significance:** The BCRP prediction assumes the drug dose is completely soluble in 250 mL; however, TLV has pH independent solubility of ~0.1g/250 mL.<sup>2</sup> For OATP1B1 and OAT3, the guidance instructs that fraction unbound for plasma protein binding (PPB) < 1% be set to 1%.

**Poster Number: 043 Table 1. Geometric Mean Ratios and 90% Confidence Intervals for Rosuvastatin (BCRP, Tolvaptan as Inhibitor; OATP1B1, DM-4103 as Inhibitor) and Furosemide (OAT3, DM-4103 as Inhibitor)**

Comparison <sup>a</sup>	C <sub>max</sub>	AUC <sub>t</sub>	AUC <sub>∞</sub>
Rosuvastatin+Tolvaptan (T) vs Rosuvastatin Alone (R), N=14	1.538	1.691	1.281 <sup>b</sup>
Rosuvastatin in presence of DM-4103 (T) versus Rosuvastatin Alone (R), N=14	1.129	1.045	0.998 <sup>c</sup>
Furosemide in presence of DM-4103 (T) versus Furosemide Alone (R), N=14	0.995–1.335	0.881–1,239	0.876–1.138
	0.907	1.04	1.018 <sup>d</sup>
	0.794–1.035	0.938–1.152	0.916–1.131

C<sub>max</sub>: maximum plasma concentration, AUC<sub>t</sub>: area under the curve to the time of the last measurable concentration, AUC<sub>∞</sub>: AUC from time 0 to infinity.

<sup>a</sup>T is test; R is Reference.

Number of subjects with parameter in both treatment periods: <sup>b</sup>n=6, <sup>c</sup>n=5, and <sup>d</sup>n=12.

DM-4103 has PPB >99.8% (data on file). Use of actual drug substance solubility and unbound fraction in plasma would produce predictions consistent with the clinical results.

#### References

1. Slizgi JR, et al. *Toxicol Sci.* 2016;149(1):237–250.
2. Australian Public Assessment Report for Tolvaptan. Feb. 2019. <https://www.tga.gov.au/sites/default/files/auspar-tolvaptan-180209.pdf>

#### Poster Number: 044

##### Do hERG Blocking Agents Further Increase the Risk of Sudden Cardiac Death in Type 1 Diabetics?

J. Taubel<sup>1</sup>, S. Cole<sup>1</sup>, H. Wibberley<sup>1</sup>, D. Camilleri<sup>1</sup>, C. Spencer<sup>2</sup>, A. Freier<sup>2</sup>, J. Camm<sup>3</sup>

<sup>1</sup>Richmond Pharmacology Ltd, London, United Kingdom; <sup>2</sup>Richmond Research Inst, London, United Kingdom; <sup>3</sup>St Georges Univ, London, United Kingdom

#### Statement of Purpose, Innovation or Hypothesis:

Type 1 diabetics have been shown to be at higher risk of sudden cardiac death (SCD) and QTc-prolongation may be a predisposing factor. It has become apparent that insulin therapy could increase the risk of hypoglycemia and lead to QT-prolongation. However, the cardiac effects of insulin therapy in the hyperglycemic state are not well studied. We have previously demonstrated that a hyperglycemic state prolongs the QTcF interval. This effect was seen to be more pronounced in female than male patients. Application of a hERG-blocking drug, moxifloxacin, during a state of hyperglycemia further prolonged the QTc interval. The variability we observed between individuals prompted our investigation into the role of the volunteers' long-term insulin regime on the response of QTc to hyperglycemia and to moxifloxacin.

#### Description of Methods and Materials:

This was a post-hoc analysis of data from 12 female type 1 diabetics who participated in a single-blinded, placebo-controlled, Phase 1 study over three days. Seven volunteers were using short-acting insulin, two were using long-acting insulin and three were using ultralong-acting insulin. On Days 1 and 3, glucose was administered intravenously to achieve blood concentrations of  $\geq 25$  mmol/L, sustained for an hour. On Day 3, 300 mg of moxifloxacin was also infused during the period of hyperglycemia. On Day 2, the volunteers were normoglycemic and a moxifloxacin placebo was administered. Time course analysis was used to assess to what extent the insulin regime modulated the effect on the QTc interval of hyperglycemia alone and in combination with moxifloxacin.

**Data and Results:** All volunteers exhibited QTc-prolongation during the hyperglycemic state, peaking two hrs after glucose administration. On Day 1, volunteers on a long-term insulin regime using either short- or long-acting insulin exhibited a similar QTc-prolongation. QTc-prolongation was 10–14 ms shorter in volunteers on ultra long-acting insulin. There was no difference in QTc-prolongation on Day 3 vs Day 1 for volunteers using long- and ultra long-acting insulin. However, QTc-prolongation was 12 ms longer on Day 3 compared to Day 1 for volunteers on short-acting insulin.

**Interpretation, Conclusion or Significance:** Our findings highlight differing responses to hyperglycemia for type 1 diabetic volunteers taking different insulins. A regime consisting of ultra long-acting insulin appeared to diminish the QTc-prolongation effect of hyperglycemia. Insulin can induce hypokalemia, which has been shown to have a prolonging effect on QTc. As endogenous insulin itself has no direct effect on the QTc interval, the observed differences may be due to the effects of the insulin regime on serum potassium. In all groups, we observed increased serum potassium during the hyperglycemic state, in line with previous findings. Volunteers using long- and ultralong-acting insulins did not exhibit QTc-prolongation upon administration of moxifloxacin, however, those using short-acting insulin exhibited a further prolongation of 12 ms. Limitations of this study included a small sample size and assessment of only female type 1 diabetics. Our findings warrant further investigation to explore how different insulin regimes impact the effects of serum potassium, hyperglycemia and moxifloxacin on QTc subintervals. Glucose concentration-effect modeling will be used to investigate how these insulin regimes differentially affect hyperglycemia and serum potassium and hence the QTc interval.

#### Poster Number: 045

##### Evaluation of Drug-Drug Interaction Potential of Vorasidenib (AG-881), a Mutant IDH1/2 Inhibitor, on the Pharmacokinetics of Lamotrigine in Healthy Adults

K. Le<sup>1</sup>, C. Prakash<sup>1</sup>, X. Jiang<sup>1</sup>, I. Hassan<sup>1</sup>, L. Steelman<sup>1</sup>, F. Yin<sup>1</sup>, R. Guo<sup>1</sup>, S. S. Pandya<sup>1</sup>, H. Yang<sup>1</sup>

<sup>1</sup>Agios Pharmaceuticals Inc, Cambridge, MA, USA

#### Statement of Purpose, Innovation or Hypothesis:

Mutant isocitrate dehydrogenase 1 and 2 (mIDH1/2) proteins catalyze production of the oncometabolite D-2-hydroxyglutarate, leading to tumorigenesis. mIDH1 and mIDH2 are found in ~70% of low-grade gliomas (LGGs). Vorasidenib is a potent, brain-penetrant, oral, pan-IDH inhibitor currently in a pivotal trial for the treatment of LGGs. The anti-epileptic drug lamotrigine is often prescribed to treat seizures and may be

**Poster Number: 045 Table 1. Statistical Comparisons of Plasma Lamotrigine PK Parameters Following 50 mg Lamotrigine Coadministered With Multiple Doses of 50 mg Vorasidenib vs Alone**

Parameter	Lamotrigine + vorasidenib (Test)		Lamotrigine alone (Reference)		GMR (%)	90% Confidence Interval	Intra-subject CV%
	Geometric LSM	n	Geometric LSM	n			
AUC <sub>0-48</sub> (ng*hr/mL)	19,440	21	20,420	22	95.16	92.98–97.39	4.36
AUC <sub>0-t</sub> (ng*hr/mL)	31,090	21	33,550	22	92.67	88.99–96.50	7.62
AUC <sub>0-inf</sub> (ng*hr/mL)	33,330	21	36,170	22	92.15	88.23–96.25	8.19
C <sub>max</sub> (ng/mL)	732.3	21	769.4	22	95.18	89.51–101.22	11.62

Geometric least-squares means (LSMs) calculated by exponentiation of the LSMs from the analysis of variance (ANOVA).

Geometric mean ratio (GMR) = 100\*(test/reference).

Intra-subject coefficient of variation (CV%) calculated as 100 x square root (exp[residual variance]-1), where the mean squared error = residual variance from ANOVA.

taken concomitantly with vorasidenib in patients with glioma. *In vitro*, vorasidenib appeared to be an inducer of uridine 5'-diphospho-glucuronyl transferase (UGT) 1A4, enzymes responsible for lamotrigine elimination. This Phase 1 study evaluated the effect of multiple doses of vorasidenib on the pharmacokinetics (PK) of a single dose of lamotrigine in healthy participants.

**Description of Methods and Materials:** This was a two-period, fixed-sequence study in 22 healthy adults (Clinicaltrials.gov NCT04015687). In Period 1, participants received a single oral dose of lamotrigine 50 mg on Day 1 and were confined for two days. In Period 2, participants were inpatient and received once-daily oral vorasidenib 50 mg on Days 1–15, and a single dose of lamotrigine 50 mg on Day 14. There were three dosing groups: Group 1 (n=4) participants initiated the study; Group 2 (n=9) participants initiated Period 1 after safety and tolerability data from ≥7 days of vorasidenib dosing in Group 1 had been reviewed; Group 3 (n=9) participants initiated Period 1 after safety and tolerability data from ≥7 days of vorasidenib dosing in Group 2 had been reviewed. Lamotrigine PK samples were taken predose and over 7 days after dosing on Period 1 Day 1 and Period 2 Day 14. Vorasidenib PK samples were taken predose and over 14 days in Period 2. Pharmacokinetic parameters were determined using noncompartmental methods. The magnitude of drug-drug interaction was assessed using a linear mixed effect model (PROC MIXED of SAS®).

**Data and Results:** Coadministration of a single dose of lamotrigine 50 mg following multiple doses of vorasidenib 50 mg resulted in similar overall and peak exposure (area under the concentration-time curve [AUC] and maximum observed concentration [C<sub>max</sub>], respectively), half-life, apparent oral clearance and volume of distribution of lamotrigine vs lamotrigine alone. AUCs and C<sub>max</sub> of lamotrigine were 5–8% lower with vorasidenib coadministration vs lamotrigine alone, and the 90% CIs of the geometric mean ratios for AUC<sub>0-t</sub>, AUC<sub>0-inf</sub> and C<sub>max</sub> all fell

within the prespecified 80% to 125% no-effect boundary, indicating that vorasidenib had no significant impact on the PK of lamotrigine (Table 1). There were no high-grade adverse events reported with lamotrigine administered alone or when coadministered with vorasidenib.

**Interpretation, Conclusion or Significance:** Vorasidenib did not affect the PK of lamotrigine when coadministered following multiple doses of vorasidenib. Therefore, no dose adjustment is recommended when lamotrigine is coadministered with vorasidenib.

#### Poster Number: 046

#### Physiologically-based Pharmacokinetic Modeling of Drug-Drug Interactions Between GB001, a DP2 Antagonist, and Substrates of CYP2C8, CYP2C9, OATP1B1/3 and P-gp

J. Shen<sup>1</sup>, I. Templeton<sup>2</sup>, H. Ortega<sup>1</sup>

<sup>1</sup>Gossamer Bio Inc, San Diego, CA, USA; <sup>2</sup>Certara UK Ltd, Sheffield, United Kingdom

**Statement of Purpose, Innovation or Hypothesis:** GB001 is a potent and highly-selective oral prostaglandin D<sub>2</sub> (DP<sub>2</sub>) antagonist in development as an orally-administered treatment for moderate to severe asthma and chronic rhinosinusitis. This study assessed the potential for drug-drug interactions (DDIs) between GB001 and substrates of CYP2C8, CYP2C9, OATP1B1/3 and P-gp using physiologically-based pharmacokinetic (PBPK) modeling and simulation.

**Description of Methods and Materials:** IC<sub>50</sub> values of GB001 against major CYPs and transporters were studied *in vitro*. A full PBPK model of GB001 was developed using SimCYP Simulator® (v17) and verified with clinical data. The PBPK model was applied to simulate DDIs between GB001 and probe substrates of CYP2C8 (rosiglitazone and repaglinide), CYP2C9 (warfarin), OATP1B1/3 (rosuvastatin) and P-gp (digoxin) in 100

**Poster Number: 046 Table 1. PBPK Simulation Results for GB001**

CYP/Transporter, Probe Substrate	Median Ratio of Probe $C_{max}$ and $AUC_{(0-\infty)}$ (5 <sup>th</sup> –95 <sup>th</sup> percentile)
CYP2C8, rosiglitazone	1.00 (1.00-1.00), 1.01 (1.00-1.02)
CYP2C8 (1/10 $K_i$ ), rosiglitazone	1.00 (1.00-1.02), 1.07 (1.03-1.19)
CYP2C8, repaglinide	1.01 (1.00-1.02), 1.05 (1.03-1.08)
CYP2C8 (1/10 $K_i$ ), repaglinide	1.02 (1.00-1.05), 1.09 (1.06-1.16)
CYP2C9, warfarin	1.00 (1.00-1.01), 1.06 (1.03-1.10)
OATP1B1/3, rosuvastatin	1.05 (1.02-1.08), 1.03 (1.02-1.06)
OATP1B1/3 (1/10 $K_i$ ), rosuvastatin	1.33 (1.15-1.60), 1.26 (1.13-1.50)
P-gp, digoxin	1.00 (1.00-1.01), 1.00 (1.00-1.01)
P-gp (1/15 $K_i$ ), digoxin	1.04 (1.01-1.09), 1.02 (1.00-1.10)

virtual subjects divided equally into 10 trials. A “worst-case” DDI was assessed by reducing calculated GB001  $K_i$  10-fold for CYP2C8 and OATP1B1/3 and 15-fold for P-gp.

**Data and Results:** The PBPK model of GB001 sufficiently described clinical pharmacokinetic (PK) profiles [ $0.5 < \text{simulated/observed ratios} < 2$  for peak drug concentrations ( $C_{max}$ ) and area under the concentration time curve (AUC)]. Physiologically-based pharmacokinetic simulations indicated a minimal effect of GB001 on PK of probe substrates at doses up to 60 mg administered once a day (Table 1).

**Interpretation, Conclusion or Significance:** Physiologically-based pharmacokinetic modeling and simulations indicate that clinically-significant DDIs between GB001 and substrates of CYP2C8, CYP2C9, OATP1B1/3 and P-gp are unlikely at GB001 doses up to 60 mg administered once a day.

Sponsored by GB001 Inc, a wholly owned subsidiary of Gossamer Bio Inc.

## Experimental Pharmacology in *In Vitro* / *In Vivo* Studies

**Poster Number: 047**

**Methotrexate Disposition, Anti-folate Activity and Metabolomic Profiling to Identify Molecular Biomarkers of Efficacy in the Collagen-induced Arthritis Mouse Model**

Y. Cho<sup>1</sup>, K. Polireddy<sup>1</sup>, R. Funk<sup>1</sup>

<sup>1</sup>Univ of Kansas Medical Ctr, Kansas City, KS, USA

**Statement of Purpose, Innovation or Hypothesis:** Methotrexate (MTX) is the cornerstone of therapy

for autoimmune arthritis. However, response to MTX is variable and unpredictable among patients. Therefore, a critical need exists to identify biomarkers to guide MTX therapy. This study aims to evaluate MTX metabolites and circulating folates as biomarkers of response to MTX treatment using the collagen-induced arthritis (CIA) mouse model and explores an untargeted metabolomic approach to identify potentially novel biomarkers of disease activity and MTX efficacy.

**Description of Methods and Materials:** Following a standard CIA disease induction protocol, DBA/1J mice were left untreated (n=8) or treated weekly with 20 mg/kg MTX subcutaneous injections (n=9). A healthy control group (n=10) was maintained for comparison and mice were sacrificed after 44 days. Disease activity was monitored using an established scoring system and by paw volume measurement using limb water volume displacement. Blood samples were collected for MTX and folate analysis and were submitted to the National Institute of Health West Coast Metabolomics Center to measure intermediates of primary metabolism, biogenic amines and lipids. Normalized peak intensity data was utilized to identify and rank metabolites using MataboAnalyst v4.0. Metabolites with a false discovery rate adjusted  $p$  value  $< 0.25$  were subjected to enrichment analysis using Chemical Similarity Enrichment Analysis (ChemRich) and metabolic networks were visualized using MetaMapp in Cytoscape v3.7.2.

**Data and Results:** Successful disease induction resulted in elevated measures of disease activity in the untreated CIA mice compared to the control group by both disease activity scores (Mean  $\pm$  SEM,  $9 \pm 1$  vs  $0 \pm 0$ ,  $p < 0.001$ ) and paw volume ( $0.48 \pm 0.02$  mL vs  $0.35 \pm 0.01$  mL,  $p < 0.001$ ). Treatment with MTX resulted in reduced disease activity compared to the untreated CIA group by both disease activity scores ( $1 \pm 0.4$  vs  $9 \pm 1$ ,  $p < 0.001$ ) and paw volume ( $0.37 \pm 0.01$  mL vs  $0.48 \pm 0.02$  mL,  $p < 0.001$ ). Erythrocyte (RBC) and plasma 5-methyl-tetrahydrofolate (5mTHF) concentrations were reduced in the MTX treated mice by 28% ( $p < 0.001$ ) and 79% ( $p = 0.003$ ), respectively. Reduced disease activity scores correlated with reduced RBC 5mTHF ( $p = 0.74$ ,  $P = 0.0007$ ) and plasma 5mTHF ( $p = 0.77$ ,  $p = 0.01$ ) and increased RBC MTX ( $p = -0.86$ ,  $p = 0.003$ ). Reduced paw volume correlated with reduced RBC 5mTHF ( $p = 0.71$ ,  $p = 0.001$ ) and plasma 5mTHF ( $p = 0.83$ ,  $p = 0.005$ ). Metabolomic enrichment analysis by ChemRich revealed that disease induction was associated with a significant class-wide reduction in unsaturated triglycerides ( $p = 2.2 \times 10^{-20}$ ) and that MTX treatment was associated with a class-wide increase in unsaturated phosphatidylcholines ( $p = 1.5 \times 10^{-8}$ ).

**Interpretation, Conclusion or Significance:** Our study demonstrated that MTX treatment was effective in

reducing arthritis disease activity in the CIA mouse model and was associated with increased RBC MTX levels and a reduction in erythrocyte and plasma 5mTHF. Association of folate level with MTX efficacy suggest that the antifolate activity of MTX is important in its efficacy and supports its role as a biomarker of drug response. Plasma metabolomic analysis suggests that lipidomic profiling may represent a useful approach to clinical biomarker development.

**Poster Number: 048**

**Predictive Performance of a Novel *In Vitro* Dissolution Setup for Nasal Suspensions. Development and Validation of a Level A *In Vitro-In Vivo* Correlation**

S. M. Berger<sup>1</sup>, U. Schilling<sup>1</sup>, E. Amini<sup>1</sup>, R. Cristofolletti<sup>1</sup>, G. Hochhaus<sup>1</sup>

<sup>1</sup>Univ of Florida Coll of Pharmacy, Gainesville, FL, USA

**Statement of Purpose, Innovation or Hypothesis:** For the assessment of nasal suspensions, an array of *in vitro* tests are described, dissolution testing is currently not playing a major role. However, dissolution might be an important descriptor for the drug development as it directly relates to pharmacokinetic (PK) and pharmacodynamic effects. A novel *in vitro* drug release method was designed and a quantitative relationship between *in vitro* drug release and *in vivo* absorption is desired in order to evaluate the biopredictive performance. The objective of this study was to develop an *in-vitro in-vivo* correlation (IVIVC) model to validate the predictive capacity of the newly-described *in vitro* method for corticosteroid nasal suspensions.

**Description of Methods and Materials:** The dissolution method employed a Transwell<sup>®</sup> system which has been recently successfully tested for inhaled corticosteroids. In comparison to conventional dissolution methods, the Transwell<sup>®</sup> system mimics the fluid capacity limited conditions in the nasal cavity. Dissolution data were generated for four highly-lipophilic intranasal corticosteroids Fluticasone propionate, Mometasone furoate, Triamcinolone acetonide and Budesonide, which are among the most commonly prescribed and over-the-counter medications used for the treatment of allergic rhinitis. Plasma concentrations of those four nasal suspensions and corresponding intravenous administrations were obtained from literature. For each drug, the *in vivo* dissolution profiles were deconvoluted from the respective plasma profile using the WinNonlin<sup>®</sup> deconvolution toolkit. A level A linear IVIVC between deconvoluted *in vivo* and *in vitro* dissolution profiles was established. To generate the predicted concentration–time profiles, % *in vivo* absorbed was calculated from the *in vitro* data based on IVIVC model and then convolved. Prediction error of the PK

parameters  $C_{max}$  and  $AUC_{last}$  were calculated and in line with the US Food & Drug Administration recommendations, predictability is established when an average absolute percent prediction error of 10% or less can be provided.

**Data and Results:** A regression analysis of the IVIVC correlation supports the conclusion that one regression line adequately fits the combined data from all three drugs and the relationship was estimated as: % *in vivo* absorbed = 0.956 % *in vitro* dissolved + 1.0526 ( $R^2 = 0.9718$ ).

The concentration–time profiles predicted by the IVIVC model adequately describe the observed data and attained a Level A correlation based on the internal and external validation since the average prediction error is less than 10%.

**Interpretation, Conclusion or Significance:** In conclusion, a Level A IVIVC describing the entire time-course of plasma concentrations was developed and validated, both internally and externally for the drug class of corticosteroid nasal suspensions. This study commends the novel Transwell<sup>®</sup> dissolution setup as a discriminative *in vitro* method that closely reflects the behavior of drug absorption *in vivo*.

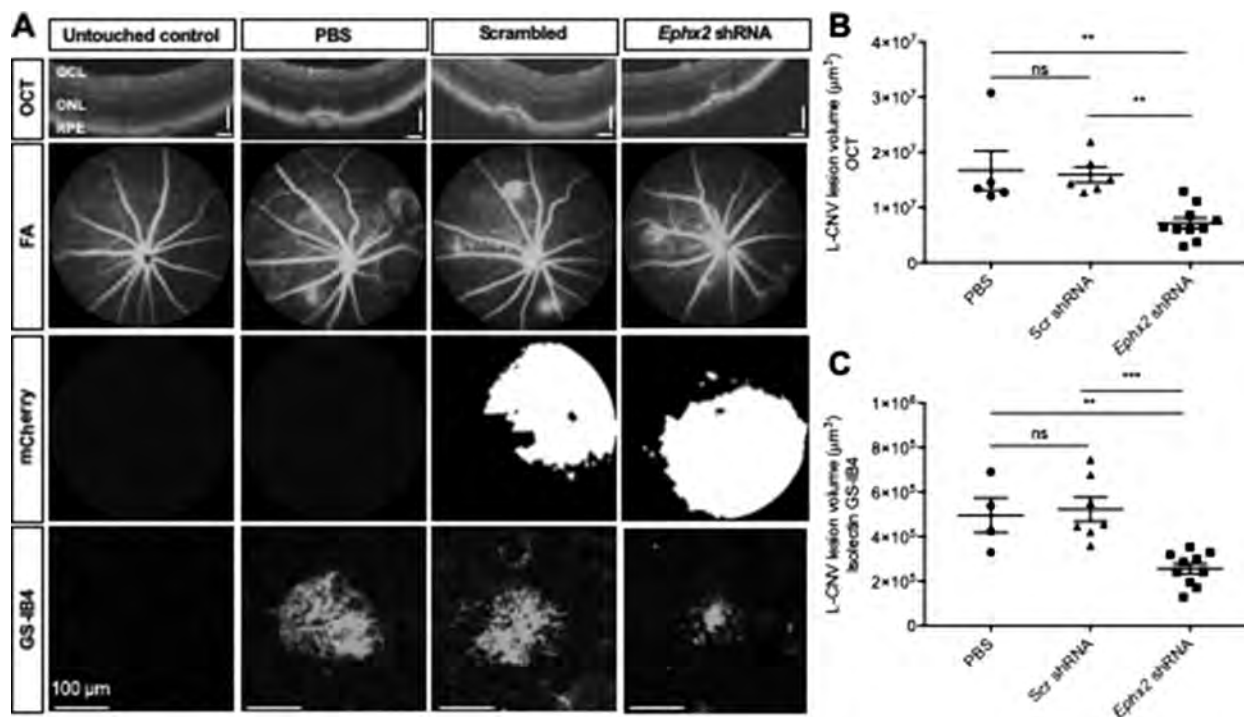
**Poster Number: 049**

**AAV8-mediated Expression of shRNA Targeting Soluble Epoxide Hydrolase Suppresses Choroidal Neovascularization**

B. Park<sup>1</sup>, S. Sardar Pasha<sup>2</sup>, K. Sishtla<sup>1</sup>, T. Corson<sup>1</sup>

<sup>1</sup>Indiana Univ School of Medicine, Indianapolis, IN, USA; <sup>2</sup>Univ of California Davis, Davis, CA, USA

**Statement of Purpose, Innovation or Hypothesis:** Wet age-related macular degeneration (AMD) is a leading cause of blindness in older people. Choroidal neovascularization (CNV), abnormal growth of new choroidal blood vessels into the neuroretina is a key pathological feature of wet AMD. Current treatment options have drawbacks and do not work for all patients. Therefore, identification of novel therapeutic targets and inhibitors is critical to address the unmet needs in antiangiogenic treatment. We identified soluble epoxide hydrolase (sEH) as a target of a novel antiangiogenic small molecule, SH-11037, and showed that intravitreal chemical inhibition of sEH suppresses CNV in mice. Other studies reported that systemic knock-out or inhibition of sEH also reduces CNV. However, ocular knockdown of sEH and gene therapy approaches targeting sEH to treat CNV have not been investigated to date. Here, we examined antiangiogenic effects of sEH knockdown using an adeno-associated virus (AAV) serotype 8 vector expressing shRNA against sEH, delivered intravitreally in a mouse laser-induced CNV model.



**Poster Number: 049** **Figure 1.** Suppression of Laser-induced CNV Formation by AAV mediated Delivery of Ephx2-shRNA

**Description of Methods and Materials:** AAV8 vectors (0.5 µl of  $1 \times 10^{11}$  gc/µL) with CMV promoter-driven sEH (*Ephx2*) shRNA, scrambled control shRNA (each with mCherry reporter) or 0.5 µL of vehicle (PBS) were injected intravitreally in 7 wk-old C57BL/6J male mice. After seven days, mice were treated with laser to induce CNV. Transduction level (mCherry fluorescence) and neovascular volume were assessed by weekly noninvasive ophthalmic imaging tools: funduscopy and optical coherence tomography. On Day 14 post laser, retina and choroid tissue of each treatment group were harvested for choroidal flatmounts, cryosectioning, protein and RNA analyses. Expression of sEH and relevant targets in treated retina and choroid tissue was assessed by qPCR and immunoblot. Choroidal neovascularization lesion volume was calculated using OCT measurements and by confocal Z-stack imaging of choroidal flatmounts stained with isolectin GS-IB4.

**Data and Results:** Fluorescence funduscopy showed efficient viral transduction and microscopic assessment revealed transduced cells localized in the photoreceptors and retinal pigment epithelial layers. Soluble epoxide hydrolase expression was reduced in retina and choroid at protein and mRNA levels. Compared to vehicle and AAV8-scrambled shRNA controls, AAV8-*Ephx2* shRNA delivery significantly-reduced CNV (Figure 1). In addition, gene expression analysis showed reduced *Vegfc* and inflammatory markers *Tnfa*, *Il1b* and *Vcam1*, but increased cytoprotective *Hmox1* in the

AAV8-*Ephx2* shRNA treatment group compared to scrambled control.

**Interpretation, Conclusion or Significance:** Intraocular knockdown of sEH inhibits CNV. Thus, depletion of sEH phenocopies the antiangiogenic effects seen with small molecule inhibitors, further demonstrating sEH as a promising therapeutic target in the treatment of CNV associated with wet AMD.

#### Poster Number: 050

##### Pharmacokinetics of Centhaquine Citrate in a Mouse Model

G. Pais<sup>1</sup>, M. Hornick<sup>2</sup>, S. Avedissian<sup>3</sup>, J. Liu<sup>1</sup>, S. Briyal<sup>1</sup>, A. Gulati<sup>1</sup>, M. Scheetz<sup>1</sup>

<sup>1</sup>Midwestern Univ Chicago Coll of Pharmacy, Downers Grove, IL, USA; <sup>2</sup>Roosevelt Univ, Schaumburg, IL, USA; <sup>3</sup>Univ of Nebraska Medical Ctr, Omaha, NE, USA

**Statement of Purpose, Innovation or Hypothesis:** Centhaquine citrate is a resuscitative agent that has significantly improved survival in hypovolemic shock. Centhaquine exhibits a biphasic decrease in concentration in rat and dog studies. The purpose of this study was to determine if centhaquine decreased glomerular filtration rates (GFR) as measured by inulin clearance. This study utilizes optical imaging techniques to visualize the effect of centhaquine citrate on inulin clearance.

**Description of Methods and Materials:** Male SKH-1 Elite mice (Crl:SKH1-*Hr<sup>hr</sup>*, n=6) were randomized to receive an intravenous bolus of near infrared fluorescent-labeled form of inulin (GFR-Vivo™ 680) plus 0.05 mg/kg centhaquine or saline. After a washout period, animals received the other treatment. Fluorescence imaging of the heart *in vivo* (BioFLECT 200 Tomographic Optical Imaging System [TriFoil Imaging, Chatsworth, CA]) was used to detect and quantify blood levels of GFR-Vivo 680 at 8, 15, 22, 29, 35, 42, 49 and 56 mins postinjection. Pharmacokinetic analyses for inulin were conducted using a standard two-compartment clearance model in Pmetrics for R. Pharmacokinetic parameters were obtained from the fitted model. A paired t-test (GraphPad Prism v8) was used to compare the clearance of inulin between groups.

**Data and Results:** A two-compartment model fit the data well (Bayesian:  $R^2=0.79$ ). The final model population median (CV%) estimates for clearance (CL), volume of distribution (V), rate transfer from central to peripheral ( $K_{CP}$ ) and peripheral to central ( $K_{PC}$ ) were: 0.12 L/h (101.2%), 0.39 L (70.6%), 4.4 h<sup>-1</sup> (90.1%) and 16.32 h<sup>-1</sup> (65.9%). Results were as follows for centhaquine and saline, respectively (mean, *p*-value): CL (0.29 L/h vs 0.43 L/h, *p*=0.51), and V (0.3 L vs 0.75 L, *p*=0.03).

**Interpretation, Conclusion or Significance:** In healthy mice, inulin clearance as a surrogate of GFR does not change with centhaquine.

**Encore:** Presented at the 32<sup>nd</sup> Meeting of the Great Lakes Chapter ASPET regional meeting, June 2019.

## Immunology/Immunotherapy

**Poster Number: 051**

### Localized Pleural Immune Conditioning to Support Immuno-oncology Therapies in MPE

V. S. Donnenberg<sup>1</sup>, A. D. Donnenberg<sup>1</sup>, D. P. Normolle<sup>2</sup>, J. D. Luketich<sup>1</sup>

<sup>1</sup>Univ of Pittsburgh School of Medicine, Pittsburgh, PA, USA; <sup>2</sup>Univ of Pittsburgh, School of Public Health, Pittsburgh, PA, USA

**Statement of Purpose, Innovation or Hypothesis:** Malignant pleural effusions (MPE) have a US incidence of more than 150,000 cases per year, a life expectancy measured in months and no effective treatment. When cancer metastasizes to the pleura, it is invariably accompanied by an influx of immune cells, but rather than mounting an effector response, these cells support invasion, angiogenesis and therapy resistance.

**Description of Methods and Materials:** Our recent studies indicate that the pleural secretome, dominated

the IL-6/IL-6R axis, plays an important role in directing local immune responses. Despite the immunosuppressive MPE environment, low levels of effector cytokines (IFN $\alpha$ , IFN $\gamma$ , TNF $\alpha$  and CXCL10) are detectable, suggesting a blunted local antitumor response. The unique physiology of the pleura and the composition MPE present an opportunity to therapeutically manipulate the tumor environment in ways that are not possible in other metastatic lesions. These include local delivery of antibody, cellular therapeutics and cytokines. Localized delivery of drugs to the pleura has the potential advantage of lowering systemic exposure and attendant toxicities.

**Data and Results:** Malignant pleural effusions provide a window into the immunobiology of metastatic cancer, a biology that is obscured in solid tumors. In addition to tumor, MPE often have abundant pleural infiltrating CD3+ T-cells, CD19+ B-cells, CD14+ macrophages and mesothelial cells, all of which are readily accessible for study when pleural fluid is drained during routine care. It is often impossible to monitor the effects of immune checkpoint therapy (other than tumor shrinkage) in solid tumors. In contrast, the routine use of tunneled pleural catheters for pleural effusion drainage provides the opportunity for sequential sampling of the metastatic environment, allowing prospective treatment monitoring, including the determination of local concentrations of cytokines/chemokines and therapeutic agents, and assessing the therapeutic alteration of immune repolarization and gauging anti-tumor effector responses. The physiologic isolation of the pleura from the systemic circulation provides an ideal anatomical space for the localized administration of large protein drugs. High molecular weight protein therapeutics remain concentrated when administered to the pleura; *e.g.* intrapleurally administered IL-2 levels are 6,000-fold higher than in the plasma. Similarly, intrapleural delivery of therapeutic antibodies should result in high local levels, but very low systemic concentrations, that may mitigate adverse reactions that are common when these drugs are given intravenously.

**Interpretation, Conclusion or Significance:** Despite recent therapeutic advances with immune checkpoint inhibitors, immunostimulatory cytokines and cellular therapeutics such as culture expanded tumor infiltrating lymphocytes and chimeric antigen receptor T cells (CAR-T), it is unknown how these therapeutics behave in the extreme MPE immune environment. We suggest that the efficacy of immuno-oncology therapeutics could be enhanced by conditioning the local environment using combinatorial immunotherapies, in which several mechanisms of tumor-mediated immune suppression are simultaneously targeted. Local delivery of combination antibody therapy to the pleural space also has the potential to decrease total delivered dose and

reduce systemic toxicities. Understanding pleural milieu and the factors that condition it will be widely applicable to all cancers that metastasize to the pleura, and may also be applicable to intraperitoneal metastases, facilitating rapid combinatorial immunotherapeutic regimens and paving the way for personalized therapy of malignant effusions and peritoneal cancers.

## Interprofessional Communication/Teams

Poster Number: 052

### Types of Interventions Made by Student Pharmacists on a General Medicine Ward at a Veterans Affairs Medical Ctr

H. Traveilyn<sup>1</sup>, N. Asal<sup>1</sup>

<sup>1</sup>Univ of Rhode Island Coll of Pharmacy, Providence, RI, USA

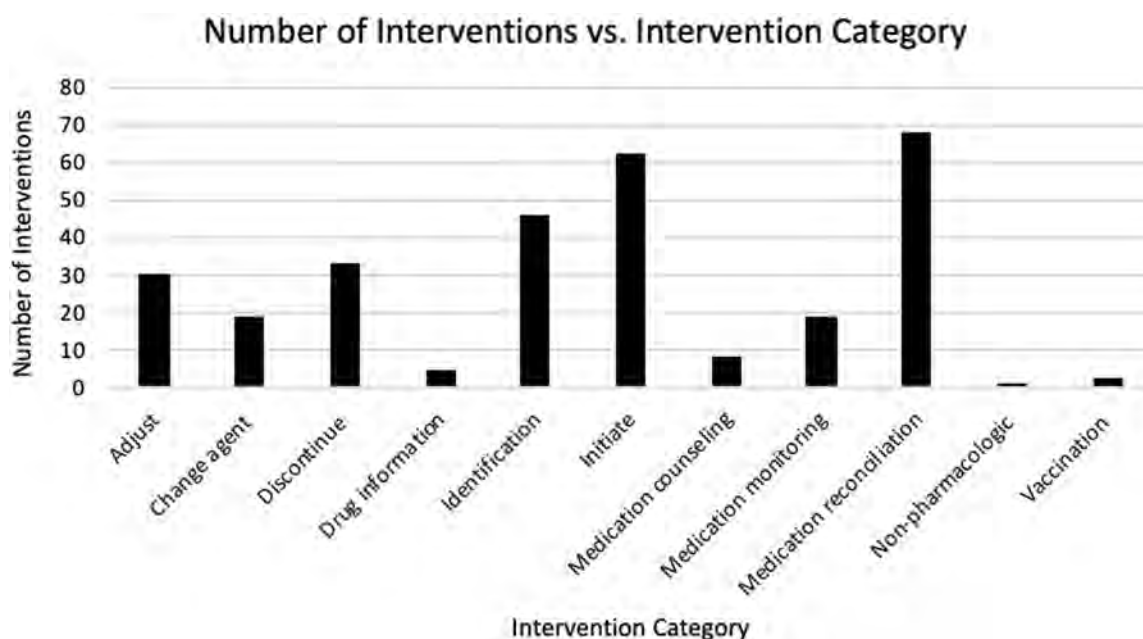
**Statement of Purpose, Innovation or Hypothesis:** The objective of this study is to describe the distribution of intervention categories made by student pharmacists in veterans on the general medicine floors at the Providence VA Medical Ctr (PVAMC) from May 13, 2019 to August 16, 2019.

**Description of Methods and Materials:** Student pharmacists on the PVAMC general medicine floors were required to document and describe the clinical interventions they made while on rotation. This deidentified data will be classified into one of 11 categories consisting of adjust (medication dose, frequency, duration or dosage form), change to a different agent, discontinue medication, drug information, identification (drug-drug interaction; drug-disease state interaction; drug allergy or adverse drug reaction), initiate medication, medication education/counseling, medication monitoring (no dosage change required or continue to monitor and assess), medication reconciliation (documented discrepancy), non-pharmacologic intervention (lifestyle/disease state education/counseling (verbal or written), referrals for additional care, or recommendation for improved adherence (i.e. pill-box)), and vaccination intervention. These categories originated from the Dept of Veterans Affairs' (VA) Pharmacists Achieve Results with Medications Documentation (PhARMD) tool; a program through which pharmacists voluntarily submit interventions they have made to the VA's national database. This information is then used to quantify pharmacists' impact on patient care. The distribution of interventions into categories will be recorded using an Excel spreadsheet. Inclusion criteria are veterans admitted to the PVAMC general medicine floors from May 13, 2019 to August 16, 2019 who received an intervention from a student pharmacist.

discontinue medication, drug information, identification (drug-drug interaction; drug-disease state interaction; drug allergy or adverse drug reaction), initiate medication, medication education/counseling, medication monitoring (no dosage change required or continue to monitor and assess), medication reconciliation (documented discrepancy), non-pharmacologic intervention (lifestyle/disease state education/counseling (verbal or written), referrals for additional care, or recommendation for improved adherence (i.e. pill-box)), and vaccination intervention. These categories originated from the Dept of Veterans Affairs' (VA) Pharmacists Achieve Results with Medications Documentation (PhARMD) tool; a program through which pharmacists voluntarily submit interventions they have made to the VA's national database. This information is then used to quantify pharmacists' impact on patient care. The distribution of interventions into categories will be recorded using an Excel spreadsheet. Inclusion criteria are veterans admitted to the PVAMC general medicine floors from May 13, 2019 to August 16, 2019 who received an intervention from a student pharmacist.

**Data and Results:** Deidentified intervention lists were collected electronically over time as a routine assignment for APPE students. They contain a brief assessment of the deidentified patient, the date of the intervention and the intervention made. Medication reconciliation, initiation of a medication and identification of discrepancies were the most common interventions made.

**Interpretation, Conclusion or Significance:** The information collected for this study can be analyzed further



Poster Number: 052 **Figure 1.** Number of Interventions vs Intervention Category

to identify educational opportunities for hospital staff and quantify the significance of the implementation of clinical pharmacists and student pharmacists into interdisciplinary teams within medical settings. Adverse drug reactions impose a heavy burden within the healthcare system accounting for up to 35.5% of older adult visits to the emergency department, increasing hospital length of stay and accumulating 30.1 billion dollars in costs per year. However, rounding pharmacists perform many important functions, such as medication reconciliation and patient counseling, resulting in fewer adverse drug events, reduced hospital stays, improved compliance and lower hospital readmission rates and costs due to the pharmacist's ability to recommend medications, modify dosages and strengths and review patient information in real-time with the interprofessional team. This information is important as it allows for better allocation of resources within healthcare systems in order to deliver exceptional patient care.

## Mechanism of Action

### Poster Number: 054

#### **SIRT6 Activation by DNA Hypomethylating Agents and Clinical Consequences on Combination Therapy in Leukemia**

H. Carraway<sup>1</sup>, A. Shatnawi<sup>2</sup>, Y. Cen<sup>3</sup>, S. Malkaram<sup>4</sup>, T. E. Fandy<sup>2</sup>

<sup>1</sup>Cleveland Clinic, Cleveland, OH, USA; <sup>2</sup>Univ of Charleston, Charleston, WV, USA; <sup>3</sup>Virginia Commonwealth Univ, Richmond, VA, USA; <sup>4</sup>West Virginia State Univ, Morgantown, WV, USA

**Statement of Purpose, Innovation or Hypothesis:** The US Food & Drug Administration-approved DNA hypomethylating agents (DHAs) like 5-azacytidine (5AC) and decitabine (DAC) demonstrated efficacy in the treatment of hematologic malignancies. Despite previous reports that showed histone acetylation changes upon using these agents, the exact mechanism underpinning these changes is unknown. In this study, we investigated the relative potency of the nucleoside analogs and non-nucleoside analogs DHAs on DNA methylation reversal and screened their effect on the enzymatic activity of the histone deacetylase sirtuin family.

**Description of Methods and Materials:** Quantitative DNA methylation reversal was assessed by DNA pyrosequencing using specific primers for *CDKN2B* (p15) gene and for the transposable element Long interspersed nuclear elements (LINE-1) in leukemia cells. The effect of DHA on sirtuins was measured using recombinant sirtuin proteins (SIRT1, SIRT2, SIRT3, SIRT5 and SIRT6) and HPLC. Bone marrow mononu-

clear cells derived from six Acute Myeloid Leukemia (AML) patients were treated with decitabine and followed by genome-wide ChIP-Seq analysis of acetylated H3K9, which is the physiological substrate for SIRT6.

**Data and Results:** The nucleoside analogs were the most potent DHAs and increased the activity of SIRT6 without showing any significant increase in other isoforms. Data pooling of the ChIP-Seq data from the six AML patients showed significant acetylation changes in 187 gene loci at different chromosomal regions including promoters, coding exons, introns and distal intergenic regions. Table 1 shows the list of genes that demonstrated acetylation decrease of H3K9. Signaling pathway analysis showed that H3K9 acetylation changes are linked to AML-relevant signaling pathways like EGF/EGFR and Wnt/Hedgehog/Notch.

**Interpretation, Conclusion or Significance:** To our knowledge, this is the first report to identify the nucleoside analogs DHAs as activators of SIRT6. Our findings provide a rationale against the combination of DHAs with SIRT6 inhibitors or chemotherapeutic agents in AML treatment due to the role of SIRT6 in maintaining genome integrity and DNA repair.

## Medication Adherence

### Poster Number: 055

#### **Identifying Determinants of Reported Lack of Affordability of Prescription Drugs**

N. S. Donnenberg<sup>1</sup>, I. Hernandez<sup>1</sup>, D. Normolle<sup>2</sup>

<sup>1</sup>Univ of Pittsburgh School of Pharmacy, Pittsburgh, PA, USA; <sup>2</sup>Univ of Pittsburgh, School of Public Health, Pittsburgh, PA, USA

**Statement of Purpose, Innovation or Hypothesis:** Rising prices of prescription drugs in the US are placing increasing barriers to accessing medications for patients. According to the National Health Interview Survey (NHIS), in 2017 nearly 8% of Americans refused at least one medication prescribed due to cost. It remains unclear, however, which factors are associated with decreased medication affordability. The objective of the study was to identify determinants of patients' failure to fill prescribed medications due to cost.

**Description of Methods and Materials:** The sample included 17,869 NHIS respondents who reported having been prescribed a medication in the past year. The outcome variable was the reported failure to fill a prescription due to cost. Independent variables included age, sex, income, a comprehensive list of comorbid conditions and social dispositions such as feelings

**Poster Number: 054 Table 1. List of Genes Showing Decrease in H3K9 Acetylation After DAC Treatment. Gray Shading Indicates Acetylation Decrease Within 2000 bp Upstream the TSS**

Gene symbol	Gene biotype	Fold change	Distance from TSS
AC002059.2	Transcribed unprocessed pseudogene	-1.7	592
AC006333.2	Antisense	-1.6	-467
AC008837.2	processed_pseudogene	-1.6	48121
AC021683.5	LincRNA	-1.7	108769
AC022558.2	Antisense	-1.7	28117
AC064807.1	Antisense	-1.5	-824
AC123912.5	processed_pseudogene	-1.8	-19674
ACTG1P21	processed_pseudogene	-1.7	-4163
ADARB2	protein_coding	-1.7	-534875
AGAP1	protein_coding	-1.9	558012
AL022318.4	protein_coding	-1.6	-62
AL137145.1	LincRNA	-1.7	35785
AL596087.2	sense_intronic	-1.5	-694
ANKRD39	protein_coding	-1.7	-2794
ATAD2B	protein_coding	-1.6	-91213
BCO1	protein_coding	-2.1	52953
BMS1P1	transcribed_unprocessed_pseudogene	-1.8	-173
CACNA1C	protein_coding	-1.8	468115
CAP1	protein_coding	-1.8	-28932
CCDC171	protein_coding	-2	567915
CECR2	protein_coding	-1.8	60852
CFAP61	protein_coding	-1.7	-813
COQ3	protein_coding	-1.8	-303
COQ8A	protein_coding	-1.9	41065
CUX1	protein_coding	-1.7	-72603
DACT1	protein_coding	-2.3	-2966
DCAF17	protein_coding	-1.6	384
DIP2C	protein_coding	-1.8	-389667
DLK1	protein_coding	-1.8	5696
DTX3L	protein_coding	-1.6	-537
EEA1	protein_coding	-2	-74930
EPN1	protein_coding	-1.6	24875
FAM129B	protein_coding	-1.9	-23288
FNDC8	protein_coding	-1.8	2522
GALNT18	protein_coding	-1.8	-198604
GAREM2	protein_coding	-1.6	13510
GDF6	protein_coding	-2.2	-5791
GPAM	protein_coding	-2.2	-368976
GRB10	protein_coding	-2.3	-171761
HAND2	protein_coding	-1.9	-13028
HMGB1P48	unprocessed_pseudogene	-2.2	-826
HOXB8	protein_coding	-1.7	-1738
HSPA9	protein_coding	-1.6	-823
ICA1L	protein_coding	-1.9	-1584
IFNGR1	protein_coding	-2.2	92852
IRF8	protein_coding	-1.8	298
KLF13	protein_coding	-1.5	-1354
KMT5B	protein_coding	-1.8	-30727
KPNA2	protein_coding	-1.9	-518
LINC02360	LincRNA	-2.1	-24267
LINC02580	LincRNA	-2.1	38010

(Continued)

Poster Number: 054 Table 1. Continued

Gene symbol	Gene biotype	Fold change	Distance from TSS
MAP4K2	protein_coding	-1.6	-10940
ME2	protein_coding	-2.1	5767
MGA	protein_coding	-1.7	39577
MIR193A	MiRNA	-1.8	-1995
MPP5	protein_coding	-1.9	-908
MT2A	protein_coding	-1.7	-398
NAPG	protein_coding	-2	18896
NDC1	protein_coding	-1.8	-559
NDUFA10	protein_coding	-1.7	-86001
OR2B11	protein_coding	-2	10796
OXSM	protein_coding	-1.5	184
PIK3C2B	protein_coding	-2	-37223
PKD1L2	polymorphic_pseudogene	-2.1	-119769
PLA2G2E	protein_coding	-1.7	-4316
PLCH1	protein_coding	-1.7	-203466
PPP1R1C	protein_coding	-2	35160
PRRC1	protein_coding	-1.8	51992
PTCH1	protein_coding	-1.8	34544
RBPJ	protein_coding	-1.6	156846
RCSD1	protein_coding	-1.6	-292
RNA5SP428	rRNA_pseudogene	-2.4	-74508
RNU6-1325P	SnRNA	-1.7	21938
RNU6-1332P	SnRNA	-1.7	-929
RPL7P6	processed_pseudogene	-2	-11350
RPS6KA2	protein_coding	-1.7	-429050
RTRAF	protein_coding	-1.7	-474
SIX1	protein_coding	-2.2	2242
SLC9A1	protein_coding	-1.8	-11980
SNAP23	protein_coding	-2	-332
SNHG5	processed_transcript	-1.9	-1047
SPAG16	protein_coding	-1.7	749422
SRCIN1	protein_coding	-2.1	-48529
TBL1XR1	protein_coding	-2	-32299
TENM4	protein_coding	-1.8	-479747
TM2D3	protein_coding	-1.8	-34590
TMEM62	protein_coding	-1.5	9822
TNFAIP8	protein_coding	-1.6	-591
TNFSF14	protein_coding	-1.9	113
TPM1	protein_coding	-2.2	25769
TRIO	protein_coding	-2.4	411399
UACA	protein_coding	-1.9	-1792
UTP18	protein_coding	-1.6	173
VCPIP1	protein_coding	-1.9	-43316
VIPR2	protein_coding	-1.8	-60456
VPS13C	protein_coding	-1.6	-972
VWF	protein_coding	-1.7	-156769
WDR27	protein_coding	-1.7	-221766
ZBTB7A	protein_coding	-1.6	-1244
ZC3H12D	protein_coding	-1.8	-2560
ZIC4	protein_coding	-1.8	-16859
ZSCAN20	protein_coding	-1.7	-944

Poster Number: 055 Table 1. Variables Associated With Failure to Prescriptions Due to Cost

	Estimate	Standard Error	p-value	Bonferroni Adjusted p-value
Intercept	-2.41	0.159		
Annual income	-1.69E-05	1.90E-06	2.00E-16	2.00E-15
Is worried about bills	1.43	0.0988	2.00E-16	2.00E-15
Feels mostly satisfied with medical care	-1	0.123	3.10E-16	3.10E-15
Has visited the emergency department in the past year	0.673	0.0971	4.20E-12	4.20E-11
History of asthma	0.63	0.105	2.00E-09	2.00E-08
History of diabetes mellitus	0.738	0.13	1.30E-08	1.30E-07
Has considered purchasing insurance through the AHCA	0.544	0.1	5.70E-08	5.70E-07
Feels mostly sad	0.511	0.137	0.00021	0.0021
Feelings mostly interfere with life	0.307	0.112	0.0065	0.065
Feels mostly hopeless	0.19	0.151	0.21	2.1

about one's neighborhood, emotions and quality of sleep. We tested the association between 33 independent variables and the outcome using univariate tests. Variables that were associated with the outcome in univariate tests, but were redundant were isolated by the Lasso sparse modeling technique in ElasticNet. The probabilities of each respondent being unable to afford his or her prescriptions was predicted from the logistic regression model.

**Data and Results:** Lack of prescription affordability was significantly associated with several demographic, clinical and socioeconomic factors (Table 1). The respondent was categorized as "unable to afford" if his or her probability was greater than a cutpoint of 0.1. The reported *p*-values are from a Type 2 likelihood ratio test and are Bonferroni adjusted. The sensitivity of the model is 71.5%, the specificity is 81.1% and the accuracy is 80.3%.

**Interpretation, Conclusion or Significance:** This study demonstrates that, in the environment of the community pharmacy, cost-based prescription refusal is a multifactorial drug therapy problem. Prescription refusal can lead to adverse events, as patients are electively forgoing pharmacotherapy as prescribed by a qualified provider. A salient finding of this study is the revelation that income is not the sole factor determining whether or not a prescription is filled. In the landscape of pharmacy and pharmacotherapy, other predisposing factors influence the decision concerning whether to use available funds to fill a prescription. Disease states, emotional dispositions and relationships between patient and provider can play key intervening roles in the successful flow of pharmacotherapy from the prescriber to the patient. To provide successful pharmacologic therapy, prescribing and dispensing providers alike must recognize and account for these risk factors as well as their downstream effects when caring for a patient.

## Model-informed Drug Development

Poster Number: 056

### Population Pharmacokinetics of Tremfya® (Guselkumab) in Subjects With Active Psoriatic Arthritis

X. Miao<sup>1</sup>, Y. Chen<sup>1</sup>, Y. Zhuang<sup>1</sup>, C. Hsu<sup>1</sup>, A. Kollmeier<sup>1</sup>, Z. Xu<sup>1</sup>, H. Zhou<sup>1</sup>, A. Sharma<sup>1</sup>

<sup>1</sup>Janssen Research & Development LLC, Spring House, PA, USA

**Statement of Purpose, Innovation or Hypothesis:** Guselkumab, a fully-human immunoglobulin G1 lambda (IgG1λ) monoclonal antibody (mAb) that binds to the p19 protein subunit of human interleukin-23 (IL-23) with high specificity and affinity, is currently being investigated in adult patients with psoriatic arthritis (PsA). Population pharmacokinetic (PopPK) analysis was conducted to characterize guselkumab pharmacokinetics (PK) following subcutaneous (SC) administration in adult patients with PsA, to identify and quantify covariates, which significantly influence PK, and to evaluate the necessity of covariate-based dosing adjustment.

**Description of Methods and Materials:** The PopPK analysis was performed using integrated data through Wk 24 from two Phase 3, randomized, double-blind, placebo-controlled, multi-center studies (DISCOVER-1 and DISCOVER-2) in adult patients with active PsA. In both studies, guselkumab 100 mg SC at Week 0, 4 and followed by every 8 wks (q8w) and guselkumab 100 mg SC every 4 weeks (q4w) were investigated. A total of 746 patients and 5,626 serum guselkumab concentration-time records were used in the PopPK analysis. The influence of subject demographic characteristics, laboratory characteristics, baseline disease characteristics and other intrinsic and extrinsic factors

on guselkumab PK were examined and quantified. Covariates model selection was conducted using a full-model approach with backward elimination (nominal  $p < 0.001$ ). The covariate model was then reduced by removing covariates with effect sizes less than 10% of the typical values of the respective PK parameter. Population pharmacokinetic analyses were performed using NONMEM<sup>®</sup>. The first-order conditional estimation with interaction (FOCE-I) method was used.

**Data and Results:** The guselkumab concentration-time profiles in PsA patients were adequately described by a one-compartment linear PopPK model with first-order absorption and first-order elimination. The typical population estimates for CL/F and V/F were 0.596 L/day and 15.5 L, respectively, at the median body weight of 84 kg. The model-derived elimination half-life was approximately 18.1 days. Body weight and diabetic comorbidity were identified as significant covariates contributing to the observed PK variability of guselkumab. Body weight was the primary covariate contributing to the observed PK variability of guselkumab and heavier subjects tend to have higher clearance and lower exposure following SC administration of guselkumab. Diabetic comorbidity was associated with 15% increase in CL/F. Nevertheless, the impact of body weight and diabetic comorbidity on PK exposure does not warrant dose adjustment based on subgroup efficacy analyses where consistent efficacy was observed regardless of body weight subgroups and diabetic status. None of the other covariates examined such as age, sex, race, subject-level positive immune response to guselkumab, hepatic function measurement, prior use of anti-TNF $\alpha$  agents, concomitant use of methotrexate, non-biologic disease-modifying antirheumatic drugs or corticosteroids and nonsteroidal anti-inflammatory drugs were found to have apparent impact on guselkumab CL/F.

**Interpretation, Conclusion or Significance:** The final PopPK model adequately described the variability and typical pharmacokinetics of guselkumab and no dose adjustment is needed for subgroups with different body weight or diabetic comorbidity.

**Poster Number: 057**

#### **Landmark Exposure-Response Modeling Analyses of Guselkumab in Patients With Psoriatic Arthritis**

Y. Chen<sup>1</sup>, Y. Zhuang<sup>1</sup>, C. Hsu<sup>1</sup>, X. Miao<sup>1</sup>, A. Kollmeier<sup>1</sup>, Z. Xu<sup>1</sup>, H. Zhou<sup>1</sup>, A. Sharma<sup>1</sup>

<sup>1</sup>Janssen Research & Development, LLC, Spring House, PA, USA

**Statement of Purpose, Innovation or Hypothesis:** Guselkumab, a fully-human immunoglobulin G1 lambda (IgG1 $\lambda$ ) monoclonal antibody (mAb) that binds to the p19 protein subunit of human interleukin-

23 (IL-23) with high specificity and affinity, is currently being investigated in adult patients with psoriatic arthritis (PsA). Landmark exposure-response (E-R) modeling analyses were conducted to characterize the relationships between guselkumab exposure metrics and clinical efficacy measures at Wks 20 and 24 following subcutaneous (SC) administration of guselkumab in adult patients with PsA, and to identify and evaluate the impact of covariates that influence clinical efficacy, and to subsequently support dose recommendation for treatment of PsA in adult subjects.

**Description of Methods and Materials:** The E-R analyses were performed using pooled data from the placebo-controlled phase (24 wks) of two randomized, double-blind, and placebo-controlled Phase 3 studies in patients with PsA (DISCOVER-1 and DISCOVER-2). In both studies, subjects were randomized to one of the following treatment groups: guselkumab 100 mg SC at Week 0, 4 and followed by every 8 wks (q8w), guselkumab 100 mg SC every 4 wks (q4w) and placebo. Data from 1,120 patients were included in the final dataset for the E-R analyses. The probability of achieving the American College of Rheumatology response (ACR20/50/70) and the Investigator's Global Assessment (IGA) response (IGA0/1 and IGA0) was parameterized to ordered categorical variables. Ordinal logistic regression models, which assumed a maximum drug effect ( $E_{max}$ ) relationship between pharmacokinetic exposure metrics and efficacy response rates, were developed to explore the relationship between systemic guselkumab exposure (model-predicted cumulative AUC from Week 0 to Week 24,  $AUC_{0-24w}$ ; model-predicted average concentration at steady-state  $C_{ave,ss}$ ; and observed trough serum concentration at Week 20,  $C_{trough,wk20}$ ) and the probability of achieving ACR responses and IGA responses at Weeks 20 and 24.

**Data and Results:** The final E-R models adequately described the observed data. For the E-R models of the ACR20/50/70 responses, the baseline DAS28(CRP) score and baseline Psoriasis Area and Severity Index (PASI) score were identified as significant covariates based on  $E_{max}$ , with a trend indicating that patients with lower baseline DAS28 scores or with higher baseline PASI scores tended to have higher ACR20/50/70 responses. For the E-R models of the IGA1/0 and IGA0 responses, the baseline PASI score was identified to be a covariate on the intercept and  $E_{max}$ , with a trend showing that patients with lower baseline PASI scores had higher IGA0/1 and IGA0 responses. Simulation results suggested that the differences in ACR and IGA responses between SC guselkumab 100 mg q8w and 100 mg q4w dose regimens were minimal in each of the subgroups stratified by either the baseline DAS28 (CRP) score ( $\leq 5.1$  vs  $> 5.1$ ) or the baseline PASI score ( $\leq 5.8$  vs  $> 5.8$ ).

**Interpretation, Conclusion or Significance:** The landmark E-R modeling has confirmed that SC guselkumab 100 mg q8w and 100 mg q4w have similar effects in improving the signs and symptoms of PsA, as measured by ACR20/50/70 and IGA0/1 responses in patients with PsA; and no dose adjustment is needed for subgroups with different baseline DAS28(CRP) or baseline PASI score.

**Poster Number: 058**

**Longitudinal Exposure-Response Modeling Analyses of Guselkumab in Patients With Psoriatic Arthritis**

C. Hsu<sup>1</sup>, Y. Chen<sup>1</sup>, Y. Zhuang<sup>1</sup>, X. Miao<sup>1</sup>, A. Kollmeier<sup>1</sup>, Z. Xu<sup>1</sup>, H. Zhou<sup>1</sup>, A. Sharma<sup>1</sup>

<sup>1</sup>Janssen Research & Development LLC, Spring House, PA, USA

**Statement of Purpose, Innovation or Hypothesis:** Guselkumab, a fully-human immunoglobulin G1 lambda (IgG1λ) monoclonal antibody (mAb) that binds to the p19 protein subunit of human interleukin-23 (IL-23) with high specificity and affinity, is currently being investigated in adult patients with psoriatic arthritis (PsA). Longitudinal exposure-response (E-R) modeling analyses were used to characterize the relationships between guselkumab exposure and the progression of clinical efficacy measures (ACR20, ACR50 and ACR70) following subcutaneous (SC) administration of guselkumab in adult patients with PsA and to identify and evaluate the impact of covariates that may influence clinical efficacy.

**Description of Methods and Materials:** The analyses were performed using pooled data from the placebo-controlled phase (24 wks) of two randomized, double-blind and placebo-controlled Phase 3 studies in patients with PsA (DISCOVER-1 and DISCOVER-2). In both studies, guselkumab 100 mg SC at Week 0, 4 followed by every 8 wks (q8w) and guselkumab 100 mg SC every 4 wks (q4w) were investigated. ACR responses from 1,116 subjects were utilized in the analysis. A sequential longitudinal E-R modeling approach was used to characterize the ACR response-time profiles. The pharmacokinetics (PK)-related parameters were provided by the final population PK model, and the pharmacodynamics-related parameters were subsequently estimated. For ACR responses, a proportional-odds logistic regression model was used, with an additive placebo effect over time and a semi-mechanistic indirect response model structure.

**Data and Results:** Two covariates, the baseline Psoriasis Area and Severity Index (PASI) score and disease duration, were identified to be statistically significant during the covariate selection process and consequently included in the final longitudinal E-R model. The observed ACR response progress was well

described by the final longitudinal E-R model. Simulation results demonstrated the superiority of the guselkumab treatment over placebo and do not reveal discernible differences in ACR responses between the 100 mg q8w and 100 mg q4w regimens over 24 wks in the overall population. Results also indicated that the two identified covariates have small impacts on ACR responses.

**Interpretation, Conclusion or Significance:** Longitudinal ER modeling has confirmed that Guselkumab 100 mg at Weeks 0 and 4, then q8w and 100 mg q4w, have similar effects in improving the ACR responses and no dose adjustment is needed for subgroups with different baseline disease duration or baseline PASI scores.

**Poster Number: 059**

**Detection and Impact of Hysteresis When Evaluating a Drug's QTc Effect Using Concentration-QTc Analysis**

J. Liu<sup>1</sup>, B. Darpo<sup>2</sup>, D. Huang<sup>1</sup>, D. Marathe<sup>3</sup>, Y. Sun<sup>1</sup>, G. Ferber<sup>4</sup>

<sup>1</sup>US Food & Drug Administration, Silver Spring, MD, USA; <sup>2</sup>ERT, Rochester, NY, USA; <sup>3</sup>Merck & Co Inc, Kenilworth, NJ, USA; <sup>4</sup>Statistik Georg Ferber GmbH, Riehen, Switzerland

**Statement of Purpose, Innovation or Hypothesis:** Early phase studies quantify the QTc prolongation potential for the drug using linear concentration-QTc (C-QTc) models, assuming no delay between plasma concentrations and QTc changes, i.e., hysteresis. To detect and quantify hysteresis and its impact on study interpretation, a large number of simulation studies was conducted.

**Description of Methods and Materials:** The simulation employed a one-compartmental pharmacokinetic model with an effect compartment to produce QTc hysteresis ranging from 0.25 to 4 hrs. The study scenarios included five different dose levels (including placebo; in a crossover design), three different drug half-life and a set of dense and clinically realistic PK/ECG sampling scheme. The hysteresis was quantified using a novel proposed method (enGRI) to account for delay and magnitude of QTc effects.

**Data and Results:** With realistic sampling, the rate of false negative QT (with 10 msec prolongation) studies (FN) increased proportional to the delay, even for delays shorter than 1 hr. With an enGRI threshold ( $\gamma$ ) of 2 msec, the FN of QTc prolongation with undetected delay (i.e.,  $\text{enGRI} \leq \gamma$  as 2 msec) is well controlled, i.e., at the same level as FN without hysteresis. For  $\text{enGRI} > 2$  msec, the specificity of detecting hysteresis is  $>90\%$  throughout investigated scenarios.

**Interpretation, Conclusion or Significance:** We propose the incorporation of enGRI when interpreting

results from C-QTc analysis intended to exclude small QTc effects.

## Novel Use of Therapeutics/Drug Repurposing

Poster Number: 060

### Physiologically-based Pharmacokinetic Model to Predict Amiloride Pharmacokinetics After Intranasal Administration

V. K. Yellepeddi<sup>1</sup>, M. Azzeh<sup>2</sup>, S. Davies<sup>3</sup>, J. Strauss<sup>3</sup>, M. Battaglia<sup>3</sup>

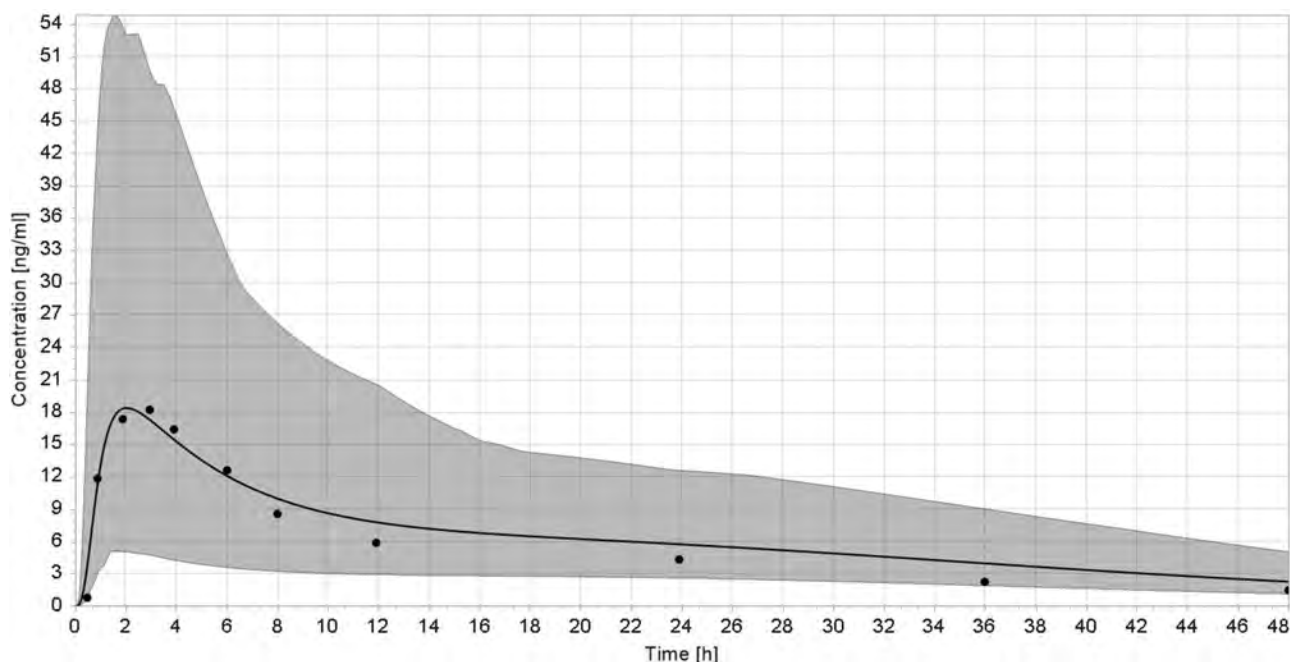
<sup>1</sup>Univ of Utah, Salt Lake City, UT, USA; <sup>2</sup>Mohammad Bin-Rashid Univ, Dubai UAE; <sup>3</sup>The Centre for Addiction & Mental Health, Toronto, ON, Canada

**Statement of Purpose, Innovation or Hypothesis:** Anxiety disorders (AD) are the most common mental illnesses in every age group, affecting 25% of children and an estimated 40 million adults in the US. Despite the advantages of newer medications, overall rates of treatment efficacy, and duration of illness have not improved. Amiloride, a diuretic agent, has shown efficacy in treating AD in preclinical models by inhibiting the acid-sensing ion channels (ASIC). By delivering amiloride via nasal route, rapid onset of action can be achieved due to direct “nose-to-brain” access. Therefore, our ultimate goal is to conduct a pharmacokinetic (PK) study of amiloride after intranasal

administration in healthy human volunteers. However, as a first step towards the preparation of the human PK study, we would like to utilize the physiologically-based PK (PBPK) modeling approach to predict the pharmacokinetics of amiloride after intranasal administration.

**Description of Methods and Materials:** We developed a whole-body PBPK model for the amiloride using the software PK-Sim<sup>®</sup>, v7.4.-Build 127. The nasal cavity compartment for humans was added using the MoBi<sup>®</sup>, v7.4. The nasal cavity was modeled using the following four default subcompartments: blood, plasma, interstitial fluid and the intracellular compartments. These subcompartments were linked to the entire PBPK model through arterial and venous blood compartments. Initially, a PBPK model of amiloride after oral administration in humans was developed and validated using digitized data obtained from published studies on oral pharmacokinetics of amiloride. The validated model was then used to simulate the concentrations of amiloride in brain tissue and plasma pharmacokinetics following intranasal administration in virtual humans.

**Data and Results:** The initial PBPK model of amiloride exposure after a single oral dose accurately described the plasma concentrations for a population of healthy human volunteers. The observed concentrations were within 5<sup>th</sup> to 95<sup>th</sup> percentiles of the predicted concentrations (Figure 1). The simulations of amiloride PK after intranasal administration showed



**Poster Number: 060** **Figure 1.** Amiloride Predicted (Solid Line) and Observed (Dots) Plasma Concentration-time Profiles After Oral Administration. Population Simulation (n=100) Geometric Means are Shown as Lines; the Shaded Area Represents the 5<sup>th</sup> to 95<sup>th</sup> Percentiles of the Predicted Concentrations

that amiloride rapidly entered the brain significantly faster (~3 mins) when compared to the oral route (~11 hrs) at the same dose of 5 mg. These data indicate the potential of the intranasal route of administration of amiloride over the oral route of administration for achieving rapid levels in the brain.

**Interpretation, Conclusion or Significance:** A whole-body PBPK model of amiloride after oral administration was developed and evaluated using observed clinical data from published literature. The evaluated model was modified to incorporate the nasal cavity compartment to enable the prediction of amiloride PK after intranasal/inhalational administration. The oral PBPK model accurately predicted the PK of amiloride of human subjects. The evaluated model predicted that at the same dose, amiloride reached rapidly in the brain after intranasal/inhalational route of administration when compared to the oral route of administration. The next step in this research is to validate the intranasal/inhalational model using clinical data. Furthermore, the relationship between exposure and pharmacodynamic activity of amiloride has to be established using pharmacodynamic data involving the efficacy of amiloride in reducing the anxiety.

## Oncology/Immuno-oncology

### Poster Number: 061

#### Evaluation of the Impact of Renal Impairment on the Pharmacokinetics of Glasdegib

N. Shaik<sup>1</sup>, R. LaBadie<sup>2</sup>, B. Hee<sup>1</sup>, G. Chan<sup>3</sup>

<sup>1</sup>Pfizer Inc, La Jolla, CA, USA; <sup>2</sup>Pfizer Inc, Groton, CT, USA; <sup>3</sup>Pfizer Inc, Collegeville, PA, USA

**Statement of Purpose, Innovation or Hypothesis:** Glasdegib is a selective, oral inhibitor of hedgehog signaling, a pathway implicated in human leukemias. This study estimated the effect of renal impairment (RI) on the pharmacokinetics (PK) of a single approved dose (100 mg) under fasted conditions.

**Description of Methods and Materials:** This open-label, parallel-group study (NCT03596567) included 18 participants (n=6 per group): age- and weight-matched controls, normal estimated glomerular filtration rate ( $\geq 90$  mL/min); moderate RI,  $\geq 30$  to  $< 60$  mL/min; severe RI,  $< 30$  mL/min. Blood was collected up to 120 hrs postdose to assess plasma glasdegib concentrations and protein binding. Pharmacokinetic parameters area under the plasma concentration–time curve from time 0 to infinity ( $AUC_{inf}$ ) and maximum plasma concentration ( $C_{max}$ ) were calculated (non-compartmental analysis of concentration–time data), and natural log-transformed  $AUC_{inf}$  and  $C_{max}$  for each RI group (Test) were compared (one-way analysis of variance) with controls (Reference). Estimates of adjusted mean dif-

ferences (Test-Reference) and 90% confidence intervals (CIs) were obtained. Adjusted mean differences and 90% CIs for differences were exponentiated to estimate the ratio of adjusted geometric means (Test/Reference) and 90% CIs for the ratios.

**Data and Results:** All participants completed the study. There were five all-causality adverse events (mild) in three participants; two were treatment related. Geometric mean ratio (90% CI) for  $AUC_{inf}$  and  $C_{max}$  vs controls: moderate RI, 205% (142–295%) and 137% (97–193%); severe RI, 202% (146–281%) and 120% (76.9–188%). Median time to  $C_{max}$ : each RI group, 2.0 hrs; controls, 1.5 hrs; range, 1.0–2.0 hrs (all groups). Mean oral clearance decreased by ~50% in both RI groups vs controls. Plasma free fraction was not altered by RI.

**Interpretation, Conclusion or Significance:** Glasdegib exposure was ~2-fold higher in participants with moderate and severe RI vs controls, with similar exposure observed in each RI group. A single approved dose of glasdegib was well tolerated in RI and in controls.

**Encore:** Published online in *Clinical Pharmacology and Therapeutics*; vol 107, March 2020.

### Poster Number: 062

#### Eflapegrastim (Rolontis), a Potent Long-acting G-CSF: Integrated Clinical Pharmacokinetic/Pharmacodynamic Results

D. Greene<sup>1</sup>, P. Kollis<sup>1</sup>, S. Huang<sup>1</sup>, S. Chawla<sup>1</sup>, F. Lebel<sup>1</sup>, J. Barrett<sup>1</sup>

<sup>1</sup>Spectrum Pharmaceuticals Inc, Irvine, CA, USA

**Statement of Purpose, Innovation or Hypothesis:** Eflapegrastim (E), a novel, long-acting G-CSF, consists of a G-CSF analog and a recombinant IgG4 Fc fragment conjugated at their N-termini via a short polyethylene glycol linker. In nonclinical studies, E showed increased uptake to bone marrow and at least three-fold increased potency vs pegfilgrastim (P). The potential of E to provide clinical benefit was demonstrated in two pivotal Phase 3 trials (NCT02643420, NCT02953340); E was noninferior ( $p < 0.0001$ ) to P at 60% of the G-CSF dose of P (3.6 mg vs 6.0 mg, respectively).

**Description of Methods and Materials:** The pharmacokinetics/pharmacodynamics (PK/PD) of E was assessed after subcutaneous (SC) administration in six studies: two studies in healthy subjects (doses of 1.1 to 350  $\mu$ g/kg; 0.3 to 96  $\mu$ g/kg G-CSF); one in breast cancer patients (BCP) treated with docetaxel and cyclophosphamide chemotherapy (TC) in the adjuvant or neoadjuvant settings at E doses of 45, 135 and 270  $\mu$ g/kg; (12.3, 36.8 and 73.6  $\mu$ g/kg G-CSF, respectively) and three studies in BCP treated with TC at a fixed dose of E of 13.2 mg (3.6 mg G-CSF). BCP received a minimum of four cycles of TC treatment. Pharmacokinetics

of E was evaluated in Cycles 1 and 3. In each cycle E or P was administered 24 hrs following TC. Serum levels of E were determined via enzyme-linked immunosorbent assay (ELISA). Pharmacokinetics was calculated by noncompartmental analysis. The pharmacodynamics (PD) of P was evaluated at a fixed dose of 6 mg G-CSF. Pharmacodynamics for both E and P was determined by calculating area under the absolute neutrophil counts (ANC) and effect curve (AUEC<sub>change</sub>) in blood samples through 22 days postdose; urine samples were studied for E in healthy subjects. Antibodies to E and P (ADA) were determined in serum by ELISA and effect on safety and efficacy evaluated. Population PK (PopPK) analysis characterized the PK of E in Phase 3 studies.

**Data and Results:** Eflapegrastim had a greater effect than P on AUEC<sub>change</sub> at comparable G-CSF doses. Consistent with the mechanism of action (target-mediated clearance by neutrophils), E showed nonlinear PK, with exposure (AUC) increasing greater than dose-proportional. Absolute neutrophil counts C<sub>max</sub> and ANC AUC increases were less than dose proportional. Statistically-significant PopPK covariates included body weight, ANC on clearance and body weight on volume of distribution. Although statistically significant, the effect of E on body weight was not clinically relevant since the effect on ANC across weight groups was similar with comparable incidence and duration of severe neutropenia across weight groups; thus, supporting a fixed dose of E. The effect of ANC on E clearance was consistent with mechanism; an increase in ANC increased E clearance resulting in decreased exposure. The presence of antidrug antibodies for E was similar to what was observed for P and did not affect PK, safety or efficacy. Eflapegrastim was not found in urine.

**Interpretation, Conclusion or Significance:** The PK/PD of E and P are consistent with target mediated clearance by neutrophils, where ANC increased with dose and clearance increased with increasing ANC. Eflapegrastim's increased potency may offer better support for highly myelosuppressive, dose-dense treatment regimens compared to current therapies.

**Encore:** Published online in *Clinical Pharmacology and Therapeutics*; volume 107, March 2020.

#### Poster Number: 063

**Pharmacokinetics and Safety of Glasdegib in Participants With Moderate or Severe Hepatic Impairment: A Phase 1, Open-label, Single-dose, Parallel-group Study**  
J. Masters<sup>1</sup>, R. LaBadie<sup>2</sup>, J. Salageanu<sup>2</sup>, J. Li<sup>1</sup>, N. Shaik<sup>1</sup>

<sup>1</sup>Pfizer Inc, La Jolla, CA, USA; <sup>2</sup>Pfizer Inc, Groton, CT, USA

**Statement of Purpose, Innovation or Hypothesis:** Glasdegib (PF-04449913) is a small-molecule selective inhibitor of hedgehog signaling, a pathway implicated in human leukemias. The majority of glasdegib is eliminated hepatically with <20% excreted renally. Mild hepatic impairment in patients does not affect glasdegib pharmacokinetics (PK); we further assessed PK and safety in otherwise healthy participants with moderate or severe hepatic impairment.

**Description of Methods and Materials:** This open-label, parallel-group study (NCT03627754) enrolled 24 participants; eight each with severe hepatic impairment (Child-Pugh class C), moderate hepatic impairment (class B), or normal hepatic function (control, age/weight-matched to hepatic impairment cohorts). After a single oral 100 mg glasdegib dose under fasted conditions, blood samples for protein binding and PK were taken up to 120 hrs. Pharmacokinetic parameters for total and unbound drug were calculated using standard noncompartmental methods and a one-way analysis of variance (ANOVA) model was used to compare cohorts.

**Data and Results:** Glasdegib plasma exposures were similar to controls in moderate hepatic impairment and lower in severe hepatic impairment, while unbound glasdegib exposures were similar to controls in both hepatic impairment cohorts (Table 1). Maximum plasma concentrations were reached within 4 hrs. No treatment-related adverse events or clinically-significant changes in laboratory values, vital signs or ECGs were observed.

**Interpretation, Conclusion or Significance:** Moderate or severe hepatic impairment did not have a clinically-meaningful effect on glasdegib exposure and a single dose was well tolerated in participants with hepatic impairment.

**Encore:** Published online in *Clinical Pharmacology & Therapeutics*, Vol 107, March 2020.

#### Poster Number: 063 Table 1. Statistical Summary (ANOVA) of Plasma Glasdegib (Unbound and Total) PK Parameters

	Unbound Glasdegib GMR, % [90% CI]	Total Glasdegib GMR, % [90% CI]
<b>Moderate Hepatic Impairment</b>		
AUC <sub>inf</sub> (ng·hr/mL)	118 [89, 157]	111 [78, 157]
C <sub>max</sub> (ng/mL)	101 [78, 130]	95 [70, 128]
<b>Severe Hepatic Impairment</b>		
AUC <sub>inf</sub> (ng·hr/mL)	116 [82, 165]	76 [52, 111]
C <sub>max</sub> (ng/mL)	89 [60, 132]	58 [38, 89]

Normal hepatic function cohort is the control group. GMR expressed as test/control. CI: confidence interval; GMR: adjusted geometric mean ratio.

**Poster Number: 064****Preliminary Clinical Pharmacokinetic Analysis of CARTITUDE-1, a Phase 1b/2 Study of JNJ-4528 (BCMA CAR-T) Cell Therapy in Patients With Relapsed and/or Refractory Multiple Myeloma**

I. Singh<sup>1</sup>, E. Zudaire<sup>1</sup>, J. Jasielec<sup>2</sup>, D. Madduri<sup>3</sup>, A. Banerjee<sup>1</sup>, J. Goldberg<sup>1</sup>, Z. Wang<sup>4</sup>, Y. Sun<sup>1</sup>, W. Wang<sup>1</sup>, A. Sharma<sup>1</sup>

<sup>1</sup>Janssen Research & Development LLC, Spring House, PA, USA; <sup>2</sup>Univ of Chicago, Chicago, IL, USA; <sup>3</sup>Mount Sinai Medical Ctr, New York, NY, USA; <sup>4</sup>Legend Biotech, Piscataway, NJ, USA

**Statement of Purpose, Innovation or Hypothesis:**

JNJ-68284528 (JNJ-4528) is a chimeric antigen receptor T cell (CAR-T) therapy containing two B-cell maturation antigen (BCMA)-targeting single-domain antibodies designed to confer avidity. The primary objectives of the study were to characterize the safety of JNJ-4528 and to confirm the Phase 2 dose in patients with relapsed and/or refractory multiple myeloma. Preliminary clinical pharmacokinetic (PK) and PK-response analyses of the ongoing Phase 1b/2 study, CARTITUDE-1 (NCT03548207), are presented here.

**Description of Methods and Materials:** JNJ-4528 was administered as a single infusion at the target dose of  $0.75 \times 10^6$  CAR+ T cells/kg. For PK, blood and bone marrow samples were analyzed to determine JNJ-4528 CAR+ T cell and transgene levels. Noncompartmental analysis and PK/pharmacodynamic modeling were conducted to describe JNJ-4528 PK properties, and the relationship between PK, biomarkers, safety and efficacy endpoints was explored.

**Data and Results:** As of data cutoff in June 2019, preliminary results show peak expansion of CAR+ T cells and transgene levels (range ~9,800–73,000 copies/ $\mu$ g gDNA; n=24) 9 to 14 days after infusion and persistence in both blood and bone marrow for at least up to 4 wks after dosing. Expansion of CAR+ T cells coincided with decreases in levels of soluble BCMA, serum M-protein and/or Free Light Chains. Levels of several serum cytokines (e.g., IL-6) increased, coinciding with expansion of JNJ-4528 and the onset of cytokine release syndrome. The overall confirmed response rate per International Myeloma Working Group criteria was 91% at a median follow-up of 3 mos (range 1–10 mos) with continued deepening of responses and achieving negative minimal residual disease status.

**Interpretation, Conclusion or Significance:** In summary, JNJ-4528 treatment of patients with relapsed and/or refractory multiple myeloma results in expansion and persistence of CAR+ T cells and strong clinical activity. Preliminary PK and PK-response analyses support continued clinical investigation of JNJ-4528 at the current dose.

**Additional authors:** Saad Z. Usmani (Levine Cancer Inst – Atrium Health, Charlotte, NC, USA), Sundar Jagannath (Mount Sinai Medical Ctr, New York, NY, USA), Jesus G. Berdeja (Sarah Cannon Research Inst, Nashville, TN, USA), Liviawati Wu (Janssen R&D, San Francisco, CA, USA), Jordan M. Schechter (Janssen R&D, Raritan, NJ, USA), Adrienne Clements Egan (Janssen R&D, Spring House, PA, USA), Dong Geng (Legend Biotech USA, Piscataway, NJ, USA), Jennifer Marino (Janssen R&D, Spring House, PA, USA)

**Encore:** Published online in *Clinical Pharmacology and Therapeutics*, Vol 107, March 2020 (<https://doi.org/10.1002/cpt.1732>).

**Pain Management****Poster Number: 065****Analgesic Effect of Delta-9-Tetrahydrocannabinol on Patients With Chronic Neuropathic Pain During a Four-week Period: A Pilot Study**

F. J. Goldstein<sup>1</sup>, K. Galluzzi<sup>1</sup>, M. Brown<sup>1</sup>, J. Smith<sup>1</sup>, J. Lubeck<sup>1</sup>

<sup>1</sup>Philadelphia Coll of Osteopathic Medicine, Philadelphia, PA, USA

**Statement of Purpose, Innovation or Hypothesis:**

The current US Food & Drug Administration (FDA) approved armamentarium for treatment of neuropathic pain (NP) includes calcium channel alpha-2-delta ligands (gabapentin, pregabalin) and a selective serotonin-norepinephrine re-uptake inhibitor (duloxetine); however, tricyclic antidepressants (amitriptyline) and antiepileptic agents (carbamazepine) have also been employed. Most have limited effectiveness and/or cause intolerable adverse reactions, leading to discontinuation. Neuropathic pain patients have also been treated with opioid analgesics, which have their own attendant risks (e.g., addiction, hyperalgesia, endocrinopathy) and limited efficacy. Delta-9-Tetrahydrocannabinol (THC) (dronabinol), C-III, is FDA-approved as an appetite stimulant and antiemetic. Doses ranging from 2.5 mg/day to 40 mg/day have been employed. As an anti-emetic, efficacy is achieved in doses of 5 mg three or four times daily. Dronabinol is not currently FDA-approved for treatment of chronic NP. Studies have found evidence supporting the analgesic effects of cannabinoids across various neuropathic disorders but many lacked scientific rigor.

**Description of Methods and Materials:** *Inclusion Criteria:* 18 to 65 years of age; diagnosis of NP of two or more months duration. *Exclusion Criteria:* non-English speaking; cardiovascular conditions; epilepsy or any seizure disorder; liver function problems; depression or other psychological problems as determined by a score

of  $\geq 10$  on the PHQ-9 screen; substance use disorder as determined by a score of  $\geq 18$  on the SOAPP-R; taking antidepressants for less than 8 wks antipsychotics, Alzheimer's Disease medications or CNS stimulants. From referring physicians, a request was made for all lab results taken within one year prior to recruitment including serum blood urea nitrogen, serum creatinine and Liver function Tests. A urine drug screening (UDS) including MS/GC confirmation of any positive results was performed. Any discrepancy between positive UDS data and information given by the patient resulted in termination from the investigation. Patients were seen weekly with vital signs taken. Each day, the study patient completed a 0–10 pain diary three times daily. In addition, they recorded how much of their pain medications they took that day. Weeks One and Two: establish each patient's baseline pain scores and analgesic usage. Week 3: up-titration process initiated; 5 mg THC orally at bedtime. Weeks Four to Six: dose increased 5 mg/week. Goal was 20 mg in Week 6. Any patient experiencing an undesirable adverse event was withdrawn.

**Data and Results:** Thus far, six patients have completed the full up-titration to 20 mg on Week 6. The average pain score dropped from 4.9 to 2.7 at end of Week 6. Of the five who were using analgesics, most were able to decrease dosages of gabapentin, carbamazepine and ibuprofen.

**Interpretation, Conclusion or Significance:** In this limited pilot study to date, six patients completed the four-week up-titration from daily 5 mg THC to 20 mg THC. The average reduction in pain scores was 44.9%. In addition, most patients used less gabapentin, carbamazepine and ibuprofen. Our investigation continues to the goal of studying a total of 20 patients who complete the 20 mg per day goal.

## Pediatrics

### Poster Number: 066

#### Postoperative Effect of Midazolam Premedication in Pediatric Patients With Obstructive Sleep Apnea

A. Garcia<sup>1</sup>, S. Rana<sup>2</sup>, D. Preciado<sup>2</sup>, C. Abdallah<sup>2</sup>

<sup>1</sup>George Washington Univ, Washington, DC, USA;

<sup>2</sup>Children's National Health System, Washington, DC, USA

**Statement of Purpose, Innovation or Hypothesis:** Midazolam is a commonly used premedication in anesthesia. Data regarding sedative effect of midazolam on pediatric patients with moderate to severe obstructive sleep apnea (OSA) undergoing tonsillectomy and adenoidectomy (T&A) is limited. We hypothesized that preoperative midazolam may increase emergence and

discharge times in pediatric patients with OSA after T&A.

**Description of Methods and Materials:** This study is a retrospective chart review of patients at Children's National Health System who underwent T&A between July 2014 and December 2015. Patients who received midazolam were compared to patients who did not receive midazolam. Demographic data included age, gender, apnea-hypopnea score, body mass index, diagnosis, American Society of Anesthesiologists physical status classification score, length of surgery and medications administered for anesthesia and recovery. Data endpoints included emergence and discharge times, perioperative desaturations, postoperative apneic episodes and delirium. Baseline demographic characteristics were compared using unpaired t-test for continuous data and Chi-square test for categorical data. Emergence and discharge times were compared using multiple linear regression adjusting for predefined potential confounding factors.

**Data and Results:** There was no significant difference between the two groups (Midazolam versus No Midazolam) regarding demographic characteristics. No significant difference in emergence time between Midazolam (n=83) versus No Midazolam (n=387) group was found. After adjusting for all potential confounders (surgery duration, dexmedetomidine and fentanyl doses adjusted to weight, and awake or deep tracheal extubation status), emergence time was found to be 5.2 minutes (95% CI: -7.1, 17.4) longer in the midazolam group (50.3 minutes, 95% CI: 39.2, 61.4) comparing to no midazolam group (45.1 minutes, 95% CI: 39.9, 50.2). This association was not statistically significant ( $p=0.41$ ). After adjusting for potential confounders (surgery duration, dexmedetomidine and fentanyl doses dose adjusted to weight), discharge time was found to be 10.1 minutes (95% CI: -6.7, 26.8) longer in the midazolam group (125.9 minutes, 95% CI: 110.7, 141.1) comparing to No midazolam group (115.8 minutes, 95% CI: 108.8, 122.9). This association was not statistically significant ( $p=0.24$ ).

**Interpretation, Conclusion or Significance:** Premedication with midazolam was not associated with a prolonged emergence or discharge time or with a higher incidence of complications after anesthesia for T&A in patients with OSA. These results would help characterize the best perioperative management approach in pediatric patients with OSA undergoing surgery.

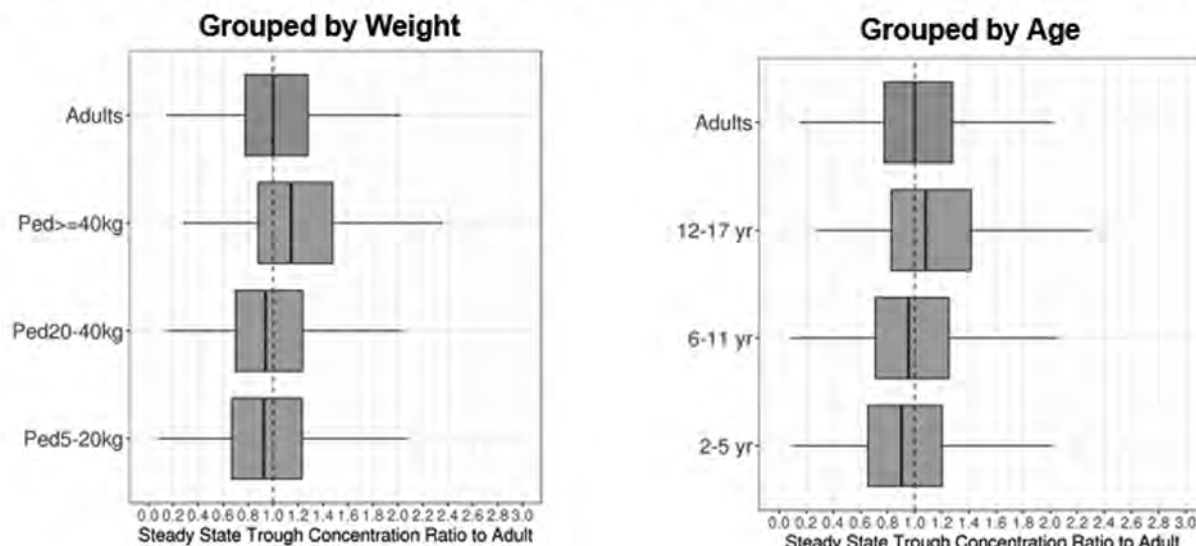
### Poster Number: 067

#### How Well the Adult-to-Children Pharmacokinetics Extrapolation Works for Monoclonal Antibodies? – Model-aided Assessment Using Case Studies and Empirical Dosing Exploration

B. Langevin<sup>1</sup>, Z. Xu<sup>2</sup>, H. Zhou<sup>2</sup>, Y. Xu<sup>2</sup>

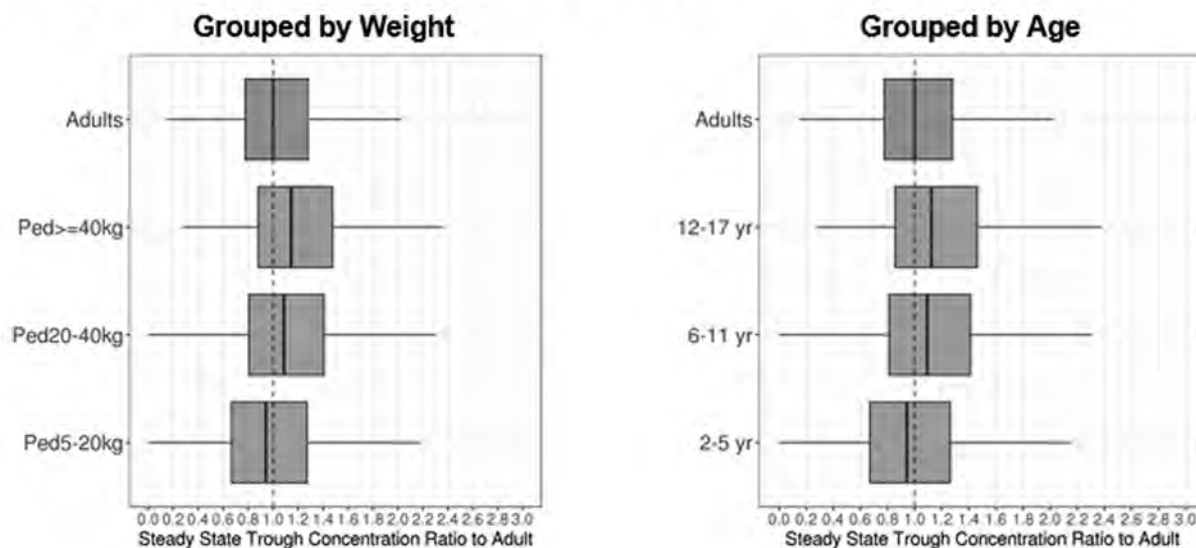
### A. Weight-Based Dosing

(<20 kg, Adult Dose/60 kg x 1.5; 20-40 kg, Adult Dose/60 kg x 1.1; ≥40 kg, Adult Dose)



### B. Body Surface Area-Based Dosing

(<40 kg: Adult Dose/1.67m<sup>2</sup>; ≥40 kg: Adult Dose)



Poster Number: 067 Figure 1. Empirical Dosing Approaches Proposed for Monoclonal Antibodies In Children 2-17 Years

<sup>1</sup>Johns Hopkins Univ, Baltimore, MD, USA; <sup>2</sup>Janssen Research & Development LLC, Spring House, PA, USA

#### Statement of Purpose, Innovation or Hypothesis:

The importance of pharmacokinetics (PK) in pediatric drug development is well recognized and a pediatric PK study is generally recommended before pivotal pediatric trials to ensure the 'right' dose in these studies. The PK of monoclonal antibodies (mAbs) is primarily affected

by body weight, where extrapolation from adults to children may conform to allometry. Therefore, PK behavior of mAbs in pediatrics, particularly for those with linear PK, is expected to be readily predictable based on data in adults. In this case, the necessity of a dedicated pediatric PK study may be of question. However, no systematic investigation has been performed. We described hereby an assessment of model-aided PK extrapolation of mAbs from adults to children (2-17 yrs) using five case studies. In addition, we

explored the empirical dosing approaches of mAbs in pediatrics.

**Description of Methods and Materials:** For each of the five case studies, population PK models were developed based on adult data, with allometric exponents of weight on clearance and volume being fixed as standard values (i.e., 0.75 for clearance [CL or CL/F], and 1.0 for volume of distribution [V or V/F]) (Approach 1) or coming from adult model estimates (Approach 2). The median weight allometric exponent from literature review was close to 0.75 for CL (0.72) and lower than 1.0 for V (0.68), but within the range. The two extrapolation approaches were used to simulate pediatric PK with pediatric subjects randomly sampled from the Center for Disease Control database. The simulated pediatric trough and peak concentrations were compared to the PK observations in pediatric trials to assess the accuracy in model predictions. Simulations were also conducted to explore the empirical dosing approaches of mAbs in pediatrics by matching the exposures in pediatrics to those of adults, with sensitivity analysis and validation.

**Data and Results:** For pediatrics 6–17 yrs, model performance was overall comparable using the two extrapolation approaches. The predicted trough concentrations were within 0.67- to 1.5-fold of the observed PK values in most cases. For children <6 yrs old, no definite conclusion could be made due to data limitation (only one case study enrolled children 2–5 yrs). Pharmacokinetic simulations support that pediatric subjects weighing  $\geq 40$  kg can generally receive adult dose, while those weighing  $< 40$  kg would require body size-adjusted dosing as follows: 1) weight-based dosing: a) pediatric subjects weighing  $< 20$  kg: adult dose/60 kg \*1.5; pediatric subjects weighing  $\geq 20$  to  $< 40$  kg: adult dose/60 kg\*1.1; 2) body surface area-based dosing: pediatric subjects weighing  $< 40$  kg: adult dose/1.67 m<sup>2</sup>.

**Interpretation, Conclusion or Significance:** Based on the data in adults and taken into accounts the weight effect on PK (allometry), model-predicted PK in pediatrics 6–17 yrs was generally comparable to the observed data. Our work supports that PK in pediatric subjects of 6–17 yrs of age is readily predictable for mAbs with linear PK based on adult PK data. Furthermore, empirical dosing calculations are also proposed to convert adult doses to equivalent pediatric doses.

**Poster Number: 068**

**US Drug Shortages Affecting Medications Included in the 2019 WHO Model List of Essential Medicines 2014–2019**

V. C. Ziesenitz<sup>1</sup>, H. Ong<sup>2</sup>, J. van den Anker<sup>2</sup>, E. Fox<sup>3</sup>, M. Mazer-Amirshahi<sup>4</sup>

<sup>1</sup>Univ Hosp Heidelberg, Baden-Württemberg, Germany; <sup>2</sup>Children's National Health System, Washington, DC, USA; <sup>3</sup>Univ of Utah Health & Univ of Utah Coll of Pharmacy, Salt Lake City, UT, USA; <sup>4</sup>Georgetown Univ School of Medicine & MedStar Washington Hosp Ctr, Washington, DC, USA

**Statement of Purpose, Innovation or Hypothesis:** Prescription drug shortages have increased significantly during the past two decades and have become a major global problem impacting all disciplines of medicine. This is especially problematic in children because suitable therapeutic alternatives for children may not be available. In order to assess the potential global impact, we analyzed the 2019 WHO Model List of Essential Medicines for Children for drugs impacted by shortages in the US.

**Description of Methods and Materials:** Drug shortage data for drugs included in the 2019 WHO Model List of Essential Medicines were retrieved from the Univ of Utah Drug Information Service over 5 yrs from 2014 to 2019. Data were analyzed focusing on drug class, formulation, route of administration, reason for shortage and shortage duration. Drugs were categorized according to the AHFS Pharmacologic-Therapeutic Classification.

**Data and Results:** There were 209 drug shortages of drugs included in the 2019 WHO Model Lists of Essential Medicines between 2014 to 2019. Of these, 36.8% were still unresolved by 2019, including 6.7% of active shortages that began before 2014. Resolved shortages had a median duration of 5.9 mos (IQR 3.6;13.2) while active shortages had a median duration of 18.3 mos (IQR 10.9,33.5) ( $p < 0.01$ ). The therapeutic categories most impacted by drug shortages were anti-infective agents (i.e. amoxicillin, (27.3%); central nervous system agents (12.9%); antineoplastic agents (11.0%); vaccines, toxoids and serums (7.7%); otic, ophthalmic, nasal preparations (7.2%); and electrolytic, caloric and water balance (6.7%). Drugs in other categories accounted for 27.3% of shortages. Most commonly, the reason for the shortage was not reported (46.4%). The most common shortage reason was manufacturing problems (29.2%), followed by a mismatch of supply/demand (15.8%) and other reasons (8.6%).

**Interpretation, Conclusion or Significance:** Drug shortages affected many medications included in the 2019 WHO Model List of Essential Medicines, which can have significant implications for the care of children globally. When essential drugs are not available, off-label use and adverse drug events may increase with implications for children's safety.

**Encore:** Published online for the Pediatric Academic Societies (PAS) Meeting, Philadelphia, May 2020.

**Poster Number: 069****Application of Updated Guidance: Full Extrapolation of Efficacy from Adults to Pediatric Patients Two Yrs of Age and Older for Antiepileptic Drug Used to Treat Partial Onset Seizures**

D. Li<sup>1</sup>, M. Bewernitz<sup>1</sup>, A. Bhattaram<sup>1</sup>, R. Uppoor<sup>1</sup>, M. Mehta<sup>1</sup>, A. Men<sup>1</sup>

<sup>1</sup>US Food & Drug Administration, Silver Spring, MD, USA

**Statement of Purpose, Innovation or Hypothesis:** Application of pediatric efficacy extrapolation guidance for antiepileptic drug.

**Description of Methods and Materials:** Summarize pediatric efficacy extrapolation guidance and approved supplemental new drug application (sNDA) submissions

**Data and Results:** Two versions of pediatric efficacy extrapolation guidance had been published. Six sNDA submissions had been approved.

**Interpretation, Conclusion or Significance:** On November 12, 2015, the US Food & Drug Administration (FDA) sent a General Advice Letter to the Antiepileptic Drug (AED) Applicants indicating that it was acceptable to extrapolate the effectiveness of drugs approved for the treatment of partial onset seizures (POS) in adults to pediatric patients four yrs of age and older. This determination was based on the similarity of the pathophysiology of POS in pediatric patients four yrs of age and older and adults as well as systematic analyses conducted by the FDA, which demonstrated a similar exposure-response relationship in pediatric and adult patients with POS. The finalized guidance for Industry: *“Drugs for Treatment of Partial Onset Seizures: Full Extrapolation of Efficacy from Adults to Pediatric Patients Four Yrs of Age and Older”* was published in February 2018. Since the General Advice Letter was sent in November 2015, five AED sNDA submissions applying pediatric efficacy extrapolation policy were approved. Among them, eslicarbazepine acetate, lacosamide, brivaracetam and perampanel were approved for monotherapy or adjunctive therapy for children four to 16 yrs of age with POS and pregabalin was approved for adjunctive therapy for children four to 16 yrs of age based on pharmacokinetic (PK) matching approach and adequate safety data in pediatric patients four yrs of age and older. In September 2019, this AED guidance was updated to extend pediatric extrapolation down to two yrs old POS patients based on accumulated experience from clinical trials and research suggesting that the pathophysiology of POS appears similar in pediatric patients two to four yrs of age and >four yrs of age, and the approved doses and clinical responses are similar in pediatric patients between two

to four yrs of age and >four yrs of age POS pediatric patients.

Key points of the finalized guidance on efficacy extrapolation from adults to pediatrics for POS include:

- Efficacy extrapolation from adults to pediatric patients can only be applied to POS
- The efficacy can be extrapolated to pediatric patients two yrs of age and older
- Adequate PK and tolerability study is required in patients two to 16 yrs of age with appropriate age distribution
- Safety cannot be extrapolated from adults to children. Clinical safety studies in pediatric patients two yrs of age and older with POS are required (open label, n ≥ 100, at least six mos)

One submission for vigabatrin was approved as an adjunctive therapy for adults and pediatric patients two yrs of age and older with refractory complex partial seizures (subset of partial onset seizures) in January 2020. It became the first case applying the updated guidance to extrapolate the effectiveness from adults to pediatric patients two yrs of age and older.

In summary, this updated guidance, which had been successfully applied to six approved AED sNDA for POS submissions, will speed up the AED development for pediatrics by waiving the efficacy trial.

**Poster Number: 070****Extrapolating Pharmacodynamic Effects from Adults to Pediatrics: A Case Study of Ustekinumab in Pediatric Patients With Moderate to Severe Plaque Psoriasis**

W. Zhou<sup>1</sup>, C. Hu<sup>1</sup>, Y. Zhu<sup>1</sup>, B. Randazzo<sup>1</sup>, M. Song<sup>1</sup>, A. Sharma<sup>1</sup>, Z. Xu<sup>1</sup>, H. Zhou<sup>1</sup>

<sup>1</sup>Janssen Research & Development LLC, Spring House, PA, USA

**Statement of Purpose, Innovation or Hypothesis:** Ustekinumab is a human monoclonal antibody targeted against interleukin-12 and -23 for the treatment of adult and adolescent (≥12 to <18 yrs of age) patients with moderate-to-severe plaque psoriasis. A Phase 3 study (CADMUS-JR [NCT02698475]) was recently completed in pediatric patients ≥6 to <12 yrs of age with psoriasis. The objectives of the current analysis were to develop a population pharmacokinetic (PopPK) model and a joint longitudinal exposure-response model using ordered categorical endpoints derived from Psoriasis Area and Severity Index (PASI) and Physician's Global Assessment (PGA) scores to characterize the pharmacokinetic (PK) and

exposure-response relationship of ustekinumab in pediatric patients with psoriasis. In addition, the potential of using adult psoriatic data to extrapolate clinical response to pediatric patients with psoriasis was also thoroughly evaluated.

**Description of Methods and Materials:** Serum ustekinumab concentrations and PASI and PGA scores were collected from 152 psoriatic subjects in two pediatric Phase 3 studies (CADMUS [NCT01090427; adolescents] and CADMUS-JR) and from 433 psoriatic subjects in two adult Phase 3 studies (LOTUS [NCT01008995] and PEARL [NCT00747344]). Post-baseline measurements of ustekinumab concentration from 4,162 blood samples, 4,565 PASI scores and 5,148 PGA scores were available. Pediatric and adult PopPK models were developed. A joint PASI response criterion [PRC] and PGA model was developed from adult data and evaluated with pediatric data.

**Data and Results:** The combined serum ustekinumab concentration-time data from pediatric patients  $\geq 6$  to  $<12$  yrs of age and adolescent patients were well described by a one-compartment model with first-order absorption and first-order elimination. Body weight effects on both the apparent clearance (CL/F) and apparent volume of distribution (V/F) were included in the base structural model. The exponents for body weight effects on CL/F and V/F were fixed to 0.75 and 1, respectively. The PopPK parameter estimates of ustekinumab for CL/F, V/F, and absorption rate constant ( $K_a$ ) in a typical pediatric subject weighing 56 kg were 0.204 L/day, 6.77 L and 0.371 day<sup>-1</sup>, respectively. All PK parameters estimated with the final pediatric PopPK model were in good precision. Both goodness-of-fit diagnostic plots and visual predictive check (VPC) plots suggested that the final pediatric PopPK model adequately captured the median serum ustekinumab concentration-time profiles, as well as associated variabilities, across the age groups in the two pediatric studies. The parameter estimates and associated variabilities of the pediatric PRC and PGA joint model were in good estimation precision, with RSE  $<30\%$  for all parameters, despite relatively small sample size in the Phase 3 pediatric studies. The VPC of the pediatric joint model suggested adequate descriptions of the observed data for both PASI response and PGA across all ordered categorical efficacy thresholds.

**Interpretation, Conclusion or Significance:** The developed pediatric joint model reasonably predicted the PK of ustekinumab and the PASI and PGA responses in pediatric patients with psoriasis. In addition, the joint PRC and PGA modeling framework was able to adequately extrapolate clinical responses to pediatric patients using data collected from adult patients with psoriasis.

**Poster Number: 071**

**Prediction of Neonatal Pharmacokinetics from Maternal Dolutegravir and Raltegravir Dosing Using Physiologically-based Pharmacokinetic Modeling**

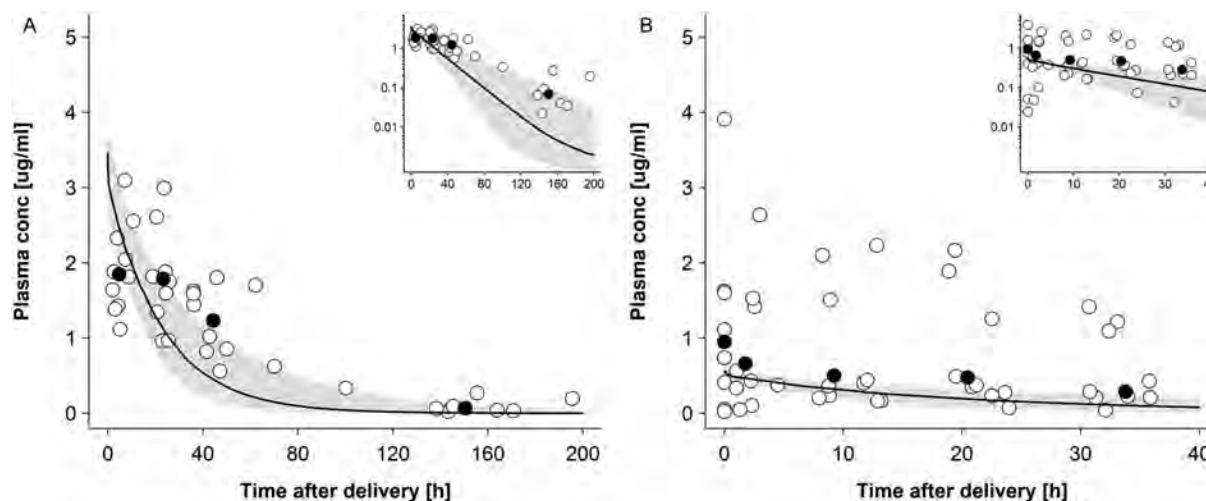
X. Liu<sup>1</sup>, J. Momper<sup>2</sup>, N. Rakhmanina<sup>1</sup>, D. Green<sup>3</sup>, G. J. Burckart<sup>3</sup>, T. Cressey<sup>4</sup>, M. Mirochnick<sup>5</sup>, B. Best<sup>2</sup>, J. van den Anker<sup>1</sup>, A. Dallmann<sup>6</sup>

<sup>1</sup>Children's National Medical Ctr, Washington, DC, USA; <sup>2</sup>Univ of California San Diego, San Diego, CA, USA; <sup>3</sup>US Food & Drug Administration, Silver Spring, MD, USA; <sup>4</sup>Chiang Mai Univ, Chiang Mai, Thailand; <sup>5</sup>Boston Medical Ctr, Boston, MA, USA; <sup>6</sup>Bayer AG, Leverkusen, Germany

**Statement of Purpose, Innovation or Hypothesis:** Little is known about pharmacokinetics (PK) of drugs in the peripartum period including placental transfer of drugs administered to the mother and drug exposure in the neonate. The objective of this study was to develop and evaluate neonatal physiologically-based pharmacokinetics (PBPK) models for predicting predominantly UGT1A1 metabolized dolutegravir (DTG) and raltegravir (RAL) concentrations in the "washout" phase after delivery among women on antiretroviral HIV therapy.

**Description of Methods and Materials:** Physiologically-based pharmacokinetics models were built with the Open Systems Pharmacology software suite (PK-Sim/MoBi<sup>®</sup>). Using two previously published maternal-fetal PBPK models, placental drug transfer was predicted in the peripartum period and the total drug amount present in the fetal compartments at the time of delivery was estimated. Subsequently, a neonatal PBPK model was developed integrating the drug concentrations in the fetal compartment as initial conditions. Elimination processes in the newborn were parameterized according to available literature. Model performance was assessed through visual comparison of the predicted with the observed plasma-concentration time profile. Additionally, the mean prediction error (MPE) and mean absolute prediction error (MAPE) were calculated. All clinical *in vivo* data for DTG were obtained from the International Maternal Pediatric and Adolescent AIDS Clinical Trials (IMPAACT) Network study P1026s (NCT00042289). For RAL, *in vivo* data were taken from the literature<sup>1</sup>.

**Data and Results:** The maternal-fetal PBPK models captured the observed plasma concentrations in the umbilical vein at delivery adequately, although for RAL a slight underestimation was seen. The neonatal PBPK models reasonably predicted plasma concentration-time profiles of DTG and RAL in newborns in the washout phase and the majority of predicted drug



**Poster Number: 071** **Figure 1.** Plasma Concentration-time Profiles of Dolutegravir and Raltegravir in Newborns Following Oral Administration to the Mother Prior to Delivery. Empty Circles Represent Observed Individual Concentration Data in the Newborns Plasma and Black Circles Represent Median Concentration Data in the Newborns; the Solid Line Represents the Predicted Median Plasma Concentration in a Population of Newborns and the Shaded Area the Predicted 5<sup>th</sup>–95<sup>th</sup> Percentile Range. Semi-log Scale Figures are given as Inset Figure in the Top Right Corners. A: Dolutegravir Plasma Concentration in Newborns; Maternal Dose of 50 mg Once a Day. B: Raltegravir Plasma Concentration in Newborns; Maternal Dose of 400 mg Twice a Day. Observed Data were Taken from Clarke et al<sup>1</sup>

concentrations fell within the range of observed data (Figure 1). For DTG, the MPE and MAPE were -33.1% and 57.2%, respectively; whereas for RAL, MPE and MAPE were 65.3% and 149.4%, respectively. However, drug clearance appeared somewhat overestimated and inter-individual variability underestimated, especially for RAL.

**Interpretation, Conclusion or Significance:** Overall, the presented PBPK modeling approach can reasonably predict DTG and RAL exposure of maternally-transferred drug in neonates, but knowledge gaps remain, e.g. with respect to the ontogeny of enzymes involved in metabolism. Nevertheless, these findings demonstrate the general feasibility of developing and applying PBPK models to predict washout concentrations in newborns which could ultimately increase the understanding of drug pharmacokinetics during the first days of life in this vulnerable population.

#### Reference:

1. Clarke DF, Acosta EP, Rizk ML, et al. Raltegravir pharmacokinetics in neonates following maternal dosing. *J Acquir Immune Defic Syndr.* 2014; 67(3): 310–5.

#### Poster Number: 072

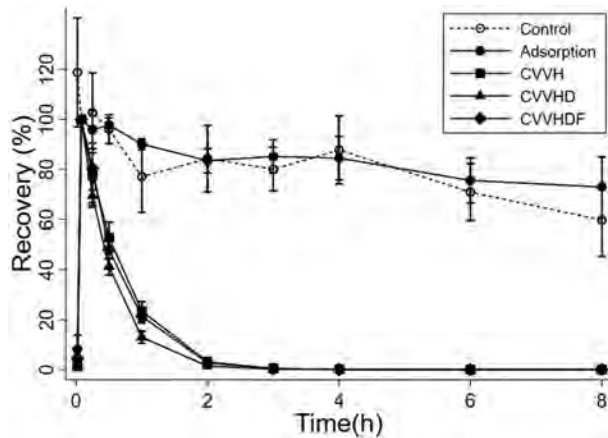
#### **Ex vivo Study of Cefepime Clearance in Continuous Renal Replacement Therapy**

A. Bensimhon<sup>1</sup>, R. Gbadegesin<sup>1</sup>, K. Watt<sup>2</sup>

<sup>1</sup>Duke Univ Medical Ctr, Durham, NC, USA; <sup>2</sup>Univ of Utah, Salt Lake City, UT, USA

**Statement of Purpose, Innovation or Hypothesis:** Continuous renal replacement therapy (CRRT), a form of dialysis, is life saving for children with acute kidney injury (AKI). Despite this, children supported with CRRT are at high risk for CRRT-related complications, including nosocomial infections. In this population, sepsis is one of the most common causes of death, with mortality rates exceeding 40%. The high mortality rates are suspected to be, in part, a result of significantly altered drug disposition by the extracorporeal CRRT circuit, resulting in suboptimal antibiotic dosing. In this study, *ex vivo* CRRT models were used to determine the extracorporeal removal via adsorption and transmembrane clearance ( $CL_{TM}$ ) of cefepime during CRRT.

**Description of Methods and Materials:** Four different closed-loop CRRT circuit configurations were constructed to independently quantify the: 1) adsorption of cefepime to the hemodiafilter and extracorporeal circuit components; and clearance via 2) hemofiltration (CVVH), 3) hemodialysis (CVVHD) and 4) hemodiafiltration (CVVHDF). Each configuration was run in triplicate. All experiments used a Prismaflex™ system and polyarylethersulfone hemodiafilter (HF-1000). Each circuit was primed with human blood and connected to a reservoir to complete the circuit. Cefepime was dosed to achieve therapeutic concentrations and urea was administered to serve as a control solute. Cefepime and urea were also added to a separate bag of blood to serve as a control. Serial blood and effluent samples were collected over eight hrs and



**Poster Number: 072** Figure 1. Cefepime Recovery in Four CRRT Circuit Configurations

concentrations were quantified with a validated assay. Drug recovery was calculated at each time point using the equation  $\text{Recovery} = [(C_0 - C_i) / C_0] * 100$ , where  $C_0$  and  $C_i$  are the concentrations at times 0 and  $i$ , respectively.

**Data and Results:** Mean (SD) recovery of drug at eight hrs in the controls and adsorption circuits was 59.6% (14.2) and 72.9% (12.0), respectively (Figure 1). In the CVVH, CVVHD and CVVHDF experiments, >96% of cefepime was eliminated from the circuit at two hrs.

**Interpretation, Conclusion or Significance:** Cefepime was readily cleared by conventional CRRT, and doses may need to be adjusted depending on the type of hemofilter, CRRT modality and ultrafiltration and dialysate flow rates. These data will be used to parameterize a CRRT compartment in a cefepime physiologically based pharmacokinetic model to determine optimal dosing in children on CRRT.

## Pharmacodynamics

**Poster Number: 073**

### Cognitive Performance and Psychedelic Effects Following Single and Multiple Ascending Doses of a New Cannabis Formulation (PPP001) Administered by Smoking/Inhalation in Male and Female Volunteers

B. Setnik<sup>1</sup>, J. Huguet<sup>2</sup>, C. Mills<sup>2</sup>, R. Ringuette<sup>3</sup>, C. Campbell<sup>3</sup>, A. De Pauw<sup>3</sup>, E. Sicard<sup>2</sup>, G. Chamberland<sup>3</sup>

<sup>1</sup> Altasciences Clinical Research, Laval, PQ, Canada & the Univ of Toronto, Toronto, ON, Canada;

<sup>2</sup>Altasciences Clinical Research, Laval, PQ, Canada;

<sup>3</sup>Tetra Bio-Pharma Inc, Longueuil, PQ, Canada

**Statement of Purpose, Innovation or Hypothesis:** PPP001 is a dried cannabis product for smoked inhalation in development for the treatment of chronic pain. Advantages of intrapulmonary administration of

cannabinoids (e.g., by smoking) include high systemic bioavailability and fast onset of action. (1) However, adverse events (AE), including cognitive dysfunction, may be observed depending on exposure levels. The objectives of this study were to evaluate the safety, tolerability and cognitive effects of PPP001 following smoked inhalation over one or seven consecutive days in an escalating fashion.

**Description of Methods and Materials:** This study was a randomized, double-blind, placebo-controlled, single (three cohorts) and multiple (three cohorts) staggered drug administration regimens (once [QD], twice [BID] or three times a day [TID]) design in 48 subjects (eight subjects/cohort; two placebo; six active). PPP001 (25 mg THC / 5.5 mg CBD) and placebo (0 mg THC / 0.8 mg CBD) were administered by smoking/inhalation with a titanium pipe at a dose of 9% (25 mg) THC / 2% (5.5 mg) CBD, QD (cohort A1), BID (cohort A2) or TID (cohort A3) daily, four hrs apart, for one day (Part A) and following a five-day titration and two days of full assigned regimens (Part B, cohorts B1 to B3). Pharmacodynamic assessments included the Bowdle Visual Analog Scales (VAS), assessing subjective drug effects, as well as Choice Reaction Time (RTI), Paired Associate Learning (PAL), Spatial Working Memory (SWM) and the Rapid Visual Information test (RVP) assessing cognition/psychomotor processing. Pharmacodynamic assessments were performed at baseline and 0.5, 1 and 2.5 hrs following each drug administration. Descriptive analysis was performed using summary statistics. Pharmacokinetic, safety assessments and cardiac safety monitoring were performed.

**Data and Results:** A marked increase was observed when compared to placebo (maximum peak effect ranging from 32.8 to 58.6 for the active arm and ranging from 0 to 15.2 for placebo arm) for the “feeling high” item in Part A. No cumulative effect was observed upon QD, BID or TID regimen (four hrs apart) administered on a single day. No clear difference with placebo was observed for “feeling drowsy” item. An increase when compared to placebo was detected for the composite scores “internal perception” (seven items) and external perception (six items). Similar trend (marked change from baseline) was observed for the psychomotor testing (e.g. processing speed, episodic learning/memory, working memory, executive function, sustained attention and psychomotor speed). Similar results were obtained for Part B. Overall AE incidence was 92% (22 / 24) in subjects who received either cannabis or placebo. Majority of the AEs were mild in intensity (80%). For THC and CBD  $T_{max}$  ranged from 0.05–0.17 hrs and 0.02–0.17 hrs, while AUC increased from 30 to 94 ng\*h/mL and 7.8 to 21 ng\*h/mL across cohorts, respectively. Both THC and CBD were eliminated in less than 1.6 hrs ( $t_{1/2}$ ).

**Interpretation, Conclusion or Significance:** Following controlled acute QD, BID or TID, 4 hrs apart, administration(s) of cannabis by smoking/inhalation, psychedelic effects and cognitive performance measures were different compared to placebo (increase or decrease), while no accumulation of the cognitive effect was observed. Pharmacokinetic results showed no evidence of accumulation and treatments were generally well tolerated.

**Poster Number: 074**

**Deciphering Mechanisms Leading to QT Hysteresis in the Context of a Thorough QT Study With Clazosentan: Influence of Food, Adverse Events and Other Factors**

P. Juif<sup>1</sup>, A. Henrich<sup>1</sup>, A. Krause<sup>1</sup>, M. Ufer<sup>1</sup>, J. Dingemans<sup>1</sup>

<sup>1</sup>Idorsia Pharmaceuticals Ltd, Allschwil, Switzerland

**Statement of Purpose, Innovation or Hypothesis:** A thorough QT study with clazosentan revealed that baseline- ( $\Delta$ ) and placebo-corrected ( $\Delta\Delta$ )QTcF dose-dependently increased after clazosentan infusion and further increased after the termination of infusion, indicating the presence of hysteresis (i.e., lack of direct relationship between plasma concentration and  $\Delta\Delta$ QTcF). Therefore, a comprehensive post-hoc analysis was performed to decipher mechanism(s) potentially leading to the observed QT hysteresis.

**Description of Methods and Materials:** A randomized, placebo- and moxifloxacin-controlled, double-blind, three-period, cross-over study was conducted in 36 healthy male and female subjects. In each period, subjects received clazosentan, moxifloxacin or placebo and this post-hoc analysis was done based on data from the clazosentan period only. The effects of food intake, excipients in the vehicle solution, use of concomitant medications and adverse events (AEs) were investigated as potential factors contributing to QT hysteresis. QTcF,  $\Delta$ QTcF and  $\Delta\Delta$ QTcF data were dichotomized and averaged by occurrence vs absence of AE of interest or concomitant medication.

**Data and Results:** The maximum prolongation in mean  $\Delta\Delta$ QTcF (14.8 ms) following clazosentan was observed approximately four hrs after last food intake suggesting that there was no apparent association between food intake and QT hysteresis. Oral moxifloxacin administration followed by placebo infusion (i.e., vehicle containing the same excipients including TRIS) led to a similar change in  $\Delta\Delta$ QTcF (maximum  $\Delta\Delta$ QTcF of 12.9 ms) as observed after moxifloxacin only<sup>1</sup>. Therefore, excipients and intravenous infusion are unlikely to have contributed to QT hysteresis. Paracetamol was the only comedication administered during the study and not associated with QT hysteresis. The most common AEs were headache, nausea and vomiting that occurred

mainly after termination of clazosentan infusion indicating also a delayed occurrence. There was no apparent association of increased  $\Delta\Delta$ QTcF with headache, but with nausea and vomiting. At the time of vomiting,  $\Delta\Delta$ QTcF was longer suggesting a relationship between vomiting and QT prolongation. Vomiting also led to a statistically-significant lowering of potassium concentrations in plasma (4.26 vs 3.96 mmol/L) known to cause QT prolongation<sup>2</sup>.

**Interpretation, Conclusion or Significance:** These post-hoc analyses suggest an indirect effect of clazosentan on  $\Delta\Delta$ QT triggered by AEs of nausea and vomiting. Mechanistically, vomiting-induced lowering of potassium concentrations in plasma may have contributed to the observed delayed QT prolongation, i.e., PK-QT hysteresis.

**References**

1. Taubel J, Ferber G, Fernandes S, Camm AJ. *J Clin Pharmacol.* 2019; 59(1):35-44.
2. Widimsky P. *e-J ESC Council for Cardiol Practice* 2008; 7(9).

**Poster Number: 075**

**A Thorough QT Study With Clazosentan, a Selective Endothelin A Receptor Antagonist**

P. Juif<sup>1</sup>, A. Henrich<sup>1</sup>, A. Krause<sup>1</sup>, M. Ufer<sup>1</sup>, J. Dingemans<sup>1</sup>

<sup>1</sup>Idorsia Pharmaceuticals Ltd, Allschwil, Switzerland

**Statement of Purpose, Innovation or Hypothesis:** Clazosentan, a selective endothelin A receptor antagonist, is currently investigated in a Phase 3 study in aneurysmal subarachnoid hemorrhage patients (NCT03585270). It does not inhibit Ether-à-go-go-Related gene up to concentrations of 300  $\mu$ M (clinical steady-state concentration  $\sim$ 3  $\mu$ M at 60 mg/h, four times the expected therapeutic dose). This study investigated the potential QT liability of clazosentan at therapeutic and suprathreshold doses using concentration/QT data for primary analysis.

**Description of Methods and Materials:** A randomized, placebo- and moxifloxacin-controlled, double-blind, three-period, cross-over study was conducted in 36 healthy male and female subjects. In each study period, subjects received a continuous intravenous infusion of i) clazosentan 20 mg/h (therapeutic dose) followed by 60 mg/h (suprathreshold dose) for three hrs each, ii) placebo for six hrs, iii) or placebo for six hrs concomitantly with moxifloxacin (oral dose of 400 mg). At predefined time points from one hr pre-dose to 24 hrs after the end of infusion, ECGs were extracted from Holter recordings in replicates and pharmacokinetic (PK) blood sampling was performed. Safety and tolerability were evaluated based on adverse

event (AE), vital signs, 12-lead ECG, clinical laboratory and physical examination data.

**Data and Results:** Twenty-six subjects were male and ten were female with a mean age of 48.3 yrs (range: 22–65 yrs). The PK of moxifloxacin<sup>1</sup> and clazosentan<sup>2</sup> were in line with previous data. For moxifloxacin, the estimated population slope of the concentration-QTc relationship was 0.003 ms/(ng/mL) and the lower bound of the 90% confidence interval (CI) of the baseline- ( $\Delta$ ) and placebo- ( $\Delta\Delta$ ) corrected QTcF was  $>5$  ms at the time of maximum plasma concentration, demonstrating assay sensitivity. For clazosentan, the concentration-QTcF analysis was not conclusive due to observed hysteresis, i.e., delayed effect, indicating a lack of direct relationship between clazosentan concentration and  $\Delta\Delta$ QTcF. Therefore, the by-time point analysis was conducted, resulting in a mean (90% CI)  $\Delta\Delta$ QTcF of 7.2 (4.6–9.8) and 10.9 (8.2–13.5) ms 3 hrs (20 mg/h) and 6 hrs (60 mg/h) after start of initial infusion, respectively. There was no subject with  $\Delta$ QTcF  $>60$  ms or QTcF  $>480$  ms in any treatment group. Following clazosentan administration, the incidence of AEs was higher at 60 mg/h (89%) than at 20 mg/h (47%). The most common AEs were headache, nausea and vomiting with an incidence of 83, 47 and 31%, respectively. Adverse effects were of mild and moderate intensity except a single severe AE of headache that led to discontinuation of the subject. No clinically-relevant changes in other safety parameters were observed.

**Interpretation, Conclusion or Significance:** Infusion of clazosentan led to a dose-dependent QT prolongation as reflected by the upper limit of the two-sided 90% CI of  $\Delta\Delta$ QTcF exceeding 10 ms.

#### References

1. Bayer. Avelox prescribing information. 2019.
2. van Giersbergen PL, Dingemans J. Eur J Clin Pharmacol. 2007; 63(2):151-8.

## Pharmacometrics & Systems Pharmacology

Poster Number: 076

### Quantitative Evaluation of Levonorgestrel Efficacy in Drug-Drug Interaction Scenarios in Healthy & Obese Women: Applications of Physiologically-based Pharmacokinetic Modeling & Model Based Meta-analysis

K. Lingineni<sup>1</sup>, B. Cicali<sup>1</sup>, A. Chaturvedula<sup>2</sup>, R. Cristofolletti<sup>1</sup>, T. Wendl<sup>3</sup>, J. Hoechel<sup>3</sup>, H. Wiesinger<sup>3</sup>, V. Vozmediano<sup>1</sup>, P. Zhao<sup>4</sup>, S. Schmidt<sup>1</sup>

<sup>1</sup>Univ of Florida Coll of Pharmacy, Orlando, FL, USA; <sup>2</sup>Univ of North Texas System Coll of Pharmacy, Fort Worth, TX, USA; <sup>3</sup>Bayer AG, Leverkusen, Germany; <sup>4</sup>Bill & Melinda Gates Fdn, Seattle, WA, USA

### Statement of Purpose, Innovation or Hypothesis:

Combined hormonal contraceptive (CHC) formulations are currently the most common oral contraceptives. They consist of a progestin (e.g. levonorgestrel, LNG) and an estrogen component, typically ethinyl estradiol (EE). Given their wide use, also in combination with other medications, drug-drug interactions (DDIs) are of general concern. The US Food & Drug Administration held a workshop in November 2015 to seek advice from external experts on the impact of DDIs on the efficacy and safety of CHCs, which resulted in a draft guidance for industry. This guidance contains a drug class label for DDIs of CHCs with focus on cytochrome P450 (CYP) inducers. However, it is currently unclear if this drug class label is equally applicable across CHCs and to what extent other factors, such as demographics, should be considered. Therefore, the objective of this study was to develop a quantitative modeling framework to determine the impact of DDIs on the efficacy and safety of CHCs using LNG+EE as a starting point.

**Description of Methods and Materials:** We developed physiologically-based pharmacokinetic (PBPK) models for LNG and EE based on available *in vitro* enzyme kinetic and clinical trial data for normal weight and obese women. Once developed and verified, these PBPK models were used to predict the impact of the strong CYP3A4 inducers rifampicin, efavirenz and carbamazepine on the steady-state kinetics of combined LNG/EE fixed dose combinations (High dose: LNG 150 ug + EE 30 ug & Low dose: LNG 100 ug + EE 20 ug) in normal weight and obese women. The results of these simulations were compared to prospective patient level clinical trial data from Bayer AG. Predicted concentrations-time profiles were then linked to a model-based meta-analysis (MBMA) that was informed by nine literature-reported studies to determine the impact of exposure changes on the efficacy of combined LNG/EE formulations, expressed as number of pregnancies per 100 women-yrs of exposure (Pearl Index).

**Data and Results:** Physiologically-based pharmacokinetic simulations were able to predict the decreased exposure of LNG in obese women due to decreased binding of LNG to sex hormone binding globulin (SHBG). Coadministration of strong CYP3A4 inducers resulted in a decrease by 50–75 % in LNG steady-state exposure, which translated to increases in Pearl Index between 1.37–5 pregnancies per 100 women yrs of exposure. This DDI was more pronounced in obese women than normal weight subjects in terms of both decreased exposure (Normal weight: 50–65 % vs Obese: 65–75%) and increased Pearl Index (Normal weight: 1.37–3.5 vs Obese: 2.7–5 pregnancies per 100 women-yrs of exposure).

**Interpretation, Conclusion or Significance:** Our PBPK model is able to adequately predict the decrease in LNG exposure with CYP3A4 inducers. In conjunction with our findings from the MBMA, our results suggest that this leads to an increase in number of pregnancies, which may require the use of backup or alternative methods of contraception in the presence of inducers. We will now expand our quantitative framework to other progestins to determine if the findings for LNG are generally applicable.

**Poster Number: 077**

**Physiologically-based Pharmacokinetic Model Development and Simulations to Evaluate Potential Drug-Drug Interaction of Veliparib**

D. Mukherjee<sup>1</sup>, S. Nuthalapati<sup>1</sup>, C. Biesdorf<sup>1</sup>, R. A. Carr<sup>1</sup>, J. P. Gibbs<sup>2</sup>, M. Shebley<sup>1</sup>, H. Xiong<sup>1</sup>

<sup>1</sup>AbbVie Inc, North Chicago, IL, USA; <sup>2</sup>Past AbbVie employee

**Statement of Purpose, Innovation or Hypothesis:** Veliparib is a poly (ADP-ribose) polymerase (PARP) inhibitor inhibiting the repair of DNA single-strand breaks and has been evaluated in patients with breast or ovarian cancer. Renal clearance is the major route of clearance for veliparib, with contributions from multiple renal transporters including OCT2, MATE1, MATE2K and P-gp. A mechanistic physiologically-based pharmacokinetic (PBPK) model was developed for veliparib to provide drug-drug interaction (DDI) predictions and guide dose adjustment, if warranted.

**Description of Methods and Materials:** The PBPK model was developed using a middle-out approach by incorporating available *in vitro* data and utilizing clinical data in patients for calibration of parameters required to recapitulate the clinical data. The PBPK model was developed in Simcyp v17 utilizing the mechanistic kidney model (MechKiM) to incorporate the contributions of active transport by OCT2, MATEs and P-gp transporters. Kinetic parameters for the various renal transporters were measured *in vitro* using human embryonic kidney cells. The PBPK model for veliparib was calibrated with single ascending-dose pharmacokinetic data from clinical trials in patients. The PBPK model was verified using clinical data from five different studies that evaluated single and/or multiple dose pharmacokinetics of veliparib. In the absence of DDI results from dedicated clinical studies, the PBPK model was verified using observations from a renal impairment study since veliparib is primarily eliminated renally. The verified PBPK model for veliparib was used to simulate DDI with various perpetrator co-medications that inhibit the transport and minimal metabolism pathways of veliparib.

**Data and Results:** Model predictions compared well with clinical observations (less than 50% prediction error). Moderate and severe renal impairment reduced both filtration and active secretion, with the active secretion being reduced primarily due to decrease in basolateral uptake by OCT2 under renal impairment conditions. The effect of a known OCT2 inhibitor, cimetidine was comparable to the reduction of secretion clearance due to renal impairment suggesting that in lieu of clinical DDI data for OCT2, the renal impairment study results verify the relative contribution of OCT2 to the active secretion of veliparib. The PBPK model predicted negligible (<20%) DDI with CYP inhibitors, consistent with the minor contribution of CYP metabolism in the disposition of veliparib. The maximum extent of DDI predicted by the PBPK model was approximately 38% increase in veliparib AUC when coadministered with cimetidine.

**Interpretation, Conclusion or Significance:** Based on PBPK simulations, the risk of clinically-relevant DDI with veliparib as a victim, is expected to be low. This work represents a novel effort where a mechanistic PBPK model was developed and verified in the absence of clinical DDI data using a mechanistic understanding of renal transport and renal impairment. Since dedicated DDI studies in cancer patients are difficult to conduct, the veliparib PBPK model could be employed to simulate untested DDI scenarios and inform the need for dose adjustment, if warranted.

**Poster Number: 078**

**Development of a Physiologically-based Pharmacokinetic Model of Desvenlafaxine and Its Application in Prediction of Pharmacokinetics in Special Populations**

Y. Yu<sup>1</sup>, J. Lin<sup>1</sup>, S. Tse<sup>1</sup>

<sup>1</sup>Pfizer Inc, San Diego, CA, USA

**Statement of Purpose, Innovation or Hypothesis:** The objective for the present study was to develop a physiologically-based pharmacokinetic (PBPK) model for desvenlafaxine and to utilize the model to predict the pharmacokinetics of desvenlafaxine in special populations including pediatrics, Chinese, Japanese, subjects with renal impairment and subjects with hepatic impairment.

**Description of Methods and Materials:** A PBPK simulator, Simcyp (v18, release 1, Certara), was used to develop and verify the PBPK model of desvenlafaxine. The model development employed a combined “bottom-up” and “top-down” approach to fully utilize the available *in vitro* or *in silico* experimental data and *in vivo* observed clinical data. The developed model was verified by using the clinical pharmacokinetic data of desvenlafaxine from a published absolute bioavailability study and other studies in healthy volunteers.

The verified PBPK model was further used to predict the pharmacokinetics of desvenlafaxine in pediatrics, Chinese, Japanese, subjects with renal impairment and subjects with hepatic impairment as part of an assessment of the predictive performance of PBPK modeling in these specific populations.

**Data and Results:** The PBPK model for desvenlafaxine has been developed and the model adequately described the observed pharmacokinetics of desvenlafaxine after 50 mg intravenous dose and 100 mg oral dose from a published absolute bioavailability study. The ratios of the predicted vs observed  $AUC_{inf}$ ,  $C_{max}$  and  $t_{1/2}$  ranged from 0.81–1.06. The model was further verified by the other studies in healthy volunteers. The verified model was employed to predict the pharmacokinetics of desvenlafaxine in special populations, including pediatrics, Chinese, Japanese, subjects with renal impairment and subjects with hepatic impairment and compared to completed studies. In general, the model well predicted the desvenlafaxine pharmacokinetics in the special populations with all the ratios of the predicted vs observed AUC and  $C_{max}$  within 0.5- to 2-fold.

**Interpretation, Conclusion or Significance:** A PBPK model for desvenlafaxine has been developed based on available *in vitro* or *in silico* experimental data and *in vivo* observed clinical data. The PBPK model was verified with data from an absolute bioavailability and other studies in healthy volunteers. The predictive performance of the PBPK model was further evaluated for the prediction of desvenlafaxine pharmacokinetics in special populations.

#### Poster Number: 079

##### Entrectinib Dosing Strategies With CYP3A4 Perpetrators Using Physiologically-based Pharmacokinetic Modeling

N. Djebli<sup>1</sup>, V. Buchheit<sup>1</sup>, Y. Cleary<sup>1</sup>, N. Parrott<sup>1</sup>, N. Frey<sup>1</sup>, F. Mercier<sup>1</sup>, A. Phipps<sup>2</sup>, G. Meneses-Lorente<sup>2</sup>

<sup>1</sup>F Hoffmann-La Roche Ltd, Basel, Switzerland; <sup>2</sup>Roche Products Ltd, Welwyn, United Kingdom

**Statement of Purpose, Innovation or Hypothesis:** Entrectinib, mainly cleared by CYP3A4, is a CNS-active, potent and selective inhibitor of ROS1/TRK/ALK kinase activity. The aim of this physiologically-based (PBPK) modeling analysis of entrectinib and its main active metabolite, M5, was to define the dosing strategies with CYP3A4 perpetrators.

**Description of Methods and Materials:** The PBPK model qualification was performed by comparing Simcyp<sup>®</sup> (v17.1) predictions to observations, in healthy volunteers (HV) and patient populations. The model was verified using itraconazole clinical data (a strong CYP3A4 inhibitor), based on a sensitivity analysis and Non-Linear Mixed Effects modeling. It was then

used to prospectively predict and confirm the effect of rifampin (a strong CYP3A4 inducer) and for entrectinib as a perpetrator with midazolam (CYP3A4 substrate). In addition, predictions were performed with several moderate to strong CYP3A4 inhibitors, several moderate to strong CYP3A4 inducers and with CYP3A4 substrates (i.e., the oral contraceptive ethinylestradiol) to better assess the drug-drug interaction (DDI) risk.

**Data and Results:** The PBPK model showed good predictive performance for both entrectinib and M5. The DDI simulations suggested a six-fold lower dose (100 mg)–consistent with clinical data–and a three-fold lower dose (200 mg) of entrectinib when a strong and moderate CYP3A4 inhibitor is coadministered, respectively. The model captured the minor effect of entrectinib on midazolam exposure and predicted an ethinylestradiol AUC interaction ratio of only 1.11. Avoidance of both strong and moderate CYP3A4 inducers is recommended.

**Interpretation, Conclusion or Significance:** The PBPK predictions of the DDI potential of strong and moderate inhibitors and inducers of CYP3A4 and their impact on the dosing of entrectinib supported the dosing recommendations with CYP3A4 perpetrators in the label.

**Encore:** Published in *Clinical Pharmacology & Therapeutics*, Vol 107, March 2020.

#### Poster Number: 080

##### Exposure–Response Analysis of Entrectinib Supports the Recommended Dose in Patients With Advanced/Metastatic Solid Tumors

F. Mercier<sup>1</sup>, N. Djebli<sup>1</sup>, M. González-Sales<sup>2</sup>, G. Meneses-Lorente<sup>3</sup>, F. Jaminion<sup>1</sup>, A. Phipps<sup>3</sup>, N. Frey<sup>1</sup>

<sup>1</sup>F Hoffmann-La Roche Ltd, Basel, Switzerland; <sup>2</sup>Modeling Great Solutions, Andorra; <sup>3</sup>Roche Products Ltd, Welwyn, United Kingdom

**Statement of Purpose, Innovation or Hypothesis:** Entrectinib is a CNS-active, potent and selective inhibitor of ROS1/TRK/ALK kinase activity. The objective of this analysis was to characterize the exposure–response relationship for adult patients with ROS1-positive, metastatic NSCLC and NTRK gene fusion-positive solid tumors.

**Description of Methods and Materials:** A Stein-Fojo model was used to describe the temporal pattern of tumor burden. Data from 39 ROS1-positive and 50 NTRK gene fusion-positive cancer patients were analyzed. Linear and sigmoid- $E_{max}$  functions were tested to describe the relationship between model parameters and drug exposure. Logistic regression models were fitted to treatment-emergent adverse events (AEs) (grade 3 or above), and serious AEs, to assess if the probability

of safety events increases with drug exposure ( $AUC_t$  and  $C_{max}$ , on Day 1 and at steady-state [ $AUC_{ss}$ ]). Data from 298 patients were available for this analysis.

**Data and Results:** The sum of lesion diameters showed a steep decrease over time, indicating a tumor shrinkage upon treatment onset for most of the patients. The mean shrinkage rate was estimated at 0.01 day<sup>-1</sup> in either *ROS1*-positive or *NTRK* fusion-positive patients, i.e. 8–12 times larger than the mean growth rate. Adding exposure into the model did not improve the goodness-of-fit, suggesting that a plateau of efficacy has been reached at the dose of 600 mg QD. A statistically-significant relationship was found between the AUC Day 1 ( $p$ -value=0.042) or  $AUC_{ss}$  ( $p$ -value=0.03) and the occurrence of AEs  $\geq$  Grade 3. The increase in the probability of occurrence was mainly noticed at exposure levels attained with doses higher than the recommended dose of 600 mg QD.

**Interpretation, Conclusion or Significance:** Overall, the exposure–response analysis suggested that the entrectinib dose of 600 mg QD in adults provides a suitable benefit:risk ratio.

**Encore:** Published in *Clinical Pharmacology & Therapeutics*, Vol 107, March 2020.

#### Poster Number: 081

#### Is There a Relationship Between In-vehicle Exposure to Gasoline-driven Bus Fumes and Blood Pressure Among Nigerian Drivers?

R. C. Anakwue<sup>1</sup>, T. Ibom<sup>1</sup>, A. Anakwue<sup>1</sup>

<sup>1</sup>Coll of Medicine, Univ of Nigeria, Enugu Campus, Nigeria

**Statement of Purpose, Innovation or Hypothesis:** Vehicular fumes appeared to be the most common source of air pollution in Nigeria and Aba is one of the worst polluted cities. The prevalence of hypertension has continued to increase in Nigeria and the cause is largely unknown. We sort to find out the effect of the composite vehicular fume on the blood pressure of drivers of gasoline-driven commercial buses in Aba, Nigeria.

**Description of Methods and Materials:** A total of 306 commercial bus drivers and 100 controls recruited from Aba urban city and Aba local government secretariat respectively were used for the study data on duration of driving in hours, per week, per month, per year were taken to depict the degree of vehicular fume exposure. Data on risk factors, lifestyles were also obtained.

**Data and Results:** The prevalence of hypertension in the subjects exposed to fumes was 41.8%, higher than the prevalence of hypertension among the control group which was 24%. Body mass index (BMI) and age were positively correlated with exposure to vehicular fumes. There was a negative association between exposure to fumes and blood pressure of the subjects in

the short-term but in the long-term systolic blood pressure correlated positively with exposure to fumes.

**Interpretation, Conclusion or Significance:** Our study had demonstrated that gasoline bus fumes when inhaled caused hypotension in the short-term but the systolic blood pressure increased in the long-term. The high prevalence of hypertension seen among drivers in this study is linked to age, BMI and their peculiar lifestyles in addition to vehicular fumes.

#### Population Pharmacokinetics

##### Poster Number: 082

#### External Evaluation of Population Pharmacokinetic Models of Trimethoprim and Sulfamethoxazole Developed Using Opportunistic Data in Infants and Children

Y. S. Wu<sup>1</sup>, M. Cohen-Wolkowicz<sup>2</sup>, C. P. Hornik<sup>2</sup>, J. Gerhart<sup>1</sup>, J. Autmizguine<sup>3</sup>, M. Cobbaert<sup>2</sup>, D. Gonzalez<sup>1</sup>

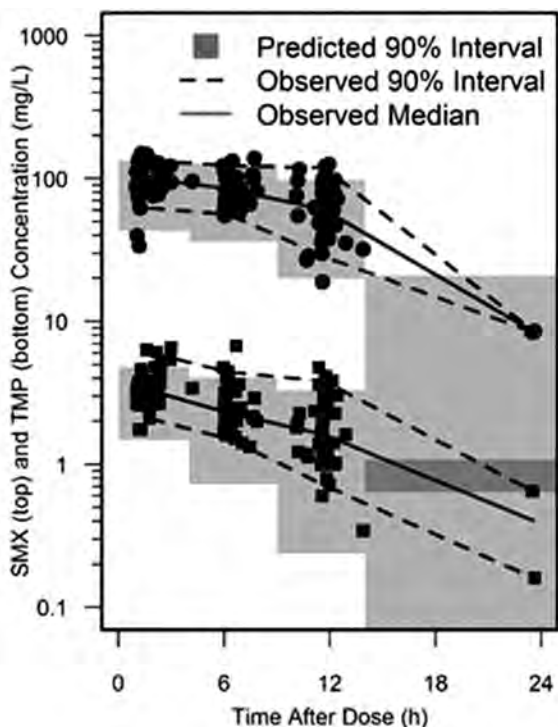
<sup>1</sup>Univ of North Carolina at Chapel Hill, Durham, NC, USA; <sup>2</sup>Duke Univ Medical Ctr, Durham, NC, USA; <sup>3</sup>Univ of Montreal, Quebec, Canada

**Statement of Purpose, Innovation or Hypothesis:** We previously applied population pharmacokinetic (PopPK) modeling to opportunistic pharmacokinetic (PK) data (collected at the time of standard of care procedures) to overcome challenges associated with assessing pediatric drug exposure in clinical trials. In this study using traditional PK data, we aimed to perform an external evaluation of our published pediatric trimethoprim (TMP) and sulfamethoxazole (SMX) PopPK models to evaluate the models' predictive performances.

**Description of Methods and Materials:** The external dataset consists of 121 plasma samples from 20 patients (median [range] age 4.4 yrs [0.23–15], serum creatinine 0.32 mg/dl [0.10–0.60]). Compared to the population in the original opportunistic PK dataset, the external dataset population was younger and excluded patients with renal impairment. The predictive performance of the published TMP and SMX models was evaluated using prediction-corrected visual predictive check (pcVPC) to adjust for different dosing regimens.

**Data and Results:** For both TMP and SMX models, most of the observed concentrations fall within the 90% prediction intervals (Figure 1), but the 90% prediction interval may be slightly lower than the observed 5<sup>th</sup> and 95<sup>th</sup> percentiles.

**Interpretation, Conclusion or Significance:** The published TMP and SMX PopPK models have acceptable predictive performance overall, although they slightly underpredict the exposures seen in the external dataset. Variability was similar between the model prediction and the external dataset.



**Poster Number: 082** **Figure 1.** Prediction-corrected Visual Predictive Check of the POPS Model Using the External Dataset

**Encore:** Published in *Clinical Pharmacology & Therapeutics*, Vol 107, March 2020.

**Poster Number: 083**

**Ethnic Similarity in Pharmacokinetics and Pharmacodynamics of TAK-906, a D<sub>2</sub>/D<sub>3</sub> Receptor Antagonist: Phase 1 Single and Multiple Ascending Dose Studies in Healthy Japanese and Non-Japanese Participants**

R.L. Whiting<sup>1</sup>, B. Darpo<sup>2</sup>, C. Chen<sup>3</sup>, H. Sekino<sup>4</sup>, H. Okamoto<sup>5</sup>, T. Yamaguchi<sup>6</sup>, R.R. Stoltz<sup>7</sup>

<sup>1</sup>Altos Therapeutics LLC, Los Altos, CA, USA; <sup>2</sup>ERT, previously iCardiac Technologies, Rochester, NY, USA; <sup>3</sup>Takeda Pharmaceuticals Int'l Co., Cambridge, MA, USA; <sup>4</sup>Medical Corp HOUEIKAI, Sekino Clinical Pharmacology Clinic, Tokyo, Japan; <sup>5</sup>PRA Development Ctr KK, Osaka, Japan; <sup>6</sup>Takeda Pharmaceutical Co Ltd, Osaka, Japan; <sup>7</sup>Covance Clinical Research Unit, Evansville, IN, USA

**Statement of Purpose, Innovation or Hypothesis:** TAK-906 is a novel D<sub>2</sub>/D<sub>3</sub> receptor antagonist in development for the symptomatic treatment of gastroparesis. TAK-906 is designed to retain the dopamine receptor antagonist profile and minimal central nervous system (CNS) penetration of domperidone whilst avoiding the cardiac effects.

**Description of Methods and Materials:** Two separate studies were conducted, one in the US and the other in

Japan. Both studies investigated safety, pharmacokinetics and pharmacodynamics of single ascending (SAD) and multiple ascending doses (MAD) of TAK-906 in healthy participants. In the US study, the SAD part consisted of seven cohorts with doses between 5 and 300 mg qd and the MAD part of two cohorts with 50 or 100 mg bid for four days and one dose on Day 5, each consisting of eight male and female participants (two randomized to placebo). In the Japan study, male participants were grouped into three SAD and MAD cohorts (a single dose of 10, 50 or 100 mg on Day 1 and multiple doses of same dose strength b.i.d for five days from Days 3–7) each consisting of eight participants (two randomized to placebo). In both studies, serum prolactin concentrations were evaluated as a pharmacodynamics marker.

**Data and Results:** TAK-906 was rapidly absorbed (median  $T_{max}$  ~1 hr) and rapidly eliminated (mean  $t_{1/2}$  ~ 4–6 hrs) following single and multiple oral doses in Japanese and non-Japanese participants. TAK-906 exposure was approximately proportional to the dose administered. Accumulation was minor (less than ~30%) with bid dosing. TAK-906 pharmacokinetic profiles, especially for mean  $C_{max}$  and AUC, were generally similar between Japanese male and non-Japanese male and female participants. The serum prolactin concentration increased rapidly following single and multiple oral doses in Japanese and non-Japanese participants. Prolactin concentrations did not increase in a dose-proportional manner. There was little accumulation in serum prolactin with bid dosing. The serum prolactin results in Japanese healthy male participants were similar to those observed in non-Japanese healthy male and female participants. Monitoring of adverse events, electrocardiogram including QT assessment, vital signs, clinical laboratory evaluations, CNS and general physical examinations indicated that oral administration of single or multiple doses of TAK-906 was well tolerated in Japanese and non-Japanese participants.

**Interpretation, Conclusion or Significance:** Pharmacokinetic and pharmacodynamic profiles of TAK-906 were similar in Japanese and non-Japanese healthy participants following single and multiple oral doses. TAK-906 was well tolerated in the Japan study, similarly to the US study.

**Poster Number: 084**

**Population Pharmacokinetic Analysis of Entrectinib, a CNS-active, Potent and Selective Inhibitor of ROS1/TRK/ALK Kinase Activity, in Patients With Solid Tumors**

M. González-Sales<sup>1</sup>, N. Djebli<sup>2</sup>, V. Buchheit<sup>2</sup>, G. Meneses-Lorente<sup>3</sup>, J. Desrochers<sup>4</sup>, P. Tremblay<sup>4</sup>, A. Phipps<sup>3</sup>, N. Frey<sup>2</sup>, F. Mercier<sup>2</sup>

<sup>1</sup>Modeling Great Solutions, Andorra; <sup>2</sup>F Hoffmann-La Roche Ltd, Basel, Switzerland; <sup>3</sup>Roche Products Ltd,

Welwyn, United Kingdom; <sup>4</sup>Syneos Health, Québec, Canada

**Statement of Purpose, Innovation or Hypothesis:** The objective of this analysis was to characterize the pharmacokinetics (PK) of entrectinib and its main active metabolite, M5.

**Description of Methods and Materials:** Data were from 276 cancer patients receiving oral entrectinib. A joint model capturing the PK of entrectinib and the active M5 metabolite was developed using NONMEM<sup>®</sup> v7.4. The parent elimination rate was assumed to correspond to the M5 production rate. The effects of patient covariates on model parameters was assessed. Model performance was evaluated using visual predictive checks.<sup>1</sup>

**Data and Results:** Entrectinib absorption was best described with a sequential zero- and first-order absorption model. The dispositions of entrectinib and M5 were best characterized with a one-compartment model for each entity with linear elimination. Moderate to high between-patient variability was quantified in model parameters (from 30.8% for apparent clearance to 122% for the first-order absorption rate constant). The mean (SD) AUC accumulation ratio of entrectinib and M5, following a 600 mg QD administration, was 1.89 (0.381) and 2.01 (0.437), respectively. The mean apparent entrectinib elimination half-life was 19.3 (SD 5.07) hrs. Except the theory-based allometric scaling using body weight,<sup>2</sup> and the relative bioavailability formulation relationship, no other covariates were retained in the population PK model. Model diagnostics indicated good predictive performance.

**Interpretation, Conclusion or Significance:** A robust population PK model was built and qualified for entrectinib and M5, describing linear PK for both entities. This model was further used for ER analysis. Body weight was retained in the model using allometric scaling, but no weight adjustment was needed, based on exposure-efficacy and exposure-safety analyses.

#### References

1. Bergstrand M et al AAPS J 2011
2. Anderson BJ et al Drug Metab Pharmacokinet 2009

**Encore:** Published in *Clinical Pharmacology & Therapeutics*, Vol 107, March 2020

#### Poster Number: 085

#### Population Pharmacokinetic Analysis of Efavirenz in Antiretroviral Therapy-naïve Adults Living with HIV-1 Starting Treatment for Rifampicin-sensitive Tuberculosis

H. Chandasana<sup>1</sup>, R. Kaplan<sup>2</sup>, N. Mwelase<sup>3</sup>, B. Grinsztejn<sup>4</sup>, E. Ticona<sup>5</sup>, M. Lacerda<sup>6</sup>, O. Sued<sup>7</sup>, E. Belonosova<sup>8</sup>, K. Dooley<sup>9</sup>, R. P. Singh<sup>1</sup>

<sup>1</sup>GlaxoSmithKline plc, Collegeville, PA, USA; <sup>2</sup>Desmond Tutu HIV Fdtn, Cape Town, South Africa; <sup>3</sup>Clinical HIV Research Unit, Johannesburg, South Africa; <sup>4</sup>Inst de Pesquisa Clínica Evandro Chagas Fiocruz, Rio de Janeiro, Brazil; <sup>5</sup>Hosp Nacional Dos de Mayo, Univ Nacional Mayor de San Marcos, Lima, Peru; <sup>6</sup>Inst Leônidas & Maria Deane Fiocruz/Tropical Medicine Fdtn Dr Heitor Vieira Dourado, Manaus, Brazil; <sup>7</sup>Fundación Huésped, Buenos Aires, Argentina; <sup>8</sup>Orel Regional Ctr for AIDS and Infectious Diseases Prevention & Treatment, Orel, Russia; <sup>9</sup>Ctr for Tuberculosis Research, Johns Hopkins Univ School of Medicine, Baltimore, MD, USA

**Statement of Purpose, Innovation or Hypothesis:** The concurrent treatment of tuberculosis (TB) and human immunodeficiency virus-1 (HIV-1) is challenging due to drug interactions, overlapping toxicities and immune reconstitution inflammatory syndrome (IRIS). Efavirenz (EFV) is commonly used, but alternatives to EFV are needed, particularly in the setting of adverse events and transmitted drug resistance to NNRTIs. Study INSPIRING (NCT02178592) was a Phase 3, randomized, open-label noncomparative, active control study describing the efficacy and safety of dolutegravir (DTG)- and EFV-containing antiretroviral therapy (ART) regimens in HIV-1/TB coinfecting patients. One of the objectives of this work was to characterize the population pharmacokinetics (PopPK) of EFV in HIV/TB co-infected patients, identify cofactors that contribute to EFV pharmacokinetics (PK) and evaluate the effect of TB treatment containing a known enzyme inducer (rifampicin) on exposure.

**Description of Methods and Materials:** Participants in the INSPIRING study were randomized to dolutegravir (50 mg twice-daily during and two wks post-tuberculosis therapy, then 50 mg once-daily) or EFV (600 mg once daily) and two nucleoside reverse transcriptase inhibitors. Participants received their DTG- or EFV-based regimen with and without TB treatment (isoniazid, rifampicin, pyrazinamide and ethambutol) for 52 wks in this study. In the EFV-treated participants, one plasma sample was collected at wks 8, 24, 36 and 48. A nonlinear mixed-effects modeling approach was used for the PopPK analysis, using NONMEM<sup>®</sup> v7.3. Once a structural model was identified, covariates (body weight, age, albumin level, TB-treatment etc.) were included in a step-wise manner in the model and tested for the improvement in objective function value using the likelihood ratio. Final model selection was driven by evaluation of goodness-of-fit plots, successful convergence, plausibility and precision of parameter estimates and the minimum objective function value. Nonparametric bootstrap and visual predictive checks analysis were performed for final model evaluation.

**Data and Results:** A one-compartment PK model with linear elimination and first order absorption was used to describe EFV pharmacokinetics (n=42). The population clearance was 10.2 L/hr. The apparent volume of distribution and absorption rate were 497.0 L and 0.10 hr<sup>-1</sup>, respectively. Bodyweight was incorporated into the model using physiological allometry with fixed allometric exponents of 0.75 and unity for clearance and volume of distribution, respectively. Tuberculosis treatment (rifampicin) did not influence the PK of EFV in this analysis. Steady-state EFV AUC, C<sub>max</sub> and C<sub>trough</sub> were calculated using final model.

**Interpretation, Conclusion or Significance:** The pharmacokinetics of EFV following repeated-oral administration in HIV/TB coinfecting patients were adequately described by a one-compartment model. After 52 wks of treatment, efavirenz clearance is comparable with and without coadministration of rifampicin.

**Poster Number: 086**

**Population Pharmacokinetic and Exposure-Response Analyses for Subcutaneous Golimumab in Children and Young Adults With Newly Diagnosed Type 1 Diabetes: TIGER Study**

J. Lee<sup>1</sup>, W. Zhou<sup>1</sup>, Z. Xu<sup>1</sup>, Y. Zhuang<sup>1</sup>, H. Zhou<sup>1</sup>, M. Rigby<sup>1</sup>, F. Vercruyse<sup>1</sup>, J. Hedrick<sup>1</sup>, R. Zoka<sup>1</sup>, J. Leu<sup>1</sup>

<sup>1</sup>Janssen Research & Development LLC, Spring House, PA, USA

**Statement of Purpose, Innovation or Hypothesis:** Type 1 diabetes (T1D) is an autoimmune disease involving abnormal activation of T-cells and targeted destruction of pancreatic β-cells. The treatment of T1D still depends on exogenous insulin therapy. Although immunomodulators have been evaluated for safety and efficacy in this disease, there are still no approved disease-modifying drugs for T1D. Golimumab, an anti-TNFα antibody approved for treatment of several autoimmune disorders, was evaluated in a Phase 2a, randomized, double-blind, placebo-controlled, multicenter study for safety and efficacy in children and young adults with newly diagnosed T1D (TIGER). Golimumab showed significant treatment effect where endogenous insulin production was preserved and clinical and metabolic parameters improved in newly diagnosed T1D patients. The objective of this analysis was to evaluate pharmacokinetic (PK) and pharmacodynamic (PD) data from the TIGER study by developing a population pharmacokinetic (PopPK) model and performing exposure-response (ER) analyses.

**Description of Methods and Materials:** In this study, patients (age range: 6–21 yrs) received induction doses at Weeks 0 and 2 (patients <45 kg, 60 mg/m<sup>2</sup> up to 100 mg; patients ≥45 kg, 100 mg) followed by maintenance doses Q2W from Week 4 (patients <45 kg,

30 mg/m<sup>2</sup> up to 50 mg; patients ≥45 kg, 50 mg). The PopPK model was developed using data from TIGER and two other pediatric studies with subcutaneous golimumab (PURSUIT-PEDS-PK (age range: 6–17 yrs) in ulcerative colitis and GO-KIDS (age range: 2–17 yrs) in polyarticular juvenile idiopathic arthritis). Exposure-Response (ER) analyses were conducted for change from baseline in C-peptide AUC (primary endpoint) and several clinically relevant secondary metabolic endpoints at Weeks 12, 26 and 52.

**Data and Results:** A one-compartment model with first-order absorption and elimination rate constants was applied to describe the concentration-time profiles. Typical parameters normalized to the values in subjects with a standard weight of 70 kg were: apparent clearance (CL/F), 0.850 L/day; apparent volume of distribution (V/F), 16.0 L; absorption rate constant (k<sub>a</sub>), 1.01 day<sup>-1</sup>. CL/F was estimated to be 34% higher in patients who were tested positive for immune response to golimumab. From the ER analyses, no clear trends were observed for changes in both C-peptide AUC and HbA1c levels for the relatively narrow exposure ranges following the BSA-based dosing regimen used in this study.

**Interpretation, Conclusion or Significance:** The developed PopPK model was able to adequately describe the observed PK of golimumab in T1D patients. Body weight and immune response to treatment were covariates with significant effects. Golimumab treatment showed significant treatment benefit in patients with newly diagnosed T1D with changes in C-peptide AUC as the primary endpoint when active treatment group is compared with placebo treatment group. Nevertheless, the ER analyses did not show clear trends within the active treatment group which may indicate that the exposure from this T1D-specific dosing regimen was at the plateau of the ER curve.

## Precision Medicine

**Poster Number: 087**

**HydroC-Precision: An Integrated Hydrocortisone Dosing and Biomarker Platform for Treating Children With Congenital Adrenal Hyperplasia**

M. M. Jaber<sup>1</sup>, K. Sarafoglou<sup>1</sup>, M. Al-Kofahi<sup>1</sup>, R. C. Brundage<sup>1</sup>

<sup>1</sup>Univ of Minnesota, Minneapolis, MN, USA

**Statement of Purpose, Innovation or Hypothesis:** Congenital adrenal hyperplasia (CAH) is a rare disease that affects the production of cortisol and adrenal steroidal hormones. Hydrocortisone (cortisol) is the standard replacement therapy in children. Disease status is monitored using 17-hydroxy progesterone (17OHP) and androstenedione (D4A) biomarkers at

**Poster Number: 087 Table 1. CAH Biometrics Analysis. Mean (%CV) [Range]**

Compound	AUC total (*hr)	AUC above (*hr)	AUC below (*hr)	Time above (hour)	Time below (hour)	Time in range (hour)
Cortisol *ug/dL	107.0 (36%) [70–258.3]	5.7 (138%) [0–42]	80.0 (21%) [29.4–100]	0.6 (89%) [0–2.6]	15.5 (17%) [6.1–18.4]	7.9 (30%) [5–15.3]
17-OHP *ng/dL	11,235.0 (103%) [106.7–47,444]	7,466.1 (225%) [0–110,373]	1,521.6 (94%) [0–4,693]	6.7 (98%) [0–24]	11.5 (72%) [0–24]	5.8 (62%) [0–13.7]
D4A *ng/dL	413.0 (123%) [24–2,426.4]	189.5 (25%) [0–5,311.9]	147.6 (136%) [0–1,029]	2.3 (221%) [0–22.1]	14.2 (60%) [0–24]	7.3 (85%) [0–19.7]

clinic visits three or four times a year. This monitoring practice is not optimal as these biomarkers have short half-lives with concentrations that fluctuate rapidly in response to hydrocortisone dosing. Furthermore, doses need to be adjusted during childhood as hypercortisolemia will over-suppress the HPA axis and restrict normal growth, and insufficient dosing will allow the overproduction of adrenal steroids that cause a multitude of unwanted effects. The objective of this work was to create the HydroC-Precision software platform to better understand hydrocortisone dosing and the time-course of biomarker response as a first step in exploring the utility of tighter hormonal control.

**Description of Methods and Materials:** The pharmacokinetics/pharmacodynamics (PK/PD) of cortisol, 17OHP and D4A are complicated and necessitated the development of bespoke software for clinical application. HydroC-Precision was built using R software. The graphical interface used for entering patient-specific information was developed in R-Shiny. The R package *mrgsolve* was used to build the PK/PD simulation model that included an endogenous circadian rhythm in cortisol production rate and turnover models with production rates of 17OHP and D4A being inhibited by cortisol concentration through Emax models. Pharmacometric exposure metrics hypothesized to be relevant to long-term outcomes included the 24-hr 17OHP and D4A area-under-the-curve (AUC); time-above- and -below-a threshold concentration; and AUC-above- and -below-threshold. Thresholds were defined by normal values in children. HydroC-Precision allows for adaptive control of the system by allowing alternative dosing regimens to be entered and the resulting exposure metrics re-calculated. The performance of HydroC-Precision was evaluated using a group of 52 pediatric patients with CAH who participated in a 6-hr PK/PD study. Each patient's demographic and PK/PD parameter data were imported and the patient-specific exposure metrics were calculated.

**Data and Results:** HydroC-Precision will be demonstrated live. Substantial between-subject variability was noted in all proposed exposure metrics. Table 1 presents the mean, %CV, and range of the calculated pharmacometric variables.

**Interpretation, Conclusion or Significance:** The HydroC-Precision platform was able to use PK/PD data over six hrs and predict biomarker metrics over 24 hrs. With the observation that dose-exposure relationships are highly variable, it is reasonable to conclude that biomarker exposure will be a more relevant surrogate marker for long-term outcomes than hydrocortisone dose. We are encouraged to pursue analyses of exposure-response relationships to improve long-term outcomes through tighter hormonal control.

## Real-world Evidence in Decision Making

**Poster Number: 088**

**Real World Utilization of CFTR Modulator Agents: Results from an Adult Cystic Fibrosis Clinic**

O. F. [Iwuchukwu](#)<sup>1</sup>, T. Jervis Serrano<sup>2</sup>, C. Lam<sup>3</sup>, R. Griffith<sup>4</sup>

<sup>1</sup>Fairleigh Dickinson Univ School of Pharmacy, Florham Park, NJ, USA; <sup>2</sup>Atlantic Health, Morristown, NJ, USA; <sup>3</sup>Univ of the Incarnate Word, San Antonio, TX, USA; <sup>4</sup>Morristown Medical Ctr, Morristown, NJ, USA

**Statement of Purpose, Innovation or Hypothesis:** There is not much data regarding tolerability and drug effectiveness of Cystic Fibrosis Modulator Agents outside of clinical trials. Our study evaluated real world utilization with ivacaftor, lumacaftor/ ivacaftor and tezacaftor/ivacaftor in a convenience sample of cystic fibrosis patients in an adult outpatient clinic.

**Description of Methods and Materials:** A single-center, 24-mos observational study involving 42 eligible (of 51) patients was conducted using de-identified clinical data. Drug effectiveness was evaluated by comparing differences in baseline FEV1 at drug initiation and final FEV1 at time of data collection. Tolerability was measured by discontinuation rates and average number of pulmonary exacerbations. Comparisons were conducted on SPSS v 24 (IBM Corp) using either independent samples T-tests with unequal variances or a one-way ANOVA test and a two-tailed level of significance set at  $p < 0.05$ .

**Data and Results:** Population genetic data showed 33 (79%) of subjects homozygous for the DF508 variant, eight (19%) had one copy of DF508 and another validated CFTR variant while one subject (2%) had an R553X/S1251N genotype. Other subject demographics include 86% White and 13% Female, Population Means ( $\pm$  SE); Age = 37.45 (range 20–58), Baseline FEV<sub>1</sub> = 63.9 ( $\pm$  3.57) with six patients' FEV<sub>1</sub>  $\leq$  40, BMI=22.69 ( $\pm$  0.47). Subjects on ivacaftor were significantly older than those on the other two agents (47.22 vs 35.26 and 32.67). Average time (mos) on drug = 15.1 ( $\pm$  1.78), 14.4 ( $\pm$  1.74 SE) and 4.5 ( $\pm$  0.96) with absolute point changes in mean FEV<sub>1</sub>=1.7, 0.03 and 4.8 for ivacaftor, lumacaftor/ivacaftor and tezacaftor/ivacaftor. Discontinuation rates were 11% and 81% for ivacaftor and lumacaftor/ivacaftor respectively ( $p < 0.001$ ). Of patients who discontinued, 78% switched to tezacaftor/ivacaftor. Average number of pulmonary exacerbations was highest ( $2.93 \pm 0.52$ ) in the lumacaftor/ ivacaftor and lowest ( $0.67 \pm 0.33$ ) in the tezacaftor/ ivacaftor group ( $p=0.01$ ).

**Interpretation, Conclusion or Significance:** Within a real-world convenience sample, there were no measurable differences in one clinical measure of effectiveness for utilized CFTR modulators and lumacaftor/ivacaftor had the least favorable tolerability profile among all agents evaluated.

## Regulatory Affairs

**Poster Number: 089**

### Characterization of US Food & Drug Administration Advice on Dose Selection and Its Impact on Individualized Dosing in Pivotal Trials and Labeling

L. Wang<sup>1</sup>, K. Maxfield<sup>1</sup>, D. Guinn<sup>1</sup>, R. Madabushi<sup>1</sup>, I. Zineh<sup>1</sup>, R. Schuck<sup>1</sup>

<sup>1</sup>US Food & Drug Administration, Silver Spring, MD, USA

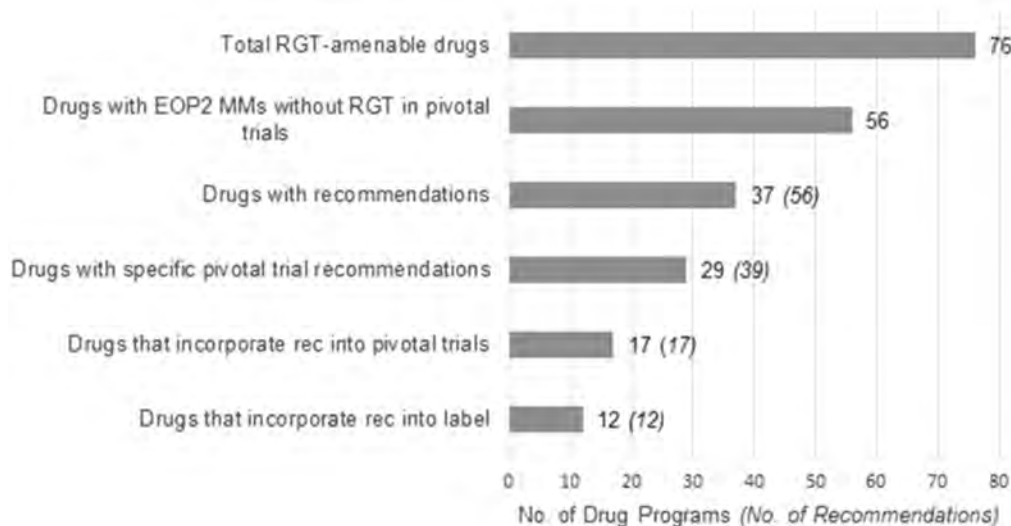
**Statement of Purpose, Innovation or Hypothesis:** Individualized dosing has the potential to maximize drug efficacy while minimizing safety risk based on specific patient characteristics. We sought to characterize the End-of-Phase 2 (EOP2) advice the US Food & Drug Administration (FDA) provided to sponsors regarding dose selection and determine if recommendations supported individualized dosing and impacted pivotal trials and drug labeling.

**Description of Methods and Materials:** We evaluated 76 drugs approved as New Molecular Entities (NMEs) from 2013–2017 that were deemed response-guided titration (RGT)-amenable, as defined in Table 1. We searched End-of-Phase 2 meeting minutes (MM) from internal FDA databases for FDA recommendations on dosing. End-of-Phase 2 MM was chosen because dose selection for pivotal trials, and therefore labeling, is typically discussed at this time. We focused on RGT-amenable drugs because these drugs are amenable to dose individualization strategies. Drug programs that did not have EOP2 MMs or already had sponsor-proposed RGT for pivotal trials were not evaluated. Recommendations were identified as (1) direct recommendations about dosing regimens to be used in pivotal trials (specific pivotal trial vs non-specific) and (2) potentially supportive of individualized dosing by providing clinicians with more dosing options to tailor treatments (Table 1). We then evaluated if the FDA recommendations from EOP2 were incorporated into pivotal trial dosing regimens and/or labeling at the time of approval by analyzing medical reviews and labeling.

**Data and Results:** *Identification of RGT-Amenable Development Programs that received FDA Dosing Recommendations at EOP2:* Seventy-four percent (56/76) of the NME programs met our criteria for analysis. Of these, the FDA provided dosing recommendations for 66% (37/56) of the drug programs. Thirty percent of the dosing recommendations were categorized as nonspecific recommendations. Of the remaining 70% that were

**Poster Number: 089 Table 1. Definitions of Terms Used**

Term	Definition
<b>Response-guided titration</b>	Titration method in which the dosing of the drug is adjusted based on an individual patient's therapeutic response for efficacy
<b>Specific pivotal trial recommendation</b>	Dosing recommendation that the Sponsor could implement during pivotal trials (e.g., the inclusion of more or fewer dosing arms)
<b>Non-specific recommendation</b>	Dosing recommendation that requested additional data from the Sponsor outside of pivotal trials (e.g., phase 2 dose ranging studies)
<b>Recommendations that support individualized dosing</b>	Specific pivotal trial recommendations that support individualized dosing through the study of more dosing regimens or the study of dosing regimens based of patient-specific characteristics
<b>Recommendations that did not support individualized dosing</b>	Specific pivotal trial recommendations that encouraged sponsor to study fewer doses or dosing independent of patient characteristics (e.g., fixed dose studies)



Poster Number: 089 Figure 1. Number of Drug Programs and Recommendations in Each Grouping

considered specific pivotal trial recommendations, 90% were categorized as supportive of individualized dosing and 10% were not supportive of individualized dosing (Figure 1). *Incorporation of FDA dosing recommendations into pivotal trials and labeling.*: Specific pivotal trial dosing recommendations were provided for 29 drug programs. Sixty percent (17/29) of the programs incorporated at least one FDA recommendation into pivotal studies. Additionally, 41% (12/29) of the original FDA-approved drug labels incorporated information resulting from implementation of FDA dosing recommendations. Of the 29 drug programs that received specific pivotal trial recommendations, only eight contained RGT in their original labeling as a dose individualization strategy. However, 75% (6/8) of these programs incorporated FDA dose recommendations received during EOP2 into pivotal studies. For the remaining 21 programs that did not contain RGT in the original labeling, only 52% (11/21) incorporated FDA dosing recommendations received during EOP2 into pivotal studies.

**Interpretation, Conclusion or Significance:** This research highlights the impact of FDA recommendations at EOP2 on choice of dosing regimens in pivotal trials and labeling. Implementation of FDA dosing recommendations in pivotal studies is more likely to lead to dosing strategies that enable individualized patient care. The views expressed in this article are those of the authors and do not necessarily reflect the official position of the FDA.

**Poster Number: 090**

**Assessing Whether Partial AUCs are Needed to Demonstrate Bioequivalence for Liposomal Doxorubicin**

K. D. Alam<sup>1</sup>, S. Sharan<sup>1</sup>, L. Fang<sup>1</sup>, W. Jiang<sup>1</sup>, M. Kim<sup>1</sup>, L. Zhao<sup>1</sup>, L. Zhang<sup>1</sup>, R. Lionberger<sup>1</sup>

<sup>1</sup>US Food & Drug Administration, Silver Spring, MD, USA

**Statement of Purpose, Innovation or Hypothesis:** The US Food & Drug Administration's (FDA) product-specific guidance (PSG) for liposomal doxorubicin recommends several *in vitro* studies to ensure similar liposome characteristics of test product to reference product. The PSG also recommends an *in vivo* single dose, crossover pharmacokinetic (PK) bioequivalence (BE) study. Bioequivalence demonstration of test versus reference product is based on 90% confidence interval (CI) of  $C_{max}$  and AUC in two analytes, i.e., free and liposome-encapsulated doxorubicin in plasma. The European Medicines Agency (EMA)'s PSG additionally recommends assessment of partial AUCs (e.g.,  $AUC_{0-48}$  and  $AUC_{48-last}$ ) only for liposome-encapsulated doxorubicin analyte. The study purpose was to determine if partial AUCs are needed as additional metrics to demonstrate BE.

**Description of Methods and Materials:** Individual patient PK data of multiple abbreviated new drug applications (ANDAs) were assessed in this study. Phoenix<sup>®</sup> software (v7.0) was used to calculate point estimate (geometric least squares means ratio of test and reference) and 90% CI of  $C_{max}$ ,  $AUC_{0-t}$  and pAUCs ( $AUC_{0-24}$ ,  $AUC_{0-48}$ ,  $AUC_{0-72}$  and  $AUC_{0-96}$ ) for both analytes except that  $AUC_{48-last}$  was only assessed for liposome-encapsulated doxorubicin analyte. Residual variabilities of the respective PK metrics of both analytes for each ANDA were also assessed to find the PK metric ( $C_{max}$  versus  $AUC_{0-t}$  versus pAUCs) that has highest residual variabilities. Individual PK metric of both analytes were compared side-by-side [e.g.,  $C_{max(free\ dox)}$  versus  $C_{max(encapsulated\ dox)}$ ] to get an insight about the variability of these analytes. Literature data were studied to

understand the exposure-response relationship of liposomal doxorubicin.

**Data and Results:** All the evaluated PK metrics of  $C_{\max}$ ,  $AUC_{0-t}$  and pAUCs for both analytes passed the BE criteria. Residual variabilities of all PK metrics associated with free doxorubicin analyte were consistently higher than that of liposome-encapsulated doxorubicin analyte suggesting that free doxorubicin analyte is presumably more variable than liposome-encapsulated doxorubicin analyte. For free doxorubicin analyte,  $C_{\max}$  showed highest residual variability in all ANDAs but one ANDA of which  $AUC_{0-t}$  showed highest residual variability. On the other hand,  $AUC_{48-last}$  of liposome-encapsulated doxorubicin analyte, showed highest residual variability in all ANDAs. When  $AUC_{48-last}$  was not considered,  $AUC_{0-t}$  of liposome-encapsulated doxorubicin showed highest residual variability in ~70% ANDAs while  $C_{\max}$  had highest residual variability for remaining ANDAs. In general, the clinical efficacy of liposomal doxorubicin is determined by evaluating disease progression and/or overall patient survival a few months later from the treatment initiation. The exposure-response relationship of liposomal doxorubicin is not well established to correlate the chronic treatment benefit with PK parameters or profiles.

**Interpretation, Conclusion or Significance:** All evaluated PK metrics including partial AUCs passed BE criteria based on in-house ANDA data which may indicate that the rigorous *in vitro* studies including comparable leakage/release rate recommended in FDA's PSG may have helped to ensure *in vivo* BE of these products. Given the large residual variability associated with partial AUCs (e.g.,  $AUC_{48-last}$ ) for liposome-encapsulated doxorubicin analyte, it implies that including these additional partial AUC parameters for BE assessment may potentially further increase the number of cancer patients needed to demonstrate BE. Considering a lack of exposure-response relationship for doxorubicin, partial AUCs as additional metrics to demonstrate BE for liposomal doxorubicin does not seem to be warranted.

## Special Populations

### Poster Number: 091

#### Effect of Renal Function Impairment on the Pharmacokinetics, Safety and Tolerability of the Iminosugar Sinbaglустat

M. Melchior<sup>1</sup>, M. Gehin<sup>1</sup>, A. Alatrach<sup>2</sup>, T. Feldkamp<sup>2</sup>, P. N. Sidharta<sup>1</sup>, J. Dingemans<sup>1</sup>

<sup>1</sup>Idorsia Pharmaceuticals Ltd, Allschwil, Switzerland;

<sup>2</sup>CRS Clinical Research Svcs Kiel GmbH, Kiel, Germany

**Statement of Purpose, Innovation or Hypothesis:** Sinbaglустat (ACT-519276), a brain-penetrating inhibitor

of glucosylceramide synthase and non-lysosomal glucosylceramidase, is developed as a new therapy for rare central nervous system diseases associated with lysosomal dysfunctions. The first-in-human study showed that sinbaglустat was primarily excreted unchanged in urine. This study was conducted to evaluate the effect of mild, moderate and severe renal function impairment on the pharmacokinetics (PK), safety and tolerability of sinbaglустat.

**Description of Methods and Materials:** In this single-center, open-label study, 32 subjects (eight per renal function group assessed using the Cockcroft-Gault formula and eight healthy subjects, with at least two female subjects per group) received a single oral dose of 200 mg sinbaglустat. The PK samples collection and the safety and tolerability observational period lasted 48 h after sinbaglустat administration. Healthy subjects were matched to average values of renally impaired subjects based upon sex, age ( $\pm 10$  yrs), and body weight ( $\pm 15\%$ ). Plasma PK parameters of sinbaglустat were derived by noncompartmental analysis. Standard safety and tolerability evaluations were analyzed descriptively.

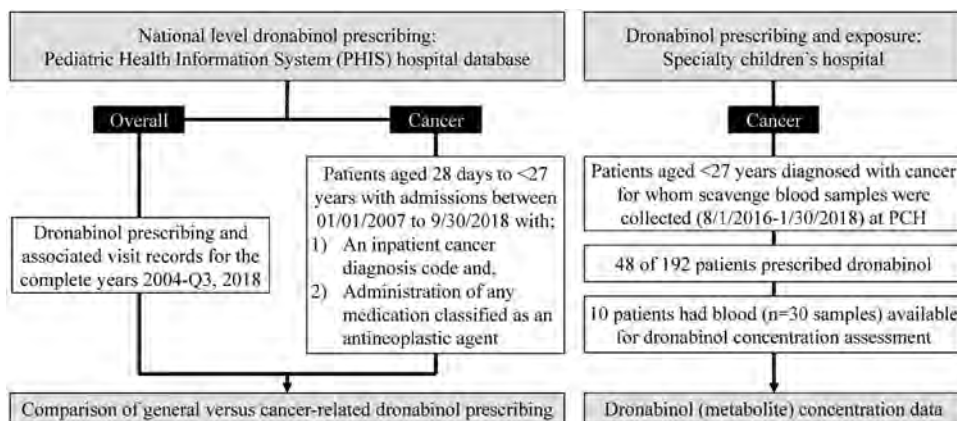
**Data and Results:** All subjects completed the study and were evaluable for safety and PK analysis. When compared to healthy subjects,  $C_{\max}$  did not show clinically-relevant differences in subjects with varying degrees of renal function impairment, but median  $t_{\max}$  was slightly delayed in subjects with moderate and severe renal function impairment with a shift of 0.25 h and 0.48 h, respectively. Overall, when compared to healthy subjects, exposure to sinbaglустat based on  $AUC_{0-t}$  increased in subjects with mild, moderate and severe renal function impairment as indicated by the ratio of geometric means (90% confidence interval) of 1.2 (1.1; 1.4), 1.8 (1.5; 2.2), and 2.6 (2.2; 3.0), respectively. No clinically-relevant findings on ECG, vital signs and clinical laboratory variables were detected. Adverse events (AEs) of headache were reported by two of 24 subjects with renal function impairment and by two of eight healthy subjects. All AEs were of mild intensity and resolved without sequelae at End-of-Study. There were no moderate or severe AEs or AEs leading to study discontinuation.

**Interpretation, Conclusion or Significance:** In conclusion, a single dose of 200 mg sinbaglустat was well tolerated in all groups. Dose adjustment should be considered for subjects with moderate and severe renal function impairment.

### Poster Number: 092

#### Tetrahydrocannabinol (THC; Dronabinol) Prescribing and Exposure Among Children and Young Adults With Cancer

J. Rower<sup>1</sup>, A. King<sup>1</sup>, D. Wilkins<sup>1</sup>, J. Wilkes<sup>2</sup>, V. K. Yellepeddi<sup>1</sup>, L. Maese<sup>1</sup>, R. Lemons<sup>1</sup>, J. E. Constance<sup>1</sup>



**Poster Number: 092** **Figure 1.** Flow Chart of Data and Sample Collection Used to Assess Dronabinol Prescribing Patterns and Exposure Among Hospitalized Children and Young Adults Diagnosed with Cancer

<sup>1</sup>Univ of Utah, Salt Lake City, Utah, USA;  
<sup>2</sup>Intermountain Healthcare, Salt Lake City, Utah, USA

**Statement of Purpose, Innovation or Hypothesis:** The therapeutic utility of Cannabis in cancer is a topic of intense interest. Dronabinol is synthetic  $\Delta^9$ -tetrahydrocannabinol (THC), the primary psychoactive component of Cannabis sativa, and is approved for treating refractory chemotherapy-induced nausea and vomiting (CINV). Little is known about dronabinol prescribing in children and young adults and no published concentration data is available. This study evaluated national level dronabinol use and assessed concentrations of THC and its primary metabolites in patients with cancer <27 yrs of age prescribed dronabinol.

**Description of Methods and Materials:** Observational review of records from the Pediatric Health Information System (PHIS) and a regional network of hospitals in the Intermountain West, including a tertiary care children's hospital, Primary Children's Hospital (PCH) for inpatients <27 yrs of age prescribed dronabinol. Prospective blood samples were collected from children with cancer at PCH.

**Data and Results:** Across PHIS institutions, overall dronabinol prescribing aligned with the pharmacy records for those with cancer ( $p < 0.0001$ ) and of these, 10.4% received dronabinol as inpatients. Blood collected within 72 hrs of dronabinol administration was available from ten children with a median age of 12.5 (range 6–17) yrs. Quantifiable concentrations were found in four (13%), 6 (20%) and one (3%) samples assayed for THC, COOH-THC and OH-THC, respectively. THC concentrations ranged between 0.100 and 0.128 ng/mL and were not associated with dose.

**Interpretation, Conclusion or Significance:** Dronabinol prescribing appears exclusive to patients diagnosed with cancer, and its use has increased steadily in the

past decade. In a small sample of children administered dronabinol, THC and metabolite concentrations were consistently low or undetectable.

**Poster Number: 093**

**Multiple-dose Pharmacokinetics, Safety and Tolerability of Aprocitentan, A Dual Endothelin Receptor Antagonist, In Healthy Japanese and Caucasian Subjects**

P. N. Sidharta<sup>1</sup>, J. Dingemans<sup>1</sup>

<sup>1</sup>Idorsia Pharmaceuticals Ltd, Allschwil, Switzerland

**Statement of Purpose, Innovation or Hypothesis:** Aprocitentan is an orally-active, dual-endothelin receptor antagonist currently in development for the treatment of difficult-to-treat (resistant) hypertension. In a dose-finding Phase 2 study in patients with essential hypertension, aprocitentan induced a dose-dependent decrease in blood pressure. In healthy subjects, the pharmacokinetics (PK), safety and tolerability have been predominantly characterized in Caucasian subjects. Metabolism and elimination of aprocitentan are not dependent on enzymes that exhibit interethnic differences in drug-metabolizing or -transporting capacity. To evaluate the acceptability of previous clinical data and assess whether dose adjustment for another ethnicity would be required this bridging study was conducted.

**Description of Methods and Materials:** This was a single-center, double-blind, placebo-controlled, randomized study. Ten healthy Japanese and ten healthy Caucasian male and female (ratio 1:1) subjects received oral multiple doses of 25 mg aprocitentan or placebo once daily for 10 days in the fasted state (ratio 4:1 for each sex). Thereafter, subjects were observed for PK, safety and tolerability until 216 hrs after last dosing. Differences in maximum plasma concentration ( $C_{max}$ ) and area under the curve during one dosing interval ( $AUC_7$ ) between ethnic groups (Caucasians as

reference) were explored by calculation of geometric means ratio (GMR) and 90% confidence interval (CI) on Day 1 and Day 10. A subgroup analysis was performed to explore differences between ethnic groups for each sex.

**Data and Results:** All 20 subjects completed the study and were evaluable for PK, safety and tolerability. The PK of apocitinan were similar in Japanese and Caucasian subjects throughout the study. Steady-state conditions were reached between Day 7 and Day 10 in both populations. At steady state,  $C_{max}$  was reached at four and three hrs and elimination half-life was 49.1 and 48.8 hrs for Japanese and Caucasian subjects, respectively. The accumulation index was approximately three for both populations. GMR values for  $C_{max}$  and  $AUC_7$  were around one with 90% CI ranging from 0.87–1.30. Results of the subgroup analysis indicated no relevant effect of ethnicity for males or females. Apocitinan was well tolerated and headache and constipation (mainly in Japanese subjects) were the only adverse events (AEs) reported. Compared to placebo, greater decreases in hemoglobin, hematocrit and red blood cells were observed after administration of apocitinan. Irrespective of treatment, a decrease in systolic and diastolic blood pressure was observed in all subjects. Treatment-emergent electrocardiogram (ECG) abnormalities were observed in 3 Japanese subjects. None of the clinical laboratory, vital signs or ECG findings were reported as AEs.

**Interpretation, Conclusion or Significance:** There were no clinically-relevant differences between Japanese and Caucasian subjects. Therefore, apocitinan can be used at a dose level of up to 25 mg in Japanese subjects without dose adjustment. Given these results and taking in consideration the metabolism and elimination of apocitinan, no dose adjustments for any ethnicity are necessary.

**Encore:** Published in *Clinical Pharmacology & Therapeutics*, Vol 107, March 2020.

## Thrombosis/Hemostasis

Poster Number: 094

**External Evaluation and Development of a Simplified Perioperative FVIII Population Pharmacokinetic Model for Adult Hemophilia A Patients Undergoing Surgeries at UNC Medical Ctrs**

J. Zhu<sup>1</sup>, S. Wu<sup>1</sup>, R. Beechinor<sup>2</sup>, R. Kemper<sup>1</sup>, L. Bukkems<sup>3</sup>, R. Mathot<sup>4</sup>, M. Cnossen<sup>5</sup>, D. Gonzalez<sup>1</sup>, S. Chen<sup>6</sup>, N. Key<sup>7</sup>, D. Crona<sup>1,6</sup>

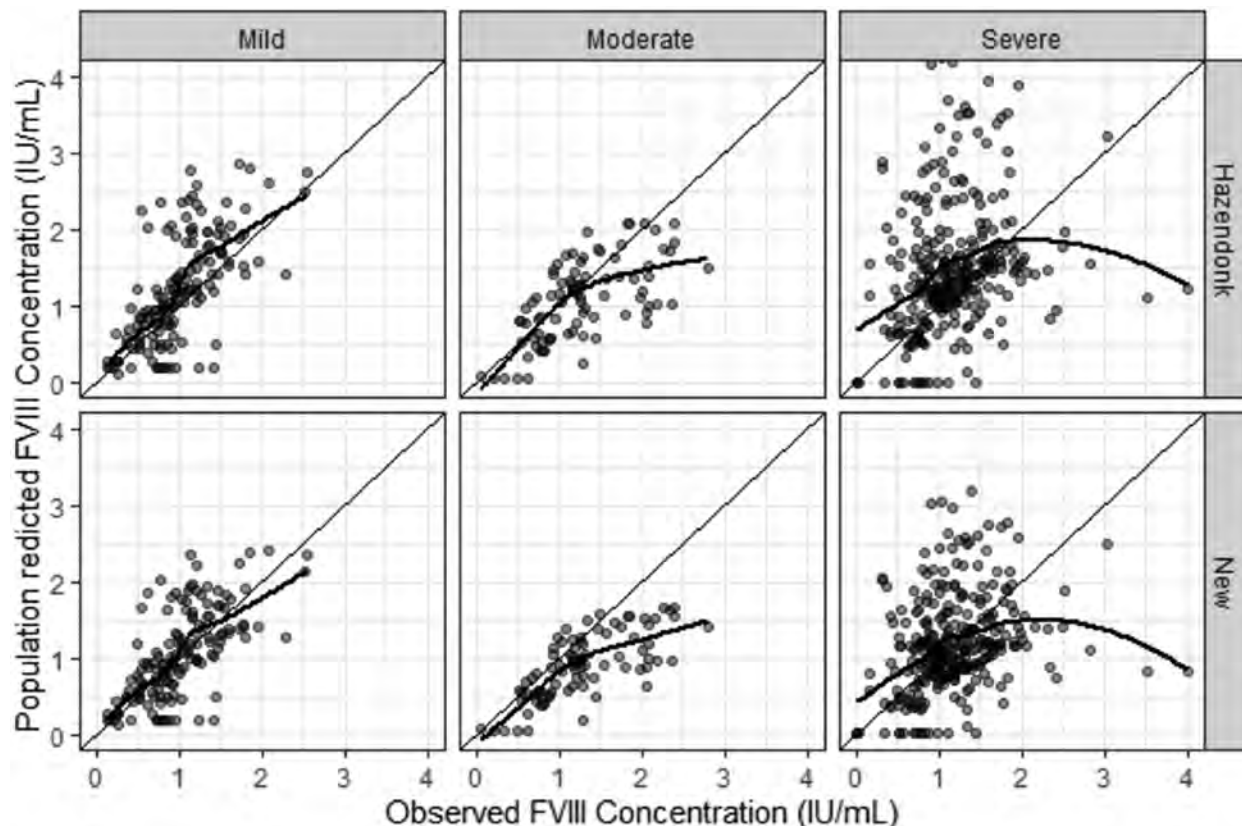
<sup>1</sup>Univ of North Carolina Eshelman School of Pharmacy, Chapel Hill, NC, USA; <sup>2</sup>Univ of California Davis Comprehensive Cancer Ctr, Davis, CA, USA; <sup>3</sup>Amsterdam Univ Medical Ctrs, Amsterdam, The

Netherlands; <sup>4</sup>Univ of Amsterdam's (UvA) Faculty of Medicine, Amsterdam, The Netherlands; <sup>5</sup>Erasmus Univ Medical Ctr, Sophia Children's Hosp Rotterdam, The Netherlands; <sup>6</sup>Univ of North Carolina Hosp, Chapel Hill, NC, USA; <sup>7</sup>Univ of North Carolina School of Medicine, Chapel Hill, NC, USA

**Statement of Purpose, Innovation or Hypothesis:** Hemophilia A is a rare X-linked bleeding disorder caused by FVIII deficiency. Patients are at high risk of joint damage requiring orthopedic surgeries due to the frequent spontaneous bleeding. Therapeutic drug monitoring is typically conducted to maintain perioperative hemophilia A patients at desired FVIII levels, but a significant proportion of patients may have supra- or subtherapeutic FVIII concentrations. Given the exorbitant cost of FVIII treatment and risk of bleeding with subtherapeutic FVIII therapy, we aim to develop a patient-specific pharmacokinetic-guided perioperative FVIII dosing strategy using population PK (PopPK) method. Here we present the results on an external evaluation of a previously-published perioperative FVIII PopPK model in a US population, and show a preliminary PopPK model simplified from the published model based on the external analysis.

**Description of Methods and Materials:** Adult hemophilia A patients who underwent surgery at Univ of North Carolina (UNC) medical centers between April 2014 and November 2019 were included in the analysis. For the external evaluation, center-based residual variabilities were estimated from the UNC dataset, and fixed effects and interindividual variability were fixed to those reported in the Hazendonk model. In addition, the simplified PopPK model was fitted to the observed data both independently and after removing covariate effects that were not significant in our dataset. Both the Hazendonk model and the new model were evaluated using a goodness-of-fit (GoF) plot, numeric predictive check (NPC) based on 1,000 simulations, and bootstrapped 1,000 times. R (v3.6.0) was used for data manipulation and interpretation, and NONMEM<sup>®</sup> (v7.4.3) was used for model simulation and model development.

**Data and Results:** A total of 521 samples from 35 adult patients with mild to severe hemophilia A were available for analysis. Patients had a median (range) age of 56 (24–80) yrs and weight of 84.5 (50.4–137) kg. The Hazendonk model reasonably predicts concentrations for mild and moderate hemophilia, but overpredicts concentrations above 1 IU/mL in severe hemophilia patients. As an abridgement of the Hazendonk model, the new model predicts the mild and severe hemophilia data with less bias than the Hazendonk model, but underpredicts exposure for the moderate hemophilia group (Figure 1). In the bootstrap analysis (Table 1), the covariate effects of blood type and surgery on clearance



Poster Number: 094 Figure 1. Mild, Moderate, Severe GOF Plot

Poster Number: 094 Table 1. Bootstrap of Hazendonk model and preliminary PopPK model using the UNC dataset

Parameter	Hazendonk Published Model		Bootstrap Median (95% Prediction Interval)	Preliminary New Model	Bootstrap Median (95% Prediction Interval)
Minimization Successful			800/1000		860/1000
CL (mL/h)	152		190 (140, 550)	205	200 (160, 250)
CL-Age	-0.172		-0.51 (-1.1, -0.12)	-0.4	-0.43 (-1, -0.013)
CL-Blood Type	1.26		1.0 (0.72, 1.4)		
CL-Surgery Type	0.933		1.1 (0.39, 1.5)		
V1 (mL)	2810		4000 (2400, 5500)	3750	3600 (2300, 4800)
V1-Age	-0.0898		-0.48 (-1.4, 0.45)		
V2 (mL)	1900		1800 (920, 5200)	1750	1800 (1100, 6700)
Q (mL/h)	160		120 (50, 1600)	116	120 (45, 1600)
ReFacto Adjustment	0.344		—		
Additive Error (IU/mL)	<b>Centers 1-3</b> 0.15	<b>Centers 4-5</b> 0.05	0.44 (0.38, 0.49)	0.45	0.44 (0.39, 0.49)
Proportional Error (%)	0.18	0.23	-1.4e-06 (-1.5e-06, -1.4e-06)		
IIV-V1 (%)	26		62 (33, 88)	64	66 (30, 93)
$\rho$ (CL-V1)	0.46		0.44 (-0.22, 0.92)	0.43	0.45 (-0.19, 0.97)
IIV-CL (%)	36		33 (23, 44)	35	35 (23, 45)

(CL) and age on volume from the Hazendonk model were negligible. The effect of age on CL also had negligible impact on predictions for both models. The 90% prediction interval captures 60.1% and 66.4% of the observed data in Hazendonk and new model, respectively.

**Interpretation, Conclusion or Significance:** The Hazendonk model may serve as an initial framework for developing a perioperative PopPK model in a US patient population. However, the inability of the external analysis to confirm the covariate effects in the

Hazendonk model may be due to the small number of subjects in the dataset, and demographic differences. Additional work is warranted to improve the precision and accuracy of the predictions. These data provide rationale to continue future lines of research inquiry aimed at tailoring FVIII perioperative dosing regimens to each hemophilia A patient using PopPK methods.

**Poster Number: 095**

**Transfusion Reactions: Implementation of Rotational Thromboelastometry in Patients Undergoing Cardiac Surgery**

I. Rodríguez Martín<sup>1</sup>

<sup>1</sup>Hosp Macarena, Sevilla, Andalucía, Spain

**Statement of Purpose, Innovation or Hypothesis:** Viscoelastic tests (rotational thromboelastometry, ROTEM<sup>®</sup>), together with the implementation of a specific algorithm for coagulation management in cardiac surgery, enable perioperative coagulopathy to be better controlled.

**Description of Methods and Materials:** Retrospective cohort study including 675 patients who underwent cardiac surgery with cardiopulmonary bypass. The incidence of allogeneic blood transfusions and clinical postoperative complications were analyzed before and after ROTEM<sup>®</sup> implementation.

**Data and Results:** Following viscoelastic testing and the implementation of a specific algorithm for coagulation management, the incidence of any allogeneic blood transfusion decreased (41.4% vs 31.9%,  $p=0.026$ ) during the perioperative period. In the group monitored with ROTEM<sup>®</sup>, decreased incidence of transfusion was observed for packed red blood cells (31.3% vs 19.8%,  $p=0.002$ ), fresh frozen plasma (9.8% vs 3.8%,  $p=0.008$ ), prothrombin complex concentrate administration (0.9% vs 0.3%,  $p=0.599$ ) and activated recombinant factor VII (0.3% vs 0.0%,  $p=0.603$ ). Increased incidence was observed for platelet transfusion (4.8% vs 6.8%,  $p=0.530$ ) and fibrinogen concentrate (0.9% vs 3.5%,  $p=0.066$ ), tranexamic acid (0.0% vs 0.6%,  $p=0.370$ ) and protamine administration (0.6% vs 0.9%,  $p=0.908$ ). Similar results were observed in the postoperative period, but with a decreased incidence of platelet transfusion (4.8% vs 3.8%,  $p=0.813$ ). In addition, statistically significant reductions were detected in the incidence of postoperative bleeding (9.5% vs 5.3%,  $p=0.037$ ), surgical reexploration (6.0% vs 2.9%,  $p=0.035$ ), and length of Intensive Care Unit (ICU) stay (6.0 days vs 5.3 days,  $p=0.026$ ).

**Interpretation, Conclusion or Significance:** The monitoring of hemostasis by ROTEM<sup>®</sup> in cardiac surgery was associated with decreased incidence of allogeneic blood transfusion, clinical hematologic postoperative complications and lengths of ICU stay.

**Poster Number: 096**

**Pharmacodynamic Effects of Clopidogrel, Prasugrel and Ticagrelor After Subcutaneous Administration of the Novel P2Y<sub>12</sub> Receptor Antagonist Selatogrel (ACT-246475)**

U. Schilling<sup>1</sup>, P. Juif<sup>1</sup>, M. Dobrow<sup>2</sup>, J. Dingemans<sup>1</sup>, M. Ufer<sup>1</sup>

<sup>1</sup>Idorsia Pharmaceuticals Ltd, Allschwil, Switzerland;

<sup>2</sup>Biotrial Inc, Newark, NJ, USA

**Statement of Purpose, Innovation or Hypothesis:** Inhibition of platelet aggregation (IPA) by P2Y<sub>12</sub> receptor antagonists is a key component in the treatment of acute coronary syndrome and prevention of thrombotic events in patients with coronary artery disease. Clopidogrel, prasugrel and ticagrelor are oral P2Y<sub>12</sub> receptor antagonists, while cangrelor is intravenously administered. Reduced pharmacodynamic (PD) effects of the prodrugs clopidogrel and prasugrel have been reported when administered during cangrelor infusion. Selatogrel is a novel P2Y<sub>12</sub> receptor antagonist for subcutaneous use with a rapid onset of action. This study investigated its PD interaction liability with oral P2Y<sub>12</sub> receptor antagonists.

**Description of Methods and Materials:** This single-center, randomized, double-blind, two-way cross-over study compared the degree of IPA achieved with clopidogrel, prasugrel and ticagrelor when given after selatogrel or placebo. A total of six groups were studied each consisting of 12 healthy subjects. In each group, a therapeutic loading dose of clopidogrel (300/600 mg), prasugrel (60 mg) or ticagrelor (180 mg) was administered 30 min (i.e., at  $t_{max}$  of selatogrel) or 12 hrs after selatogrel at the planned Phase 3 dose of 16 mg or placebo (Table 1). Inhibition of platelet aggregation was assessed at various time points for up to 48 hrs using the Light Transmission Aggregometry (data not shown) and VerifyNow<sup>®</sup> assay. Primary endpoint was the time-matched treatment difference of IPA at the last two sampling time points. Safety and tolerability were assessed based on adverse events and other safety data. Pharmacokinetic (PK) parameters of selatogrel were derived from 48-hrs plasma concentration-time profiles.

**Data and Results:** In total, 77 subjects were enrolled of which 72 completed the study and were included in the PD analysis. A similar IPA was determined for ticagrelor when administered 30 min after selatogrel or placebo. In contrast, reduced IPA was determined when clopidogrel or prasugrel were administered 30 min after selatogrel. However, when applying a 12-h interval, the reduction in IPA was either less pronounced (clopidogrel) or not observed (prasugrel) (Table 1). Selatogrel given in combination with each oral P2Y<sub>12</sub> receptor antagonist was safe and well tolerated. The most

**Poster Number: 096 Table 1. Inhibition of platelet aggregation by treatment group**

	Interval* (h)	Timepoint (h)	Placebo → Oral P2Y <sub>12</sub> RA (%IPA)	Selatogrel (16 mg) → Oral P2Y <sub>12</sub> RA (%IPA)	Treatment difference (%IPA)
Clopidogrel (600 mg)	0.5	24	54.4	12.9	-41.5
		48	44.7	1.06	-43.6
Clopidogrel (300 mg)	12	24	31.4	28.4	-3.00
		36	33.5	16.5	-17.0
Clopidogrel (600 mg)	12	24	48.7	33.7	-15.0
		36	46.9	18.7	-28.2
Prasugrel (60 mg)	0.5	24	98.8	31.7	-67.1
		36	97.9	18.8	-79.1
Prasugrel (60 mg)	12	24	99.6	98.5	-1.10
		36	99.2	96.5	-2.70
Ticagrelor (180 mg)	0.5	24	39.9	49.3	9.40
		36	20.8	21.7	0.90

Data is expressed as arithmetic mean % inhibition of platelet aggregation (%IPA) assessed with the VerifyNow® assay.  
RA: receptor antagonist - \*Interval between administration of selatogrel or placebo and oral P2Y<sub>12</sub> receptor antagonist.

common adverse events were headache and dyspnea which occurred in seven subjects each. The PK profile of selatogrel was in line with previous studies indicating rapid absorption (i.e., median  $t_{max}$  of 1 h) and elimination (i.e., geometric mean  $t_{1/2}$  of 4–6 hrs).

**Interpretation, Conclusion or Significance:** Ticagrelor-mediated IPA was unaffected despite administration at the  $t_{max}$  of selatogrel mimicking a worst-case scenario. By contrast, IPA mediated by clopidogrel and prasugrel was impaired when these were administered at the  $t_{max}$  of selatogrel. By administering clopidogrel or prasugrel 12 hrs after selatogrel, this could be partially or fully mitigated, respectively.

## Translational Medicine (Biomarkers/Imaging)

### Poster Number: 097

#### Role of Gut-Brain Axis, Pro-inflammatory Activity and Heavy Drinking in the Exacerbation of CIWA in Patients With Alcohol Use Disorder

V. Vatsalya<sup>1</sup>, J. C. Frimodig<sup>1</sup>, R. Agrawal<sup>1</sup>, I. A. Kirpich<sup>1</sup>, J. C. Verster<sup>2</sup>, C. J. McClain<sup>1</sup>

<sup>1</sup>Univ of Louisville, Louisville, KY, USA; <sup>2</sup>Univ of Utrecht, Utrecht, The Netherlands

**Statement of Purpose, Innovation or Hypothesis:** Pathways underlying the gut-brain axis and pro-inflammatory cytokines influence brain functions and behavior. Alcohol use disorder (AUD) patients frequently develop alcohol withdrawal and gut-brain axis and pro-inflammatory response may play a role in the development of alcohol withdrawal. This study examined the role of intestinal permeability,

proinflammatory cytokines and hormones on alcohol withdrawal in AUD patients.

**Description of Methods and Materials:** Forty-eight male (n=34) and female (n=14) AUD patients aged 23–63 yrs were grouped categorically using the clinical institute withdrawal assessment of alcohol scale (CIWA) as clinically-significant CIWA group (CS-CIWA [score >10] gr. [n=22]), and clinically-not significant group (NCS-CIWA [score ≤10] gr. [n=26]). Baseline clinical data and blood samples were collected at admission, which was the point of this investigation. Blood samples were analyzed for markers of intestinal permeability, proinflammatory cytokines and hormones. CIWA, 90-day timeline followback (TLFB90: TD90, NDD90, AvgD90, HDD90) and lifetime drinking history (LTDH) were also collected for analyses.

**Data and Results:** CIWA and LTDH were significantly associated in all AUD patients ( $p=0.031$ ). CIWA showed significant association with IL-8 ( $p=0.011$ ), and adiponectin ( $p=0.003$ ) in all AUD patients, with a trend toward significance for IL-6 ( $p=0.063$ ). CIWA score in CS patients (45.34% of the cohort) was three-fold more than the NCS patients. Between-group comparisons showed that the CS patients had numerically higher values in all the drinking markers (LTDH, TD90, NDD90, AvgD90, HDD90) assessed. Adiponectin was significantly higher in CS patients ( $p=0.013$ ). CS patients showed a stepwise increase in the effects of association of CIWA scores and adiponectin with liposaccharide (LPS, adjusted  $R^2=0.397$ ,  $p=0.014$ ); that augmented with absolute neutrophil count (adjusted  $R^2=0.526$ ,  $p=0.002$ ) only in the CS patients. Only CS females showed higher effects of association of CIWA with IL-8 (adjusted  $R^2=0.779$ ,  $p=0.002$ ; augmented to adjusted  $R^2=0.819$  with LPS as a covariate).

**Interpretation, Conclusion or Significance:** Clinically-significant CIWA scores in AUD patients show close association with altered candidate cytokines and adiponectin. Interaction of adiponectin accompanied with LPS and neutrophils supports the role of

inflammasome activity on CIWA supporting pathogenic role of gut-brain axis in exacerbating withdrawal. Females with elevated CIWA show greater vulnerability in withdrawal that can be characterized by the changes in gut permeability and cytokine response.







# **Clinical Pharmacology in Drug Development**

Volume 9 Number S2 September 2020

---

Abstracts: 2020 Annual Meeting of the American College of Clinical Pharmacology® September 21st-23rd Virtual